CZECH TECHNICAL UNIVERSITY IN PRAGUE

Faculty of Civil Engineering
Department of Mechanics

Stochastic Hard Packing for Heterogeneous Materials Modelling via Wang Tilings

DOCTORAL THESIS

Ing. David Šedlbauer

Doctoral study programme: Civil Engineering
Branch of study: Physical and Material Engineering

Doctoral thesis tutor: doc. Ing. Matěj Lepš, Ph.D.

Prague, 2019

CZECH TECHNICAL UNIVERSITY IN PRAGUE
Faculty of Civil Engineering
Thákurova 7, 166 29 Praha 6

DECLARATION

Ph.D. student's name: David Šedlbauer

Title of the doctoral thesis: Stochastic Hard Packing for Heterogeneous Materials Modelling via Wang Tilings

I hereby declare that this doctoral thesis is my own work and effort written under the guidance of the tutor doc. Ing. Matěj Lepš, Ph.D.
All sources and other materials used have been quoted in the list of references.

The doctoral thesis was written in connection with research on the projects:
SGS13/034/OHK1/1T/11,
SGS14/028/OHK1/1T/11,
SGS15/030/OHK1/1T/11,
SGS16/037/OHK1/1T/11,
SGS17/042/OHK1/1T/11,
SGS18/036/OHK1/1T/11.

In Prague on .....

.....
signature

Abstrakt

Tato práce se zabývá modelováním náhodných heterogenních mikrostruktur. Zvláštní důraz je pak kladen na materiálové domény, které tvoří kruhové nebo kulové částice v základní materiálové matrici. Na mikro a nano úrovni jsou tyto mikrostruktury nejčastěji tvořeny pomocí opakujících se kopií jedné buňky s periodickými okrajovými podmínkami. Na druhé straně existují úlohy na poli materiálového inženýrství, které vyžadují zachování heterogenity a minimalizace periodických artefaktů. Pro ty je vhodnější využít konceptu Wangova dláždění, který umožňuje vygenerovat aperiodické nekonečné plochy pomocí konečného počtu dlaždic.

Pro úlohy rekonstrukce nebo komprese náhodných materiálových struktur není prakticky nutné tvořit striktně aperidocká dláždění. Postačí využít konceptu stochastického dláždění. Konkrétně v této práci je stochastické Wangovo dláždění s osmi dlaždicemi v základním setu použito na rekonstrukci výše uvedených domén. Vzhledem k typu částic je součástí algoritmu generování dlaždic i molekulární dynamika. Zároveň je představen nový typ okrajových podmínek – Adaptivní stěny, který redukuje periodické artefakty i pro malý počet dlaždic v setu a také zachovává kompatibilitu dláždění bez přiřazování částic hraničním oblastem. Tyto teze jsou ověřeny na sadách testovacích domén pro 2D mono i polydiseperzní struktury spolu s realizací 3D monodisperzního vzorku.

Rekonstrukce jak umělých, tak reálných materiálových domén zde tvoří optimalizační úlohu. Pro její řešení je vybrána optimalizační metoda rojem částic – Particle Swarm Optimization method. Tato metoda je dále modifikována pro účely kompatibility s Wangovým dlážděním a molekulární dynamikou. Poté je výsledný algoritmus otestován na sadě umělých a dvou reálných mikrostruktur. Hodnocení výsledků a doporučení pro další vývoj jsou součástí závěrečné diskuze.

Klíčová slova: Náhodné heterogenní materiály, Wangovo dláždění, molekulární dynamika, Particle Swarm Optimization, Adaptivní stěny

.

Abstract

This work deals with the modeling of random heterogeneous microstructures. Special emphasis is placed on material domains, which are formed by circular or spherical particles in the matrix of basic material. These materials are formed at micro and nano level mostly with copies of just one tile with periodic boundary conditions. On the other hand, there are problems in the field of material engineering which require preservation of heterogeneity and minimization of periodicity artefacts. Here it is preferable to use concept of the Wang tiling, which is able to generate infinite aperiodic areas with finite number of tiles.

For the tasks of reconstruction or compression of random material structures it is not necessary to create strictly aperiodic tiling. It is sufficient to use a concept of stochastic tiling. In this work the stochastic Wang tiling with basic set of eight tiles servers for reconstruction of the above domains. A molecular dynamics is included to the algorithm for generation of tiles because of the type of particles. Concurently a new type of boundary condition is introduced – Adaptive walls, which reduces periodicity artefacts even for small number of tiles in a set and keep the compatibility of tiling without assigment of particles to tile edges. These theses are verified on sets of test domains for 2D mono and polydisperse structures together with a realization of 3D monodispersion sample.

A reconstruction of both artificial and real microstructure domains forms an optimization task. The Particle Swarm Optimization (PSO) method is chosen to solve this kind of problem. This method is further modified in order to be compatible with both Wang tiling and molecular dynamics. Then the final algorithm is tested on a set of artificial and two real microstructures. Evaluation of results and recommendations for further development are parts of the discussion chapter.

Key words: Random heterogeneous materials, Wang tiling, molecular dynamics, Particle Swarm Optimization, Adaptive Walls

Acknowledgements

I would like to thank all those who have supported me throughout my Ph.D. study.

- First of all I would like to thank my supervisor Matěj Lepš for inspiring comments, great patience and for opportunity to work under his leadership.
- Another thanks goes to my friends from the department of mechanics: Martin Doškář, Lukáš Zrůbek, Jan Stránský, Ondřej Zobal, Zdeněk Prošek, Tereza Otcovská, Martin Verner, Věra Hlavatá, Adéla Hlobilová, Michal Hlobil and Jan Havelka for many enjoyments I will remember for all my live.
- I also express my deep thanks to other department members for inspiring discussions and a correct attitude throughout my studies: Milan Jirásek, Bořek Patzák, Jan Zeman, Anička Kučerová, Jan Sýkora, Jan Vorel, and Pavel Tesárek.
- I would like to thank my best friends Jan Marx a Tomáš Fechtner for their enormous support in difficult moments.
- The financial support by SGS projects of the Czech technical university in Prague is gratefully acknowledged.
- Last but not least I am grateful to my colleagues and bosses from Allcons Industry without whom I would never be able to combine work and studies.
- The greatest thanks goes to my family, Renata, Kristýna and Ondra, without whom I would neither start nor finish this work. Thank for all the support and positive energy they gave me daily.

Contents

List of Figures

List of Tables

1 Introduction

The term "*Heterogeneous*" comes originally from the Medieval Latin (Ancient Greek) and consists of two words *heteros* – "another" or "different" and *genos* – "kind". One of the definitions in material engineering designates heterogeneous materials as domains (i) of different phases (materials) or (ii) of the same material in different states [1]. This work deals with the first group and its representatives – composites. If we focus on definition of composites with emphasis on the design philosophy, composites are heterogeneous materials where a single structure is created after mixing materials with very different properties. The final structure shows additional or better properties than each of individual components or simple mixture of such components. This phenomenon is called synergism [2].

Deeper knowledge in the field of material studies in micro level together with computer technologies enables both effective usage of traditional heterogeneous structures such as wood, sandstone, soils, or bones and a design of new synthetic ones, for example concrete, foams, cellular solids, fibre or particular composites. Experimental testing and optimization of material properties using already made samples is very expensive concept in terms of time and money demands. On the other hand approaches, which utilize computer modelling, numerical or analytical methods and at a later stage verification on physical samples, are able to significantly reduce these costs.

The Periodic Unit Cell (the PUC) or the Statistical Equivalent Periodic Unit Cell (the SEPUC) respectively are the most widespread concepts for modelling of heterogeneous materials in micro and nano level. They used to serve as building blocks for numerical methods on upper scale, where the main issue is to obtain effective properties of reference or reconstructed structures. On the other hand there are tasks of material engineering, which require preservation of heterogeneity with eliminated or minimized periodic artefacts.

The modelling of the random heterogeneous microstructures can be understood as a creation of 2D surfaces or 3D spaces of finite dimensions with specific boundary conditions and required final properties. Similar tasks have been solved also in other fields of science. The texture synthesis and a design of large areas with low computer demands are challenges in computer graphics or game industry [3], [4]. Also medicine face similar issues, let us mention contributions dealing with assembly of DNA string [5] [6]. These works utilize the Wang tiling approach [7], [8] to overcome problems with randomness. Over the last few years principles of the Wang tiling concept have been taken over and incorporated into material engineering as well. Now, researches are able to reduce unwanted periodicity artefacts when dealing with random heterogeneous microstructures in comparison with traditional methods based on periodical repetition of just one cell [9], [10], or [11].

1.1 Thesis objectives

This doctoral thesis focuses on Wang tiling concept and its application to random heterogeneous material microstructures, which 2D or 3D sample are composed of discrete hard inpenetrable circular/spherical particles in a continuous phase. Representatives of such a material domain are composites reinforced with unidirectional fibres. When searching for the term "unidirectional fibre composites", google scholar as a web search engine of scholarly literature (including results from databeses Scopus or Web of Science) offers more than 4800 results from the January, 2018 up to the January, 2019. This fact together with usage of the the traditional PUC for modelling of random heterogeneous materials in most of contemporary works makes the topic actual and desirable.

The main objective of the doctoral thesis is to create algorithms for generation of random heterogeneous domains with hard spherical/ circular particles via system of stochastic Wang tiles. Partial objectives are following:

1. To develop algorithms for general tiling and to implement molecular dynamics principles for material structures with circular/ spherical inclusions.
2. To create algorithms for generation of Wang tiles based on modified molecular dynamics, to define boundary conditions for efficient reduction of unwanted periodicity artefacts and to implement statistical descriptors for comparison of tiled domains.
3. To implement and/or modify optimization methods into algorithms for tile generation, to verify these algorithms on artificial samples, and to reconstruct real random heterogeneous material microstructures.

This thesis is organized as follows. The second chapter as a theoretical part introduces Wang tiling concept and its history, methods for modelling of particle domains together with restrictions given by packing problem of circles in a rectangular container, and statistical descriptors which are utilized in practical part. The third chapter defines modified molecular dynamics approach for particle motion and compares 3 types of boundary conditions in terms of periodicity artefacts reduction. The traditional concept with periodic repetition of just one tile is extended with Volume Walls and brand new Adaptive Walls technique. The fourth chapter aims at reconstruction of both artificial and real microstructures. In previous chapters material domains are generated with random distribution of particles, but match with reference sample requires usage of optimization mechanisms. In our case modified Particle Swarm Optimization method is introduced, verified on artificial samples and applied on reconstruction of two real microstructures. Later, we briefly dicsuss given results and outline possible improvements. The highlights of the thesis are summarized in conclusion.

2 Theoretical background[1]

2.1 Wang tiling

The origin of Wang Tiling is associated with search for a general algorithm that can decide validity of a statement. This Entsheidungsproblem (the decision problem) was firstly posed by German mathematician David Hilbert in 1928. Alan Turing in [12] and Alonzo Church [13] proved non-existence of such algorithm on the Halting problem. Later a mathematician Hao Wang introduced set of tiles as a tool for the study of the decision problem [7], [8]. During the tiling process, tiles were not permitted to rotate or reflect. The question was to find an effective procedure, which can decide whether copies of squares from the finite set are able to cover a whole plane (infinite plane) with restriction of adjoining edges – colours. This generalized game of dominos leads to finding periodically repeated areas. He proved that a part of such plane that is periodic can be stacked with a finite tile set.

Through the years researches proved that there exist sets of tiles enabling to cover a plate even without periodic repetition of a certain group of tiles and the competition was to find the smallest set. Wang's student Robert Berger found out that strictly aperiodic plane can be tiled with set of 20 426 tiles [14]. He later reduced in his thesis this set to 104 tiles. The last two smallest sets, up on the best author's knowledge, are shown in Fig. 2-1. The first set consists of 13 individuals with 5 different colours on edges [15]. The second set includes 11 tiles over only 4 codes [16]. Note the same codes on both vertical and horizontal edges in comparison with the Stochastic Wang tiling concept, which is described in detail within following subsection.

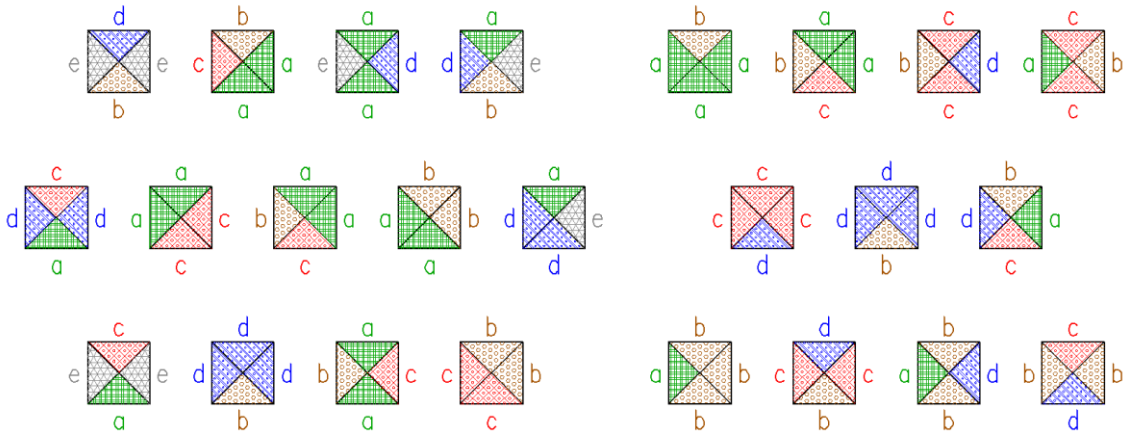

Fig. 2-1 Minimal sets for aperiodic tilings
Left – 13 tiles over 5 codes [15] Right – 11 tiles over 4 codes [16]

[1] Parts of this chapter are reproduced from author's contributions: [I], [II], [III], [IV], [V]

2.1.1 Stochastic tiling

The main reason for implementation of Wang tiling principles to the tasks of material engineering is to create naturally looking domains. Moreover real heterogeneous material microstructures might include periodic artefacts as well, representing for example clusters of pores or regularly arranged particles. Thus, the requirement for utilization of presented aperiodic tiling is quite strict and therefore substituted with principles of the stochastic Cohen-Shade-Hiller-Deussen (CSHD) tiling algorithm [4].

Tiles from a basic tiling set in 2D are placed into a regular lattice of cells with the same dimension column by column and row by row. The tiling algorithm starts with the first tile of a set that is randomly chosen and placed in the corner of the grid. In a general position of the process, the system has to propose at least two individuals for the next step in order to be called stochastic. Similar requirements with number of codes on appropriate edge define minimal number of tiles in the set. When considering n_x and n_y as numbers of different colours/codes on vertical and horizontal edges respectively, the full or complete Wang tile set includes $n_x^2 \cdot n_z^2$ tiles, whereas the minimal set forms $2 \cdot n_x \cdot n_z$ tiles. In this work minimal set of stochastic Wang tiles for 2D applications applies two different codes on both horizontal and vertical edges, unless otherwise indicated. Therefore the final set consists of 8 tiles. A visualization of both full and minimal set together with tiling process in two dimensions are shown in Fig. 2-2.

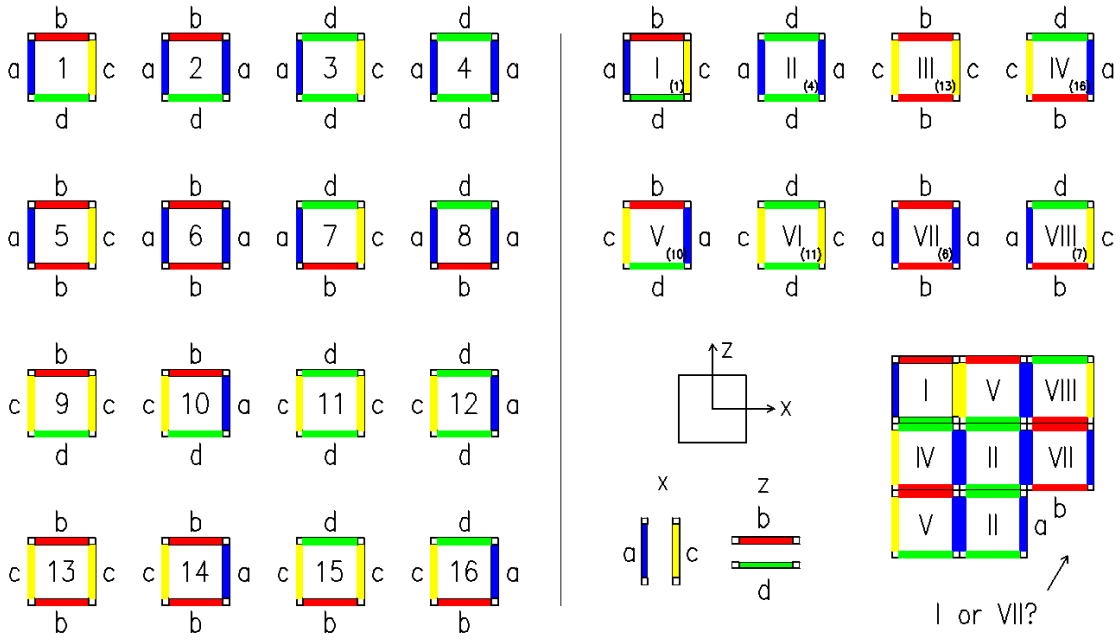

Fig. 2-2 Sets for 2D stochastic tilings
Left – full set W16/2-2, Right – minimal set W8/2-2 with tiling algorithm

Extension to the 3D system is straightforward. If we consider n_x, n_y and n_z as numbers of different colours on walls in main coordinate directions, the full set consists of $n_x^2 \cdot n_y^2 \cdot n_z^2$ 3D tiles – cubes. The tiling algorithm starts with the first cube randomly chosen and placed to the grid of a material domain. The system then adds cubes gradually row by row, column by column within a layer and then layer by layer. A choice between two individuals for any combination of codes in main coordinate system results in minimal set of $2 \cdot n_x \cdot n_y \cdot n_z$ cubes. If we have two codes for every set of walls in main directions, the minimal set for 3D stochastic tiling, designated W16/2-2-2, include 16 Wang cubes, Fig 2-3.

The nomenclature of tiles follows [9]. Here general tile description is defined as W_{nt}/n_{1c}-n_{2c}, where W_{nt} designates number of tiles in a set and n_i number of codes on edges. The lower index 1 is attributed to codes on horizontal edges while 2 on vertical edges. Extension for 3D application is straightforward.

In this work sequence of numbers which describe each tile in the set depends on designation of independent tile edges/walls. The string follows the definition and position of the main tile coordinate system, unless otherwise indicated. The centre of coordinate system lies in the centre of gravity of each tile/cube. The direction of axis goes to the centre of appropriate edge/wall. A sequention of numbers is based on code on negative and positive side of axis X, Y, and Z respectively. This procedure substitute the description based on world sites.

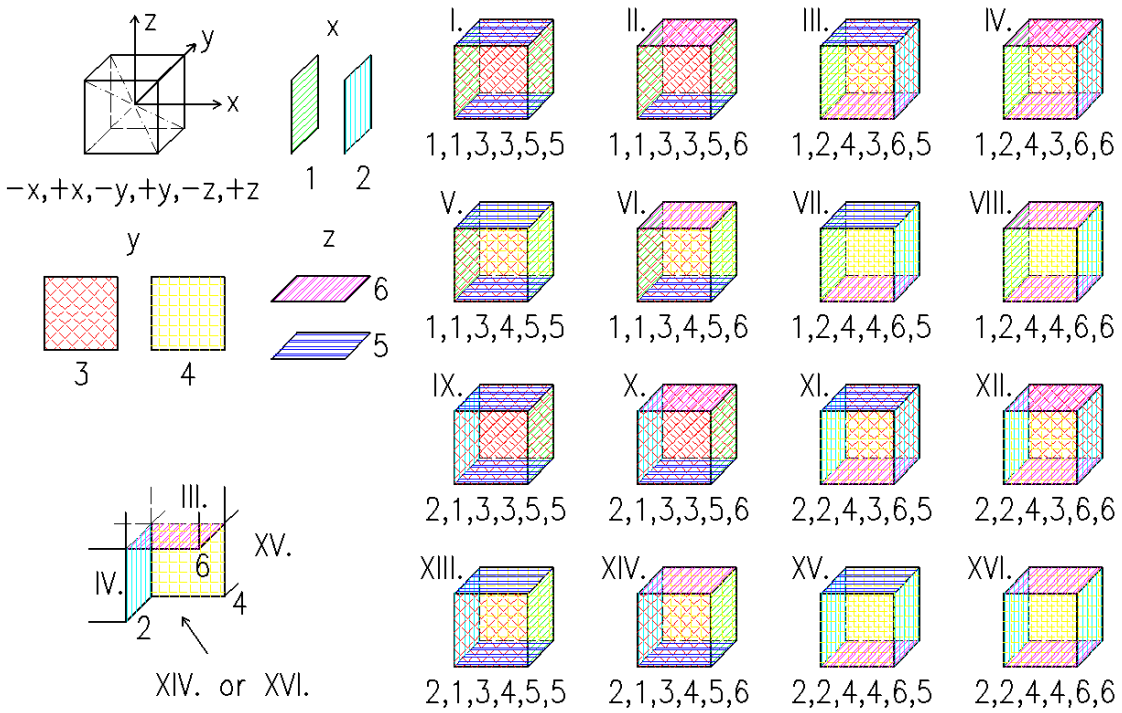

Fig. 2-3 Minimal set for 3D stochastic tiling W16/2-2-2 with tiling algorithm

2.2 Particle systems

As a first step, before both compression and reconstruction of microstructure domains, we need to select method, which is suitable for investigated type of random particle system. This contribution focuses mainly on geometrical and physics based computer methods. A reference sample is considered to be an input, therefore experimental testing and imaging techiques like X-ray tomography or optical microscopy are not in scope of this work. An interested reader is referred to [17] or [18], where is inter alia brief state of the art of these methods.

2.2.1 Modelling methods

Both geometrical and physics based methods require sorting of particle systems according to various criteria. The first one is a shape of particles (spherical, cylindrical, cubical) influencing mainly the number of parameters for description of particle position or movement. The second criterion represents mutual possible particle position (overlapping, non-overlapping) decisive for required volume fraction and repulsive or attractive forces between particles. A similar effect has a decision whether simulated system is composed of isolated particles with rare contact or most of particles are in contact. Such a system requires knowledge of mechanical stable states as well as particle packing problems. Another property is a type of particle distribution (random, regular) connected with time demands on a simulation. This preprocessing enables succesfull dealing with the main taks of boths methods: to create models with similar stastistical information.

The simplest algorithms for generation of "random" particle systems are the Simple Sequential Inhibition model (SSI) and Random Sequential Adsorption model (RSA), where particles are randomly and sequentaly placed into area of prescribed size. If another particle in a sequence overlap with any of already placed, this inclusion is discarded followed with a new trial. The stopping criterion used to be reaching required volume fraction connected with maximal number of successfully placed particles. Such systems are able to create domains with lower volume fractions. But works perfectly as a starting systems for further investigation. Detailed description with various modification can be found in [19].

More effective, from the packing posibilites point of view, are sedimentation algorithms and their modifications. Here for 3D aplications, a small set of initial particles are randomly generated and arranged usually on the bottom of the container. After this step next particles are sequentially added (dropped) into container and their motion follows principles of gravity until a stable system is reached. This process with addition of one particle is called drop-and-roll [20]. Contrary a mechanical contraction system [21] starts with simultaneously generated group of particles, but principles of their later motion are the same as in the previous work.

A group of Collective rearrangement algorithms improves the results achieved by the above methods, not only with regard to the maximum possible volume fraction and dense packings. The initial position of a given number of particles, which can overlap, can be created by adsorption or sedimentation methods. Then the entire system or just a part of it is released and the particles move or shrink their dimensions to obtain more advantageous schemes. The rearrangement can be done using different methods based on physical principles (molecular dynamics, spring systems, attractive and repulsive forces) or optmization heuristic techniques with artificial schemes. For a more detailed description of methods an interested reader is reffered to [17] or [18]. Following paragraphs offer brief set of historical contributions that have a direct impact on algorithms utilized in this work.

Jodrey-Tory [22] algorithm, in original form, divides particles (spheres) into two parts: the first rigid one, which defines the minimal distance of a pair of particles and the second, soft or deforming one, representing a repulsive core. In the course of the algorithm, the external part is reduced until only the inner part remained, and the system reached dense packing. The initial complex geometric scheme was later replaced by a simple and efficient force-biased algorithm [23]. This was later extended for generation of non-spherical particles. Such an algorithm represents an optimization method where the goal is to minimized energy of a system with reduction of outer/inner particle parts.

Molecular dynamics, as an algorithm for generation of random systems or simulation of particles behaviour, was invented at the beginning of seventies [24]. Here, Newton's motion laws were aplicated to every single member of a set. Particles moved based on artificial attractive forces. There has to be implementation of contact algorithms in order to prevent particle overlapping.

When we are dealing with dynamics and particles that work in whole process as individuals, we have to mention the Discrete (or distinct) Element Method (DEM). Its origin date back to the early eighties, and was used to analyze rock-mechanical problems [25]. Now it works as a universal numerical method for solid mechanics when solving more than just problems with dynamical processes. Therefore, it is a core of both commercial and open-source softwares [26]. The DEM principles were used even for generation of particle domains with Wang tiling [27].

Nevertheless, this work utilizes molecular dynamics for generation of particle domains, namely the modified Lubachevsky-Stillinger [28], [29]. Here, in the beginning of the whole process, particles are randomly thrown into a container with originally periodic boundary conditions. As a next step, particles are assigned with velocity vectors. After releasing particles move, grow up and collide with both walls and each other until the stopping criterion is reached.

2.2.2 Hard packing of monodisperse particles

Placement of hard particles within Wang Tile/Cube is limited via type of a packing problem. In preprocessing we need to decide how many particle of given radii are able to be placed into rectangular tiles or tile parts with specific dimension in order to be below maximal values of given particle packing states. Fundamental for solution of this problem is knowledge of traditional packing algorithms such as packing of hard particles into an arbitrary shaped container, ordered and disordered packing issues like random loose or close packing.

A packing problem was presented as 18th out of 23 mathematical problems by David Hilbert in 1900. He asked: How one can arrange most densely in space an infinite number of equal solids of given form that is how can one so fit them together that the ratio of the filled to the unfilled space may be as great as possible? [30]. But the earliest studies on the packing problem appeared already in 1661 within the Kepler Conjecture – the problem of maximum packing density of identical spheres.

A classification of packing problems (dense packing problems) can be according to various criteria. The first one is a shape of rigid particles - disc, rectangles, spheres, spheroids etc. Next criterion is an equality of investigated particles, whether they are equal or unequal. However, in the majority of contributions we meet concepts of ordered and disordered packing.

Ordered packing can be achieved with arranging the particles in regular structures using e.g. lattices. Disordered packing can be divided into two groups – random close packing and random loose packing. Random close packing should occur when the packing contains no statistically significant order and any decrease in density from this state leads to ensembles of particles which need not to be closed packed. This definition is for hard disc and hard spheres. We can achieve this state experimentally by shaking and vibrating of a container with particles. Random loose packing is then defined as a state where each particle is touching several others [31].

Packing of spheres and circles with equal radii has been studied for many years. Scientist used them to explain and understand structural and kinetic matters. Johannes Kepler in already mentioned Kepler Conjecture in 1661 believed, that the face-centred cubic lattice is the densest packing structure for spheres. A packing density was in this case $\pi / 18 \approx 0.7405$. The same values stated Berryman in [31]. This value for ordered close packing was proved by Hales in [32]. Ordered close packing of hard spheres occurs when the packing fraction is about 0.7405. For discs in 2D the determinate packing fraction is approximately 0.9069. A packing fraction of random close packing occurs with a fraction around 0.64 and for random loose packing of spheres the value is 0.60. Similar values are reported for other important sphere densities by Weitz [33].

For Wang tile generation more important are results in a field of particle packing into arbitrary, rectangular or even squared containers. Before particles are assigned to appropriate tile or tile size, one has to know the possibility of placement the given number of inclusions into a tile of certain size. This issue goes to the forefront especially with a set where each tile include different number of particles. Considering particle system with wang tiling, see following sections. Here, any of particle is able to cross border with a part of its surface. But extreme position of particle is given by range of possible movement of its centre. Therefore we still face the problem how to place *n* circles into a square. This problem is equivalent to the problem of scattering *n* points in a unit square such as the minimum distance between any two-points becomes as large as possible. This task for 2-9 discs was already solved in 1964 [34]. For 10 discs Schlüter [35]find the best solution that was later confirmed. In Fig. 2-4 are shown solutions for some number of circles up to 20 [36]. Investigation of more discs within square can be found in [37], but for the purpose of this work the packing of maximally 20 circles sufficient. A reader who is interested also in packing of polydisperse particles in a square is referred to [38], [39] or [40].

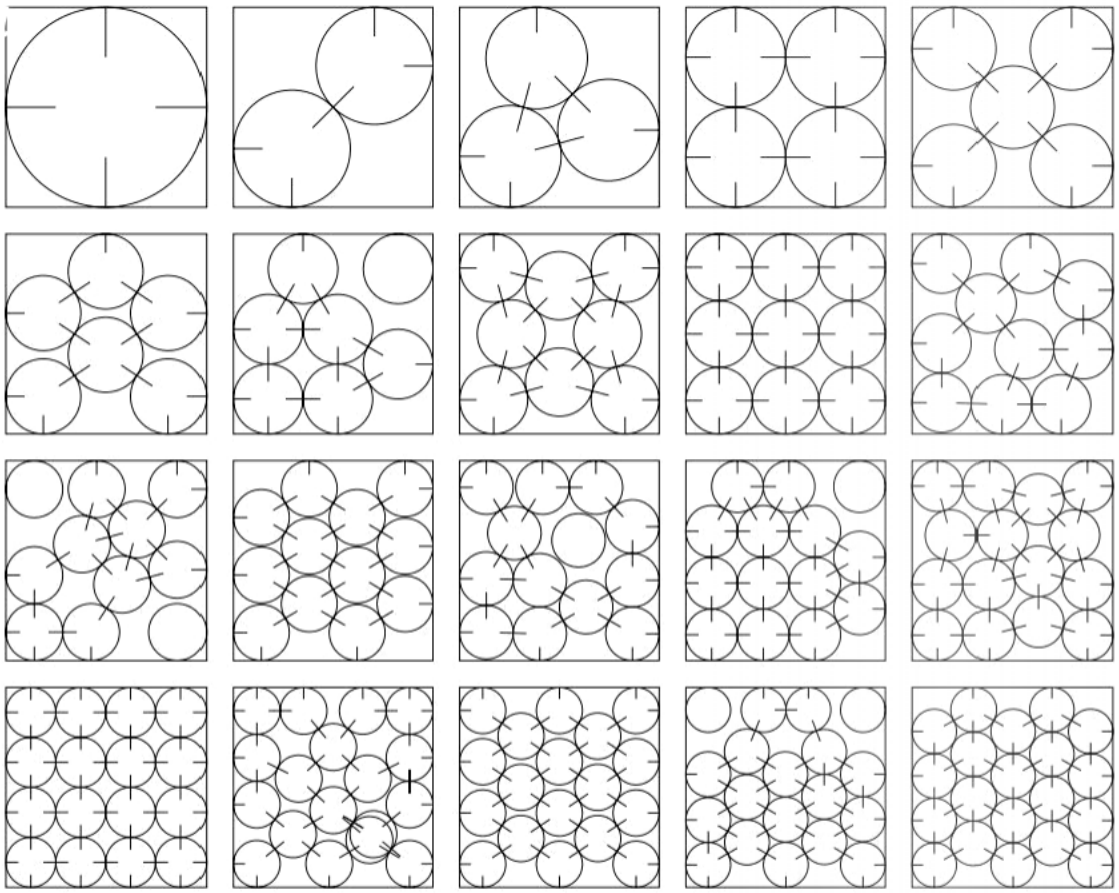

Fig. 2-4 Best known packing of equalsized circles in a square [36]

2.3 Microstructure characterization

One of the main goals of this thesis is to create a Wang tile based microstructure which mimics the statistical description of a reference domain. In order to successfully accomplish this task, we introduce a new concept for tile boundary conditions. First we have to put basis of microstructure characterization before any further investigation.

When facing random heterogeneous materials problems we use to deal with a set of representatives (micrographs) which are different from the microscopic detail point of view but identical in macroscopic detail. Such a system of realizations, if is large enough, forms the ensamble or sample space S, for detailed description see [41] or [42]. Considering an individual sample of this space α which occupies a spatial (possibly infinitely large) domain Ω, then the probability of finding a realization α in space S is $p(\alpha)$. With this concept all spatial descriptors are understood as expectations of chosen n-point microstructural functions. We consider, for simplicity and with emphasis on investigated material microstructures in this work, only two dimensional space, two phase medium and two-point probability functions. Another assumption leading to efficient computing of spatial descriptors is the statistical uniformity or homogeneity of a microstructure. With this hypothesis the ensamble average of any functions remains the same with any translation of the coordinate system within domain Ω. With this simplification we omit the calculation of probability of realization α in space S. Moreover we consider the ergodic hypothesis. Here the ensamble average coincides with spacial domain average over Ω. But this works only if domain Ω is formaly infinite. Such a premision is fulfilled when there is a periodic extension of smaller domain. In general stochastic Wang tiling process is able to create periodically repeated regions.

As stated above we focuse in this constribution on two-point probality functions which indicates probability of finding two-points in given phase, specifficaly the one occupied by particles. Therefore, this descriptor can be designated as two-point autocorellation function [43]. Detailed characterization of other lower order descriptors (Lineal path, Cluster function) as well as those of higher order (3 point probability function) can be found in [1]. When considering hypothesis of ergodicity together with statistical homogeneity, the two-point probability function has following form:

$$S_{rs}(\mathbf{y}) = \frac{1}{|\Omega|} \int_{\Omega} \chi_r(\mathbf{x}) \chi_s(\mathbf{x}+\mathbf{y}) \, \mathrm{d}\mathbf{x}, \tag{2.1}$$

where r and s designate phases. We can easily observe that for y=0 the probality of finding two-points merge into one point probability function and corresponds to the volume fraction of the sample. When the second point is theoretically in infinite distance, there is no corrrelation of investigated points and the equation is reduced to combined probability of two independent phenomena.

3 Tilings[2]

This section introduces and describes algorithm for generation of Wang tile set with emphasis on general particle motion and tile boundary conditions. Proposed improvements and methods are later compared on several artificial microstructures in order to find the best approach for tasks of random heterogeneous microstructures modelling and reconstruction.

3.1 Molecular dynamics

The main parts of dynamics that occur during the algorithm are collisions. They are of two types, bounce from the tile edges and rebounds of discs. To ensure proper movement involving boundary conditions of Wang tiles, it is necessary to determine when these phenomena occur.

The earliest time of bounce Δt_e depends on the current discs position and a velocity vector of each particle. Calculation of Δt_e in two dimensions is according to following equation:

$$\Delta \boldsymbol{t_e} = \boldsymbol{min}\left\{-\boldsymbol{dx_{i,ri}}/\boldsymbol{vx_i}\,;\, \boldsymbol{dx_{i,le}}/\boldsymbol{vx_i}\,;\, -\boldsymbol{dz_{i,lo}}/\boldsymbol{vz_i}\,;\, \boldsymbol{dz_{i,up}}/\boldsymbol{vz_i}\right\}, \tag{3.1}$$

where Δt_e is the earliest time of reflection since the previous event or time step, $dx_{i,ri}$, $dx_{i,le}$, $dz_{i,lo}$, $dz_{i,up}$ are distances of a disc centre to the appropriate borders. Velocities of the *i-th* disc in *x* and *z* directions are labelled with vx_i and vz_i respectively. The same principle is for bounce in 3D where equation (3.1) is extended by the velocities and edges in the third dimension.

The earliest time of the second type of a collision, disc rebounds, can be determined as time from certain moment until disc centres will be in the distance of their mutual radii. Such a time can be defined with the following formulas:

$$(\boldsymbol{x_j} - \boldsymbol{x_i})^2 + (\boldsymbol{z_j} - \boldsymbol{z_i})^2 = (\boldsymbol{r_j} + \boldsymbol{r_i})^2 \tag{3.2}$$

$$\boldsymbol{x_i} = \boldsymbol{x_i^t} + \boldsymbol{vx_i^t} \cdot \Delta \boldsymbol{t_c}, \qquad \boldsymbol{z_i} = \boldsymbol{z_i^t} + \boldsymbol{vz_i^t} \cdot \Delta \boldsymbol{t_c}, \qquad \boldsymbol{r_i} = \boldsymbol{r_i^t} + \boldsymbol{dr_i} \cdot \Delta \boldsymbol{t_c}, \tag{3.3), (3.4), (3.5}$$

$$\boldsymbol{x_j} = \boldsymbol{x_j^t} + \boldsymbol{vx_j^t} \cdot \Delta \boldsymbol{t_c}, \qquad \boldsymbol{z_j} = \boldsymbol{z_j^t} + \boldsymbol{vz_j^t} \cdot \Delta \boldsymbol{t_c}, \qquad \boldsymbol{r_j} = \boldsymbol{r_j^t} + \boldsymbol{dr_j} \cdot \Delta \boldsymbol{t_c}, \tag{3.6), (3.7), (3.8}$$

where $x_i,\ y_i,\ x_j,\ y_j$ are collision disc coordinates, $x_i^t,\ y_i^t,\ x_j^t,\ y_j^t$ disc coordinates and $vx_i^t,\ vy_i^t,\ vx_j^t,\ vy_j^t$ disc velocities at time ***t***; r_i, r_j, r_i^t, r_j^t are collision discs radii. The growth rate of particles is determined by a variable dr and Δt_c is time elapsed since time t. Next collision time is in this case designated as minimum of real positive roots of equation (3.2). As for disc collisions in 3D the equation (3.2) includes difference of spheres' coordinates also in *y* direction. Nevertheless, (3.2) still remains a square function. In case of rebound a change of velocity vector follows a law of impact and rebound.

[2] Parts of this chapter are reproduced from author's contributions: [I], [II], [IV], [V]

3.2 Boundary conditions

This subsection present three types of boundary conditions for particle motion while using molecular dynamics for Wang tiles generation. The new Volume and Adaptive walls approaches enrich the traditional concept of periodic conditions. The main goal of new improvements is to reduce unwanted periodicity artefacts while keeping compatibility of tiles on both edges and corners.

3.2.1 Periodic Unit Cell

The concept of a periodic unit cell is based on consideration that the final medium is stacked with identical cells which on the edges meets the conditions of periodicity. The shape of such cells in two dimensions can be regular polygons, mostly squares and rectangles or crystal lattices of given materials. In 3D cubes, blocks and appropriate crystals represent periodic unit cell can be used in accordance to a characteristic shape of material.

If the reconstructed heterogeneous medium has been already periodic, a size and distribution of particles within a unit cell corresponds to the material grid. When the reconstructed heterogeneous composite exhibits a random distribution of particles, parameters of the PUC must be set according to prescriptions that satisfy statistical conditions of the RVE. This basically defines an optimization issues.

The concept of a periodic unit cell establishes periodic boundary conditions on the edges of the cell. From the molecular dynamics point of view, this concept is based on the main central cell surrounded by its nine images that guarantee periodic boundary conditions Fig. 3-5.

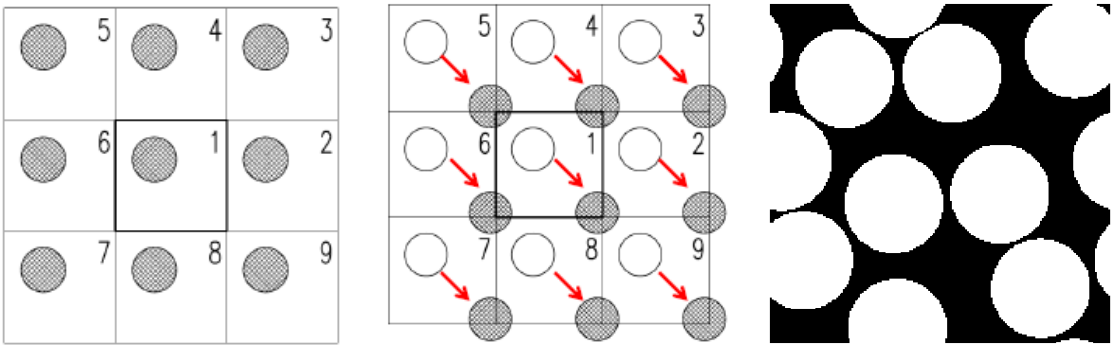

Fig. 3-5 Molecular dynamics and boundary conditions for the PUC concept

If any particle crosses with its surface any of vertical or horizontal tile edge, the copy of the same particle appears on the opposite side. The particle movement continuous until particle centre reaches the edge and rebound or any other inclusion force the original one to change the velocity vector back to the tile. The similar algorithm works for three dimensional problems, only edges in the definition above are changed to walls of the cube. Note that minimal set of stochastic Wang tiles include tiles with the same codes on opposite sites, which can be designated as PUCs.

3.2.2 Periodicity and tiling artefacts

In this contribution the principles of stochastic tiling build bases for random heterogeneous material models. The nature of classical Wang tiles with codes on edges together with application on material domains composed of arbitrary shaped particles within matrix result to corner problem. If there has to be ensured compatibility of tiling on edges, any particle cannot even touch the corner of tile. Discussed problem can be solved in different ways.

The first solution enables to have tiles directly without particles in corners. But such approach head to periodicity artefacts underlining tiling grid of composed space. In [44] Lagae and Dutré introduced a concept of corner tiles as an alternative for Wang tiling. Corner tiles take the form of squares with coloured corners in comparison with Wang tiles where colours are assigned to edges. This method enables to stack a final domain with respect to every of eight neighbour tiles. There is need to say that within our application the problem with dead space where particle centres are forbidden to be located has just moved to centres of tile edges. In general the problem is caused by the nature of molecular dynamics and principles of both Wang and corner tiling, Fig. 3-6.

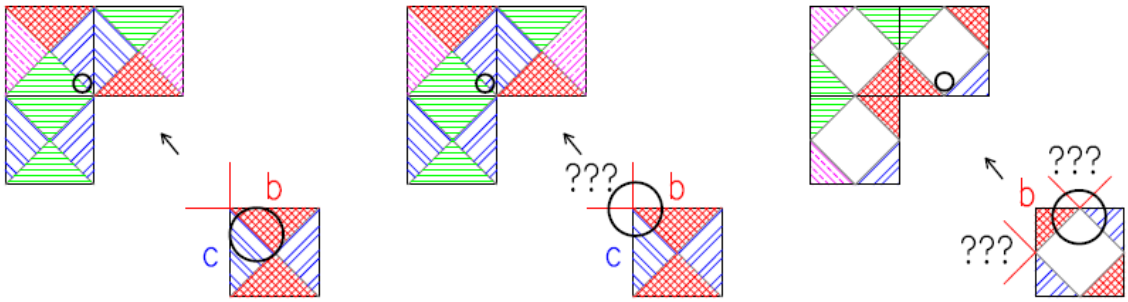

Fig. 3-6 Corner problem
a) Wang tiles without corner particles – dead spaces and grid periodicity,
b) Wang tiles with corner particle – no corner information = overlaps,
c) Corner tiles with central particle – no central infromation = overlaps
(hatch is only for ilustration)

While set of eight tiles is generated, particles grow, collide with each other and bounce of the tile walls. Considering the algorithm that prevent particle crossing a tile edge final plane will be composed using eight different tiles. With such simplification whole tiling is ordered and exhibits grid periodicity because there is no interaction between tiles. If particles can leave the tile during motion, it has to be copied into all prototiles with possibility of shared edge within tiled material domain. This approach leads to unwanted variation of volume fraction. We seek the algorithm modification which allows interference of particles to other tiles with no changes in a volume fraction. The first proposed modification is to divide each Wang tile into border and central parts – Wang tiling with Volume Walls. The second approach uses deformation of tile edges and creates a puzzle system – Wang tiling with Adaptive Walls.

3.2.3 Stochastic Wang tilings – Volume Walls

The situation with boundary conditions for molecular dynamics gets difficult considering material with hard particles together with the Wang tiling approach. When particle tends to leave the mother tile through the edge with a certain code, it has to be copied to every edge designated with the same code on any other tile in order to meet the requirements of the stochastic tiling. Such a permission leads to unwanted increasing of overall volume fractions. Therefore we present a concept with Volume Walls (VW), where volume fraction of the tile set remains the same over the whole process.

In the beginning of the generation, before particle centres are thrown into tiles, each tile is divided into central and border parts of certain volume – Volume Wall (VW). The width of the VW is equal to the diameter of the largest particle in a model. The height of the VW equals to the size of a tile edge reduced by diameter of the largest particle in a set. One half of the VW is inside the tile, the other is outside and physically belongs to the neighbour tile in a final domain, Fig 3-7. This division defines corner parts of a tile – dead spaces – where particle centre can never go to.

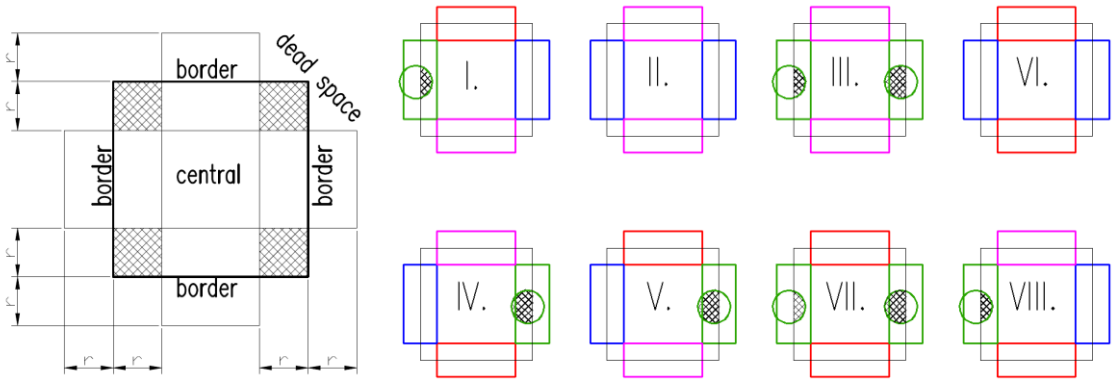

Fig. 3-7 Division of Wang tile with Volume Walls
Wang tile set W8/2-2 with Volume Walls with one border inclusion

The number of particles within border and central parts usually follows the ratio of its areas and prescribed volume fractions. The border parts have the same areas. Therefore the number of particles within these parts should be the same, no matter of the code, to avoid unwanted cluster artefacts in the final microstructure. This assumption works fine for tilings with the same number of inclusions in tiles. Even though there are rigid barriers between the tile parts, central particles can collide with the border ones. The border are valid for their centres, not for their surfaces. The rebound occurs only when the particle centre reaches the barrier. In the Fig. 3-8 there is a set of tiles for 2D application with one particle inside each VW and 3 individuals inside the central parts. The extension to 3D wang tile cubes with VW is straightforward, Fig. 3-8 right.

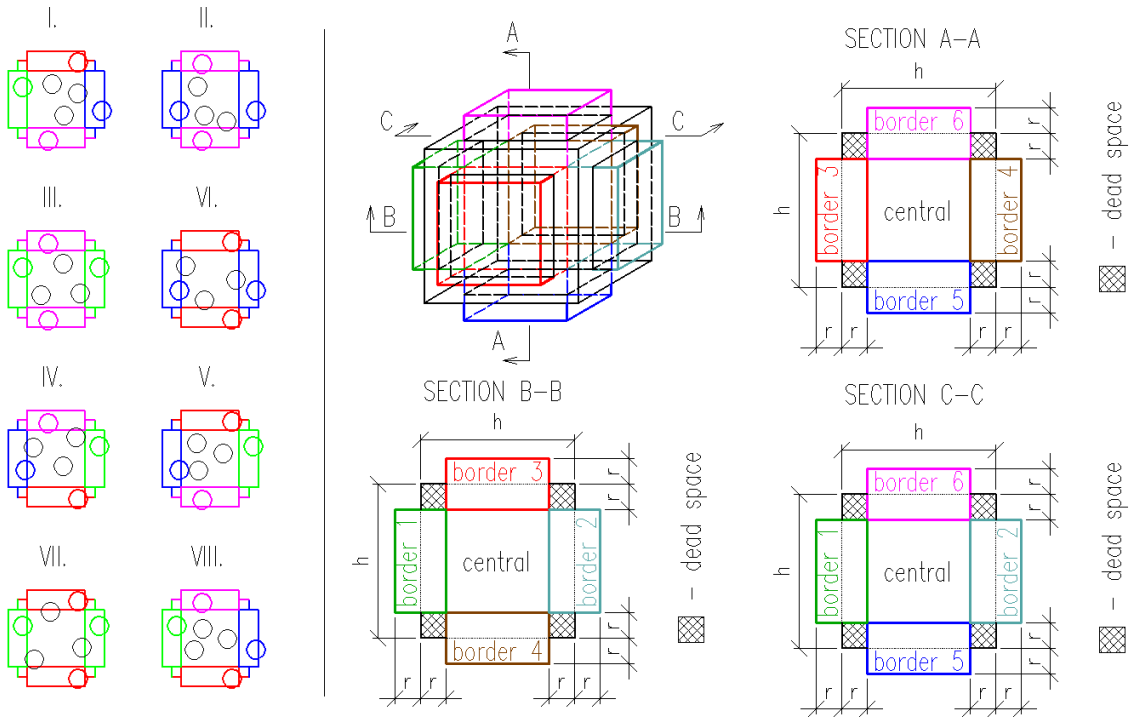

Fig. 3-8 Wang tiling with volume walls - VW:
Left – 2D set, Right – division of one 3D tile into appropriate parts

Note the corner parts, where particle centres never get to. This modification prevents copying of particles to the tile which has no common boundary part with the master one. If there is no dead space, particle leaving tile through the corner finds its copies all over the set. Aforementioned state is called corner problem, which might be solved in general case with corner tiles [44]. Unfortunately corner tiling do not fit to our case when the tile set is generated via molecular dynamics. The nature of the algorithm only removes the problem to the middle of tile edges.

3.2.4 Stochastic Wang tilings – Adaptive Walls

Random heterogeneous material domains generated via concept of the PUCs consist of copies of just one tile, which brings great periodicity number. The Wang tiling method with Volume Walls reduces significantly periodicity of the domain due to the stochastic tiling based on set of different tiles. Notwithstanding this success, still parts of tiles corresponding to the number of different codes on edges cause artificial periodicity artefacts. These artefacts get more significant with higher volume fraction of the domain.

The main task for the improvement of tile sets generated via molecular dynamics is how to keep the compatibility of tiles without repetition of tile parts. One of the solutions that fulfil this condition is to prevent any particle transition across the tile edge. Such a system leads to material domains composed of independent blocks forming lattice of vertical and horizontal lines without any particle. Contrary, a method similar to the puzzle system seems promising.

Consider a typical set of eight Wang tiles where each tile edge is designated with only one of four colours according to the principle of stochastic tiling. In the next step particle centres are sequentially thrown into tiles related to the required volume fractions of composed heterogeneous material. Each particle centre is equipped with a random velocity vector and a growth rate based on the final particle radii and time steps of simulation duration. Once the process begins particles move and collide with each other and particle centres bound of the tile walls. Graphic form of tile borders changes in time with respect to following rules.

When particle contour leaves the tile, appropriate edge copies this contour. The particle centre reaches original walls, rebounds and goes back to tile. The tile edge adapts to particle contour until whole particle is inside the tile, Fig. 3-9. In order to keep compatibility of tiling, adaptive boundaries have to be the same on every tile edge designated with the same colour.

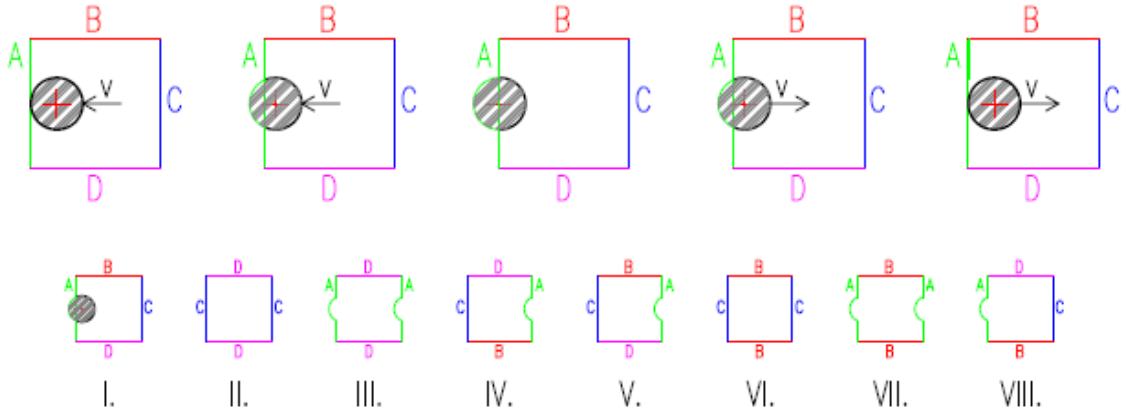

Fig. 3-9 Wang tiling with Adaptive Walls – AW
Top – principles of wall modifiation,
Bottom – Wang Tile set W8/2-2 with one master and other slave tiles

A similar process runs when particle simultaneously reach two corner edges or interferes diagonal tile (of tiled area), Fig. 3-10. There is a master tile where the leaving particle originally belongs. The edges adaptation of this tile manage all other tiles in set in terms of tiling compatibility. The modification of edges on slave tiles could be divided into three steps. Within the first step the shape of all edges, designated with the same colour as modified master tile walls, are unified. In the next step a corner deformation of a diagonal tile (in final tiling) is copied to all tiles. The most critical issue for proper modification of boundaries is to find all possible neighbour tilling of the master tile. In the last step corner deformation is copied to opposite side of each tile (either horizontal or vertical but the same for all tiles). This modification server inter alia for reduction of dead spaces. Unfortunately, there is still a bit of space without any particle – small closed corners occurring in half of tile set, see Fig. 3-10 the third step tiles IV., VI., VII., and VIII.

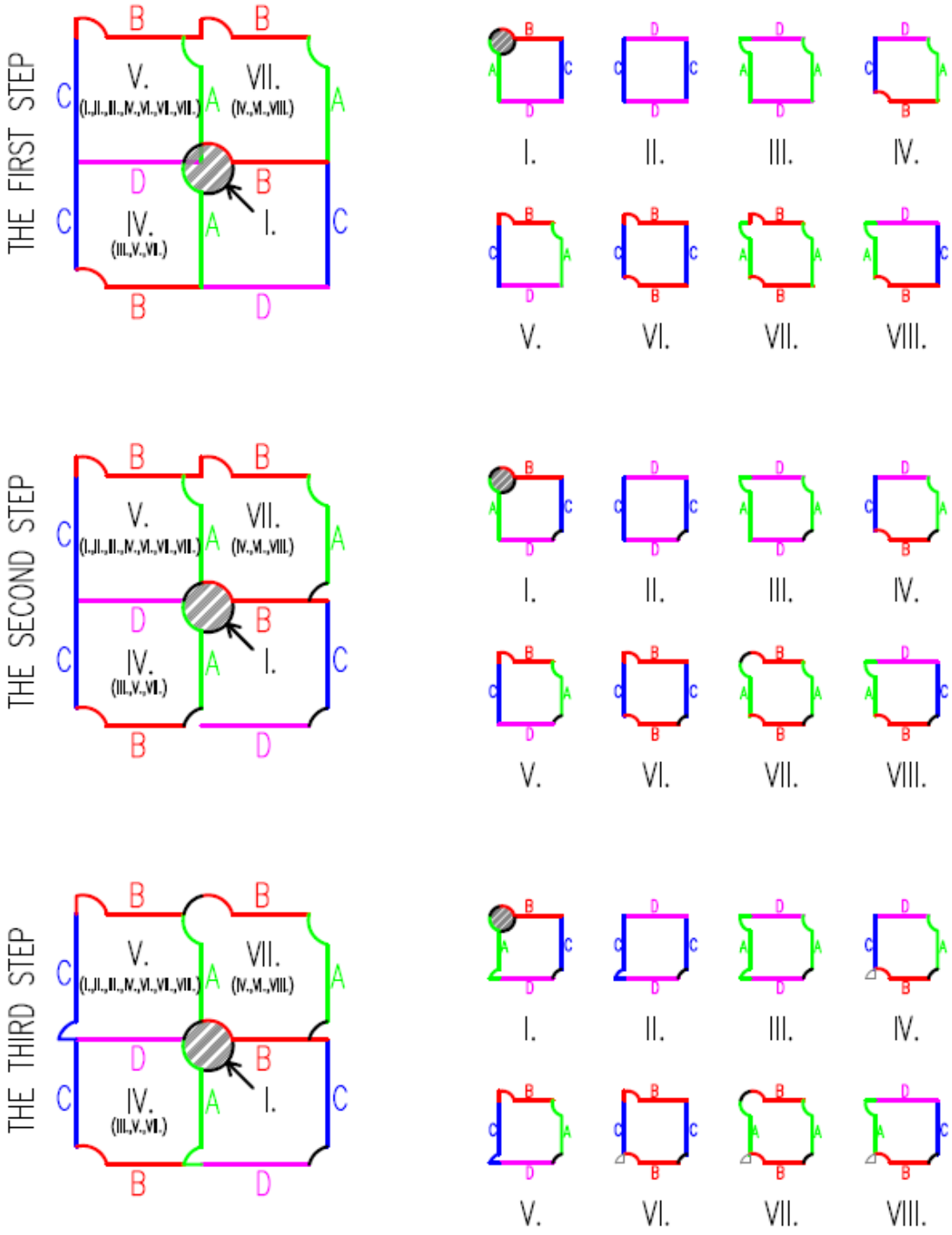

Fig. 3-10 Adaptive Walls – corner particle, algorithm of tile edges modification

The tiling then represents a puzzle system. In fact the algorithm considers eight master Wang tiles surrounded with all possible combination of neighbour slave tiles to affect changes caused by trespassed particle and to ensure compatibility of tiling, Fig. 3-11. The phenomena of particle-particle and particle-tile boundary collision for all these combinations are calculated simultaneously.

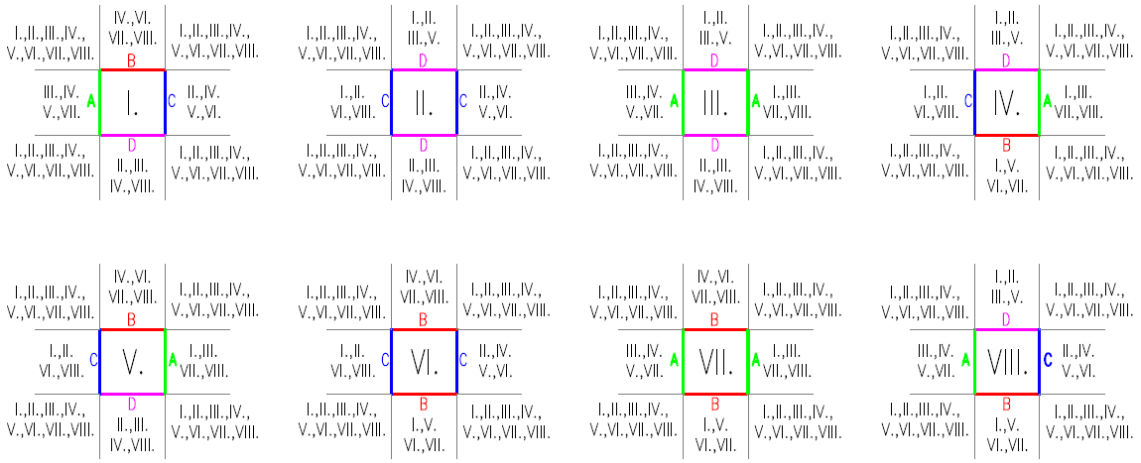

Fig. 3-11 Adaptive Walls – combinations of master and slave tiles

Adaptive walls of tiles where trespassing particle is trying to get to are dynamic in order to keep interacting system. If there occurs a collision of either concave or convex adapted tile wall with particle inside the tile, velocity vectors of these objects (as well as original particle which caused a deformation of tiles walls) are calculated according to the Momentum conservation law and the Conservation of the energy law. The entire process of the Wang tile set generation is terminated when particles grow to the desired size. The extension to the 3D space is straightforward. The modification of edges is transferred to the walls, Fig 3-12.

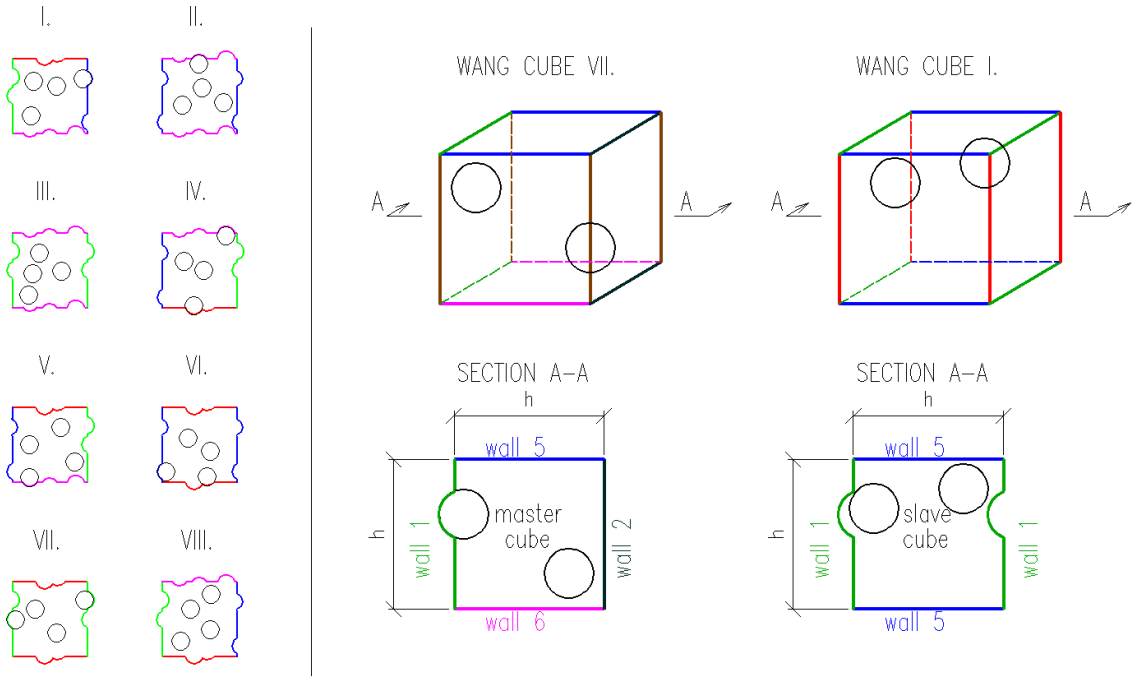

Fig. 3-12 Wang tiling with Adaptive Walls for 2D and 3D applications
Left – 2D set, Right – visualization of AW algorithm in 3D (master cube + one slave cube)

3.2.5 Comparison

This subchapter aims at comparison of the Wang tiling process with the concept of the PUC. We show the contrast in both visual and statistical way using lower order descriptor, namely the two-point probability function. I has to be noted that at this stage of research structures are not optimized in term of complete statistical information, we only focus on reduction of significant accompanying phenomenon – secondary peaks – applying different boundary conditions.

3.2.5.1 Monodisperse 2D sets

Every single example consists of four randomly generated samples: an original one with required properties and three tilings assembled by tiles with the PUC, the VW and the AW boundary conditions. The lattice of eight by eight tiles represents every tiled microstructure. The sequence of tiles is similar for each tiling within one comparable example. All tiles from the basic set in Wang tiling samples have the same number in a final domain. Only one group of samples for each example are shown for the purposes of visual comparison. The first artificial modelled microstructures contain equal sized hard discs of radius 15 pixels. We have here domains of three different particle volume fractions: 0.2, 0.4, and 0,6. The tile edge size is 100 pixels, in accordance with dynamic algorithm definition from the previous section of this work. The numbers of particles in samples and/or tiles are summarized in Tab. 3-1. While number of particles in the PUCs and the Wang tiles with the AW corresponds proportionally to the overall volume fractions, the situation on tiles with the VW differs. If we consider two neighbour tiles with certain code/colour on edges, in the system with the VW particles in common border parts completely overlap. Therefore the real number of particles per the VW tile equals to the sum of inclusions in the central part and the half of inclusions in all four border parts. The following figure Fig. 3-13 shows all three modelled states.

Tab. 3-1: Settings for comparison of boundary conditions – monodisperse sets

Volume fraction app.	Method	Particles per tile	Total number of tiles	Total number of particles
0.2	sample	--	--	256
	PUC	4	64	256
	VW	5	64	256
	AW	4	64	256
0.4	sample	--	--	512
	PUC	8	64	512
	VW	11	64	512
	AW	4	64	512
0.6	sample	--	--	768
	PUC	12	64	768
	VW	17	64	768
	AW	12	64	768

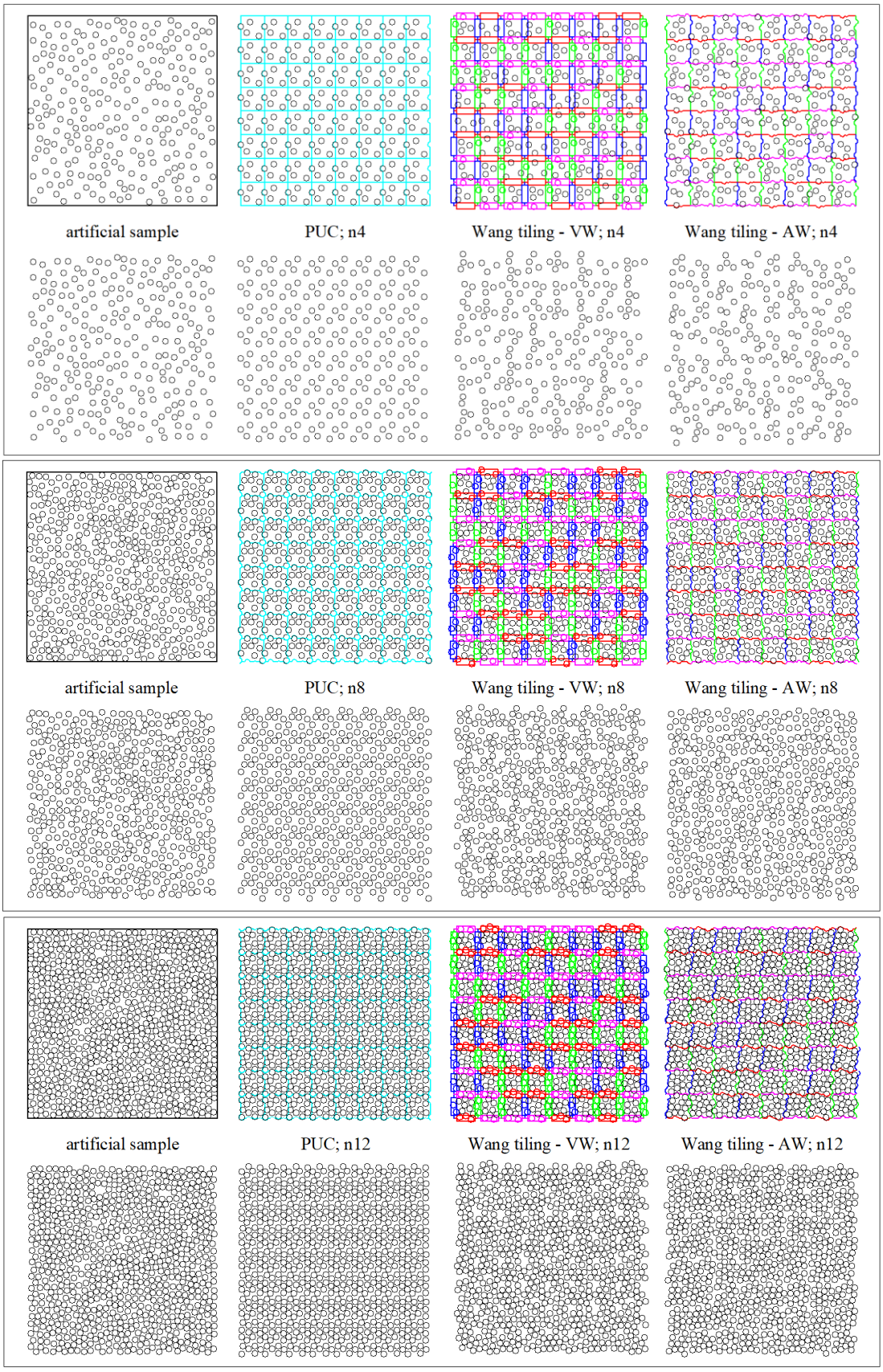

Fig. 3-13 Generated sets with monodisperse particles
Artificial sample; the PUC tiling; the Wang tilings W8/2-2 Volume Walls, Adaptive Walls.
Upper frame – 4 particles/tile; middle – 8 particles/tile, lower – 12 particles/tile

The visual evaluation focuses on the artificial periodicity artefacts in line with the task of this contribution. We briefly comment the results for each algorithm and point out problems. We are aware of the distortion due to the number of realizations for the visual comparison. Despite this fact, with these tests we gain rough insight into the behaviour of the algorithms and its benefits and disadvantages. The first column of samples represents initial domain with random distribution of particles without significant particle clusters or regular lattice.

On the other hand, samples in the second column exhibit clearly visible lattice of repeating areas given by the nature of the PUC concept. This phenomenon is supported by the same size of tile for all samples of any volume fractions. The PUC for the last case includes twelve particles whereas for the first one only four. Without input changes, representing tile size and number of particles within, the PUC approach cannot compete with Wang tiling in terms of visual results. Contrary, the lower number of particles in motion leads to savings of computer demands due to the probability of particle collisions. Such an assumption prefers the PUC (4 particles needed for the first example) from the VW (26) and the AW (32).

The concept of Wang tiles with the VW seems promising, especially for examples with a lower volume fraction. Generally, if we want to reduce periodically repeating areas, we have to minimize the number of particles in the border parts of tiles. The best way is to set this number to zero. Such a limit value is possible in fact only for cases with very low volume fractions. If similar consideration was applied to the second analysed example of particle fraction 0.4, we would have a system with visible lattice of particle-free regions. Instead, we assigned particles to certain tile parts according to its area ratio. Despite the restriction, dead spaces in final tiling arises with increasing sum of particles as a consequence of the algorithm nature.

The last group of tilings with the AW exhibits the greatest visual match with the artificial samples. The visible repetition is primarily given by the number of tiles in the basic set, since each tile is completely different. The only exception represent tile corners. If there is a master tile where any particle finds its position in the corner, the space in all other corners over the whole tile set remain free until any other particle fill this area. This result of the game of probabilities is more visible in samples with higher volume fractions. Despite the increasing probability of filling, free corner spaces (if any) cannot hide between other places without particles. Contrary, dilution of artefacts is possible for domains with lower number of inclusion. Thus these reconstructions visually match more with random reference medium.

We evaluate the artificial periodicity artefacts also via microstructure statistical description. Special emphasis is placed on secondary peaks in two-point probability function plots. The graphic form of generated samples is divided into pixels, where number of pixels per tile edge equals to the size of tile. Pixels are designated with white colour if distance from their midpoint to the certain particle centre is lower than the appropriate radius, see Fig. 3-14 – 3-16. Therefore some particles may look incomplete.

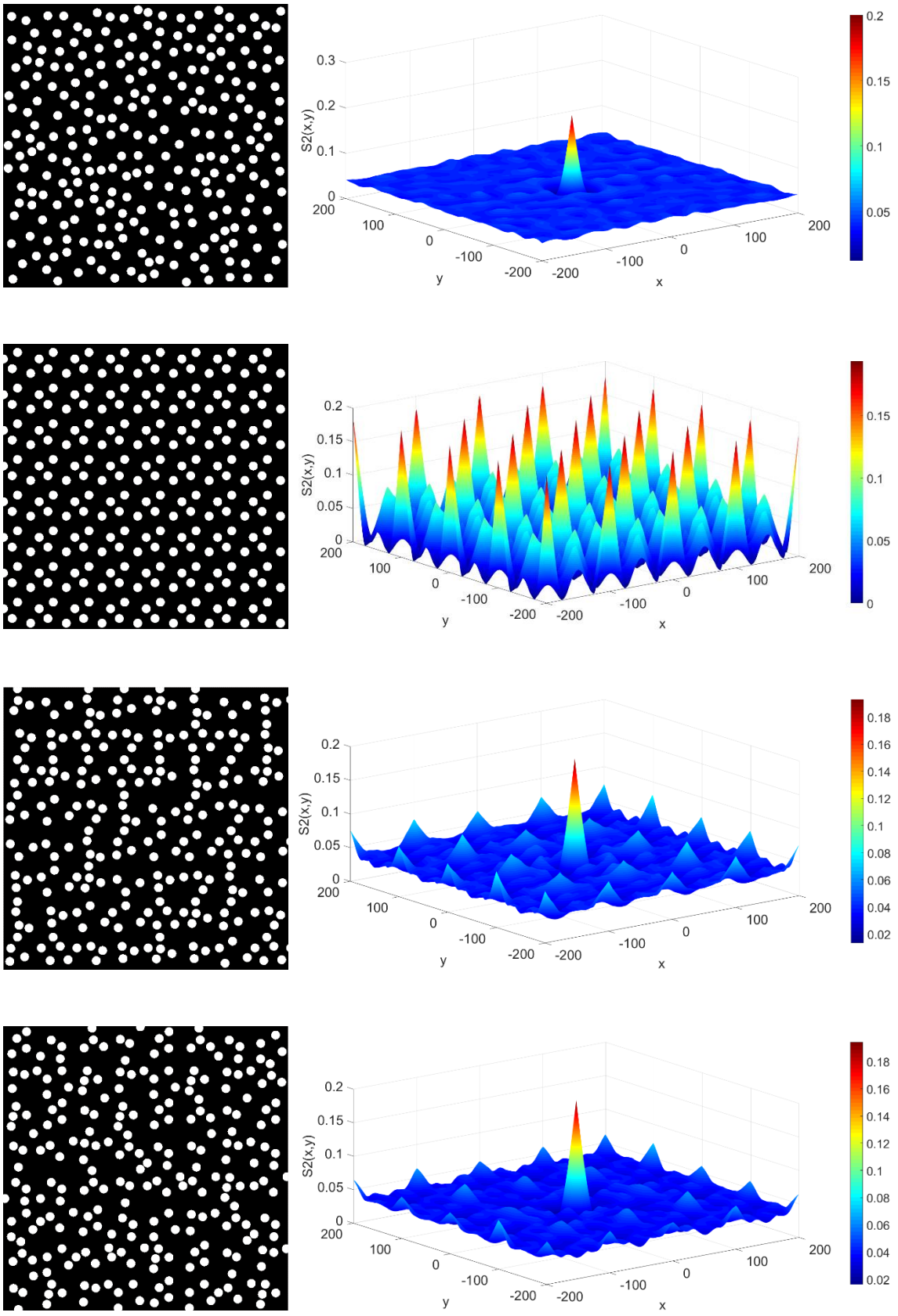

Fig. 3-14 Analysis of 2D monodisperse samples of volume fraction approximately 0.2 Systems from top to bottom: artificial sample, PUC, Wang tiling – VW, Wang tiling – AW. Right – one randomly chosen realization, Left – S2 function (average of all realizations).

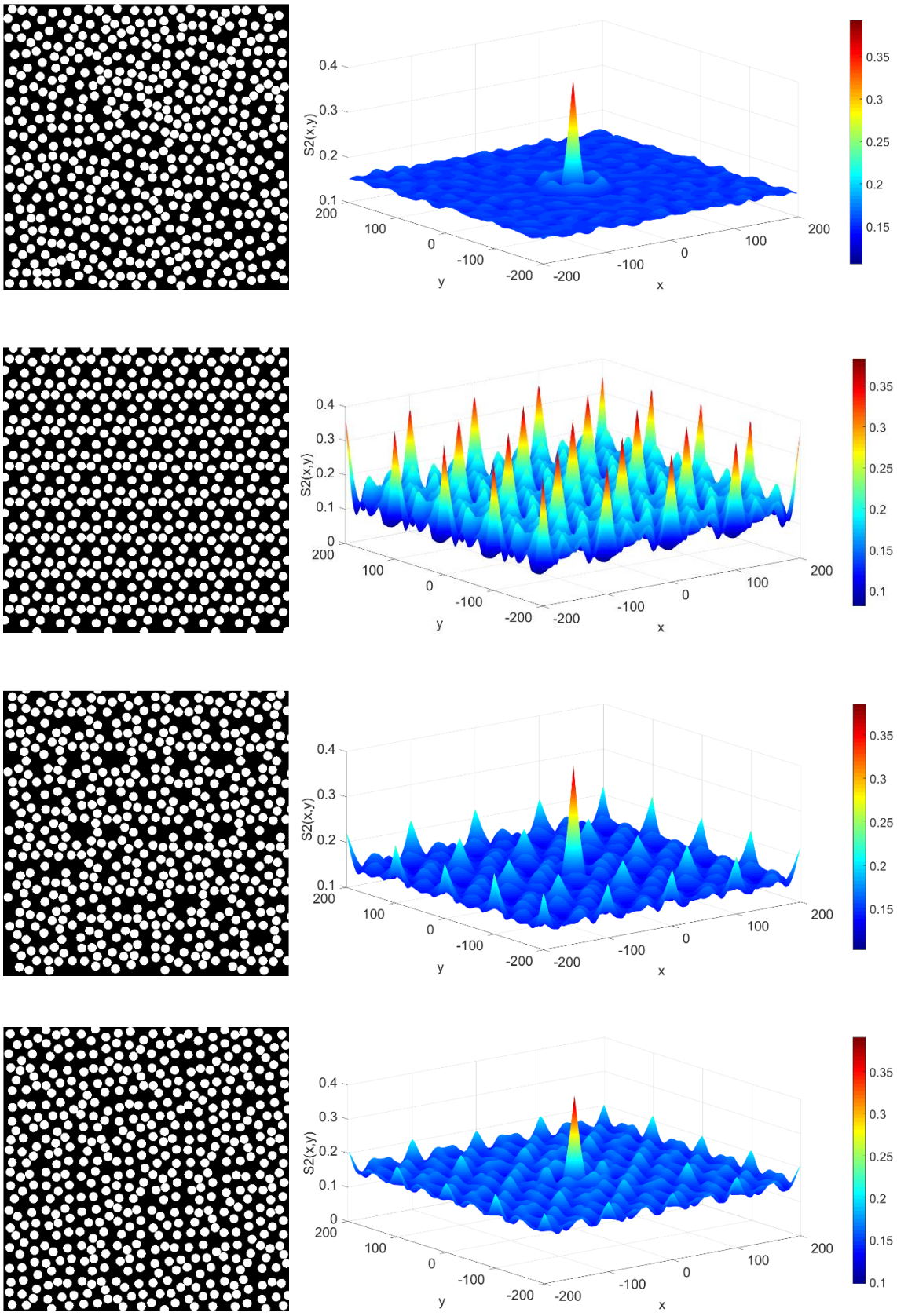

Fig. 3-15 Analysis of 2D monodisperse samples of volume fraction approximately 0.4 Systems from top to bottom: artificial sample, PUC, Wang tiling – VW, Wang tiling – AW. Right – one randomly chosen realization, Left – S2 function (average of all realizations).

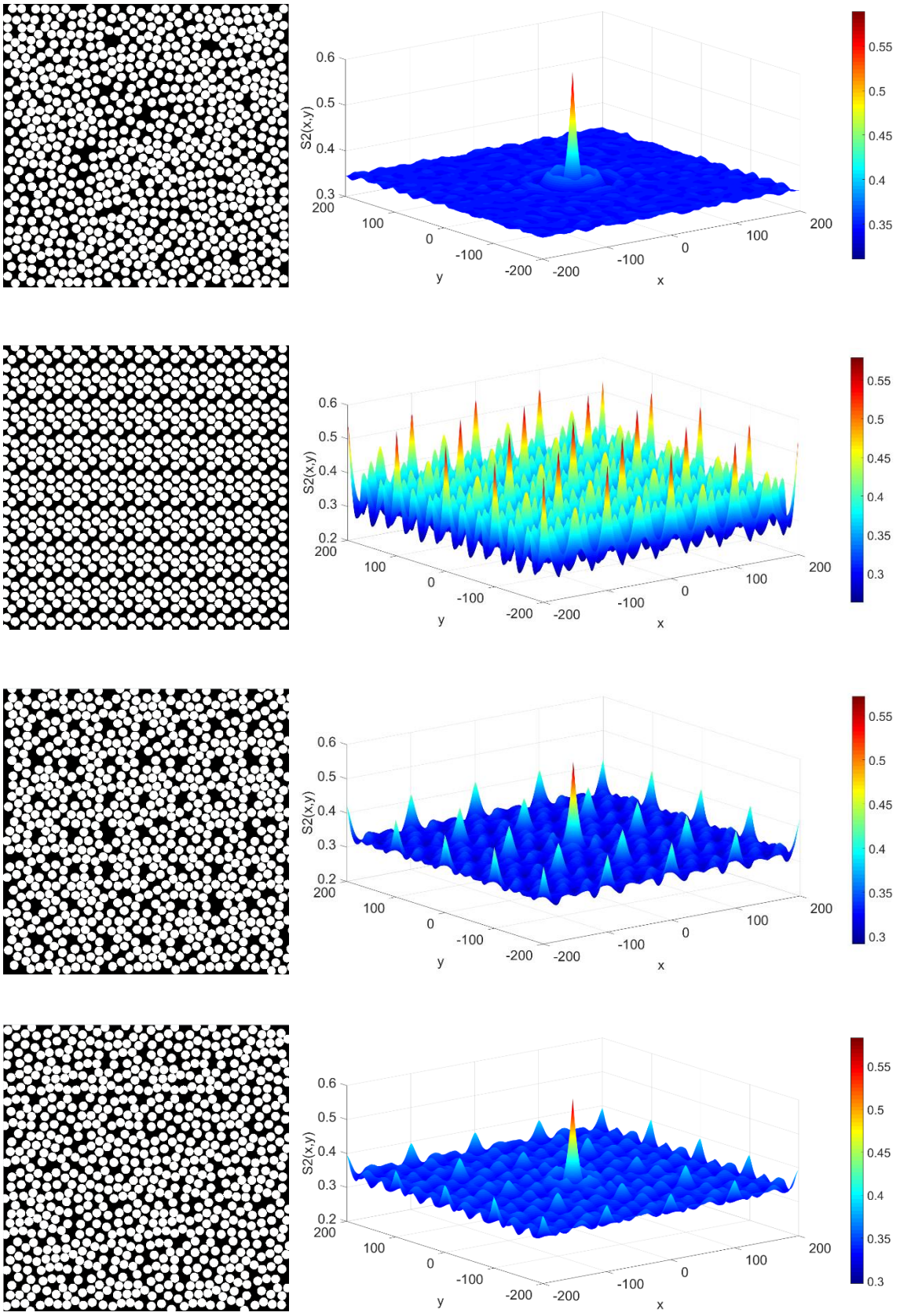

Fig. 3-16 Analysis of 2D monodisperse samples of volume fraction approximately 0.6
Systems from top to bottom: artificial sample, PUC, Wang tiling – VW, Wang tiling – AW.
Right – one randomly chosen realization, Left – S2 function (average of all realizations).

The principle when each particle has a general template was not implemented here due to the particle motion together with final random position. The range of statistical description is reduced to 400x400 points in order to keep results clear and simple. Long range dependencies give no information that would influence the assessment of observed artefacts. The two-point statistics for artificial sample and tiling made of the PUCs correspond to the binary representation of domains from Fig. 3-13, shown in left column. Whereas plotted results for Wang tiling represent average of five realization. The binary representation next to means one of the realizations and fits the microstructure in Fig. 3-13.

The word description of graphic results consider mainly the first and the group of secondary extremes complementing differences in methods of tiles generation. The highest value in every graph represents the volume fraction of certain sample in accordance with the description definition. The first extreme is the same for all samples due to the identical total number particles. However, the prescribed condition of volume fraction is met with an error given by the integer number of particles. Secondary extremes fully reflect the periodicity in the samples. There is no significant secondary peak in the first artificial samples, situation is different in tiled domains. If we look at the PUC system, here every particle in a cell repeats in main coordinate system in a distance of the tile size with the same probability. Tertiary and other extremes express the geometric relationship between the particles in one cell with the contribution of tile copies in diagonal direction.

The secondary peaks in domains based on the VW are caused mainly by two phenomena: the regular repetition of boundary particles and the usage of the same tiles. The occurrence probability of both situations is lower than for the PUC system. The first indicated factor does not affects the results of the samples with the AW. An oscillation around the squared volume fraction appears in every tested type of boundary condition as a consequence of the descriptor definition. The comparison in terms of the secondary and tertiary extremes in graphs of statistics is in favour of the AW system.

3.2.5.2 Polydisperse 2D sets

The algorithms for generation of the PUC and Wang tiles are capable to work with particles of different radii. Therefore another group of tested sets represent polydispersible material structures. The overall volume fraction remains the same as for the previous set, but inclusion are of two radii. Their relative volume ratio is approximately 60 percent for the first radius of 12.5 pixels and 40 percent for particles of radius 7.5 pixels. The other settings of both material domains and algorithms remain unchanged. The visualization of tilings and appropriate microstructures without tile edges are shown in Fig. 3-17. The sample labels are supplemented with the number of particles of given radii in each tile.

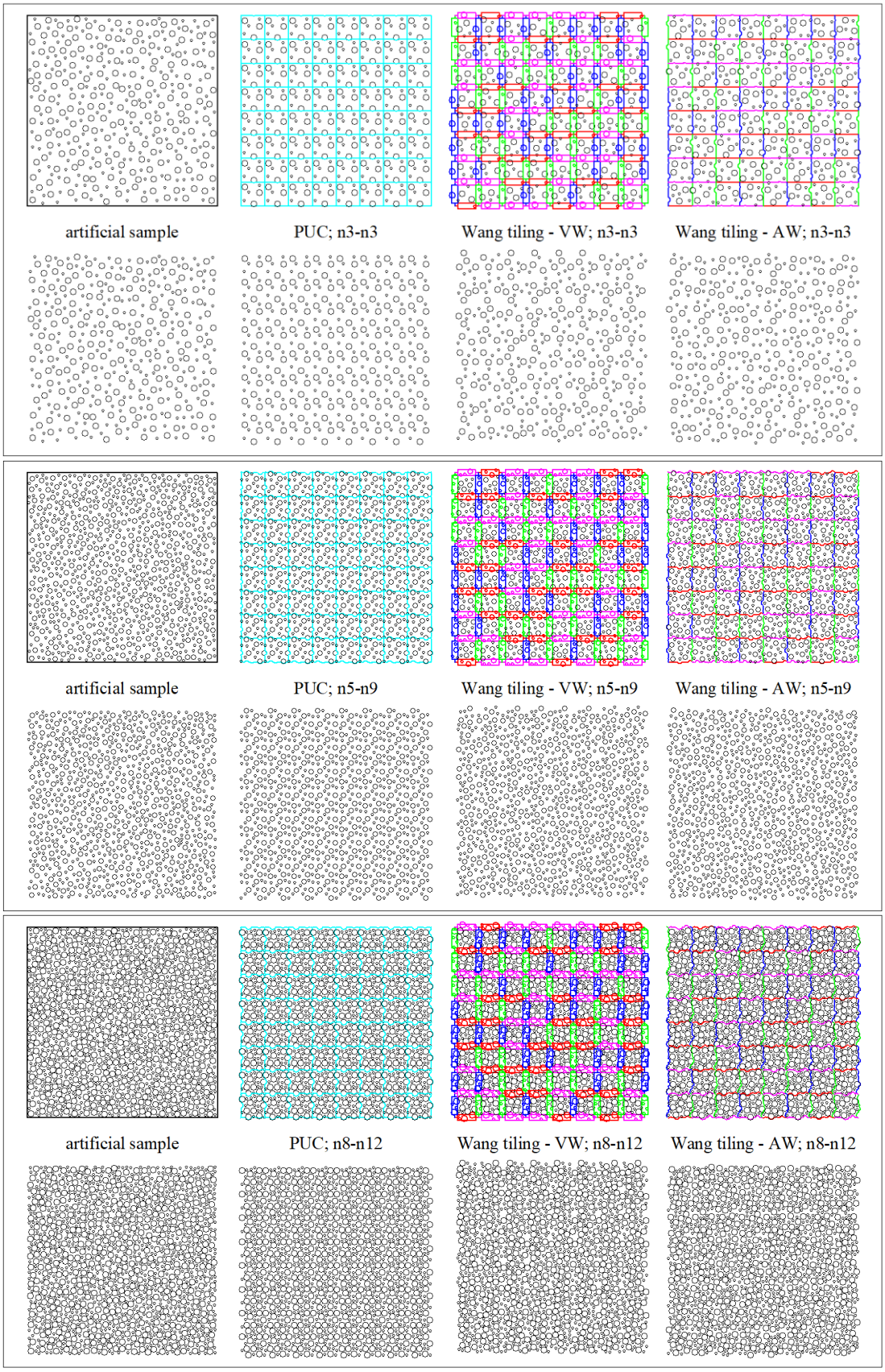

Fig. 3-17 Generated sets with polydisperse particles
Artificial sample; the PUC tiling; the Wang tilings W8/2-2 Volume Walls, Adaptive Walls.
upper frame – 3+3 particles/tile, middle – 5+9 particles/tile,lower – 8+12 particles/tile

The set of polydisperse microstructures for visual comparison includes artificial sample and tiled domains of the PUC and Wang tiling with both the VW and AW conditions. The benefits and disadvantages for monodisperse sets are generally valid in these cases as well. An emphasis has to be on prescribed volume fraction and volume ratio of particles of different radii. If we consider still the same tile size, the real volume fraction error gets up to ten percent for systems with the lowest tile particle number. This issue can be solved by modification of tile size according to an integral combination of particles with certain radii. We decided to keep the same tile size because of the main subchapter purpose – comparison of methods for tile set generation.

The lengths of tile edge, or dimensions of border areas respectively, are the decisive parameters for the size of dead spaces. The width of border areas equals the maximal particle diameter. Thus, if the centre of small particle reaches the corner, its surface is unable to cover a sufficient free area of the corner dead space. In this manner is formed visually regular lattice of islands without inclusions. This phenomenon appears with higher volume fraction and lower ratio of the largest particles to other ones. It can be found in our tested samples, particularly in domains of volume fraction 0.4 and 0.6, see Fig. 3-19 and Fig. 3-20.

On the contrary, polydisperse materials are more suitable for the method with the AW when solving the corner problem. Consider the particle of maximal radius which is located in a corner of the master tile. The deformation occurs in every corner of every tile from the set. One corner in the master tile is occupied with a particle while all others represent a free space only. These spaces are filled in the easiest way with particles of lower radii. Such a particle is "protected" by the master corner inclusion. A collision of the corner master particle with any other particle from slave tiles come earlier than a collision of these particles with the protected one. This advantage of the AW boundary conditions is visible in modelled states with both monodisperse Fig. 3-13 and polydisperse domains, Fig. 3-17.

The following pictures Fig. 3-18 – 3-20 complement the visualization with statistical information. The description of the first two examples of each volume fraction set corresponds to the binary representation located next to a certain graph. The binary form of Wang tiling examples symbolize only one of five realization, which are used for the statistics. All of these monochrome figures coincide with samples for visual comparison in Fig. 3-17. If we focus on the secondary extremes of function, we gain considerable reduction in the Wang tiling compared to the PUC. It is caused in particular by two circumstances. The first one is, naturally, usage of different boundary conditions. The second one is ability to create different tilings via just one set of tiles. Multiple realizations of material domains based on the PUC concept are not needed. Considering a statistically homogeneous microstructure, the two-point probability depends only on the relative position of tested points. The differences between statistics would only be inside tiles. However, the extremes of the final sample would be the same when there is no change of the tile size.

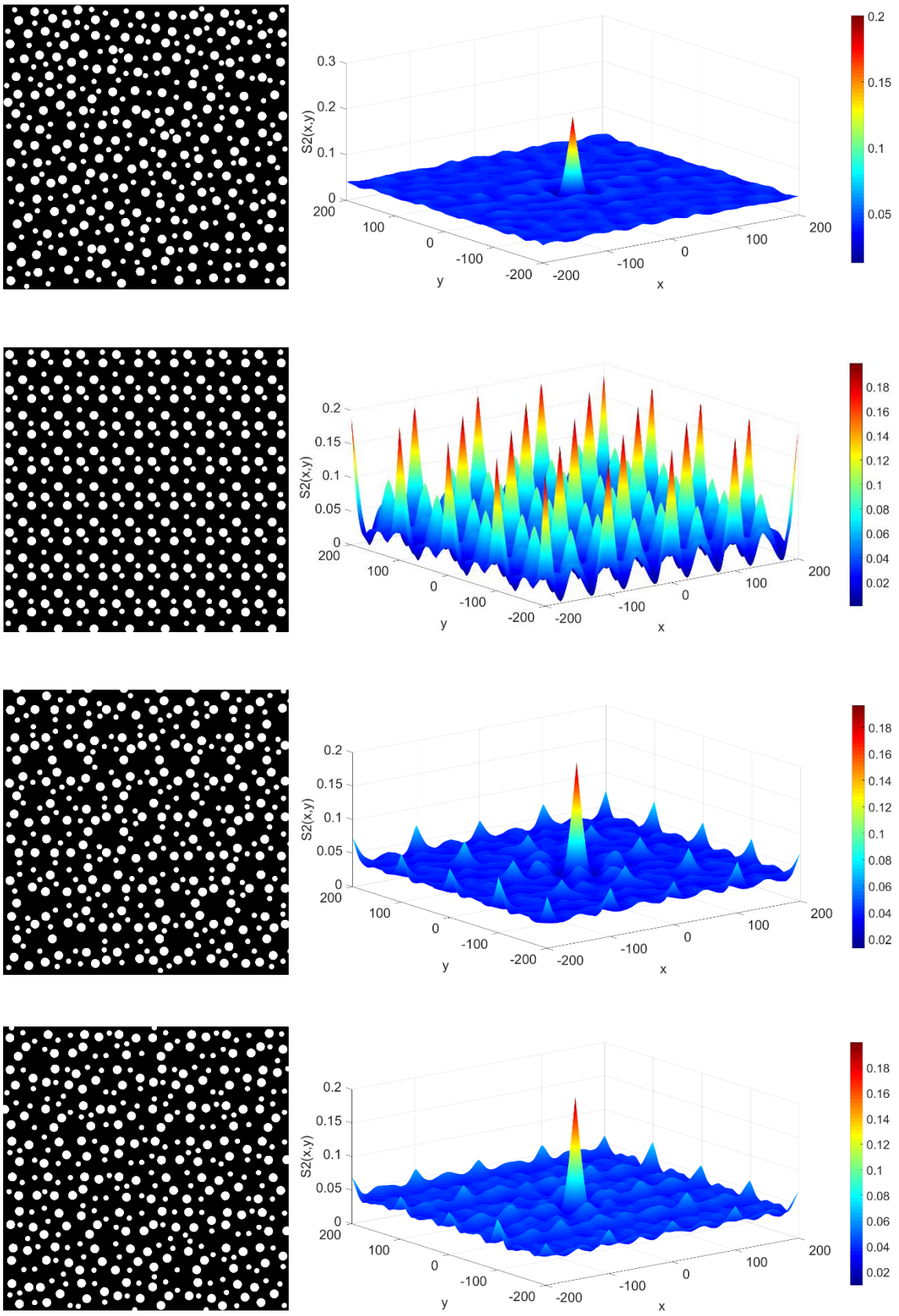

Fig. 3-18 Analysis of 2D polydisperse samples of volume fraction approximately 0.2
Systems from top to bottom: artificial sample, PUC, Wang tiling – VW, Wang tiling – AW.
Right – one randomly chosen realization, Left – S2 function (average of all realizations).

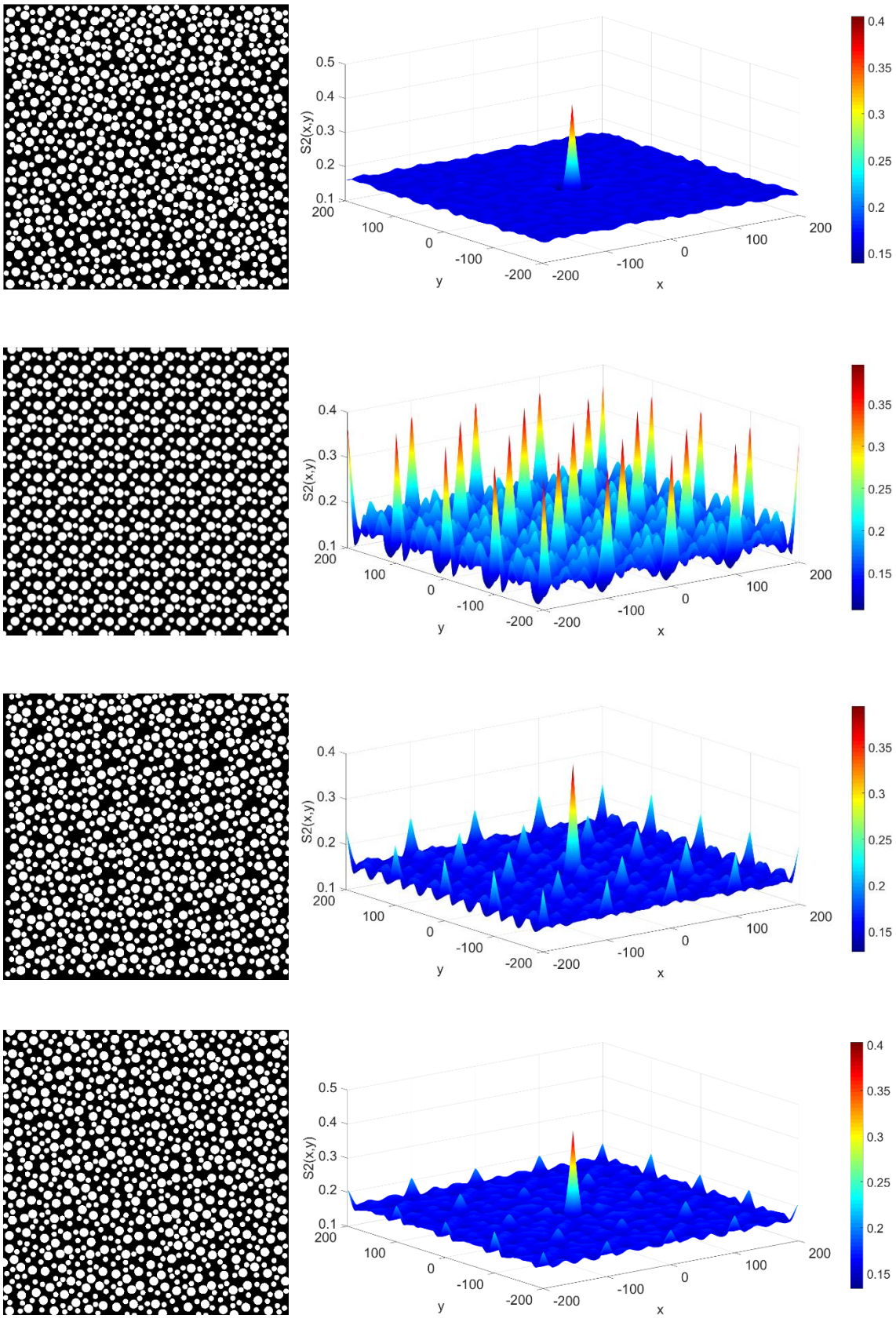

Fig. 3-19 Analysis of 2D polydisperse samples of volume fraction approximately 0.4 Systems from top to bottom: artificial sample, PUC, Wang tiling – VW, Wang tiling – AW. Right – one randomly chosen realization, Left – S2 function (average of all realizations).

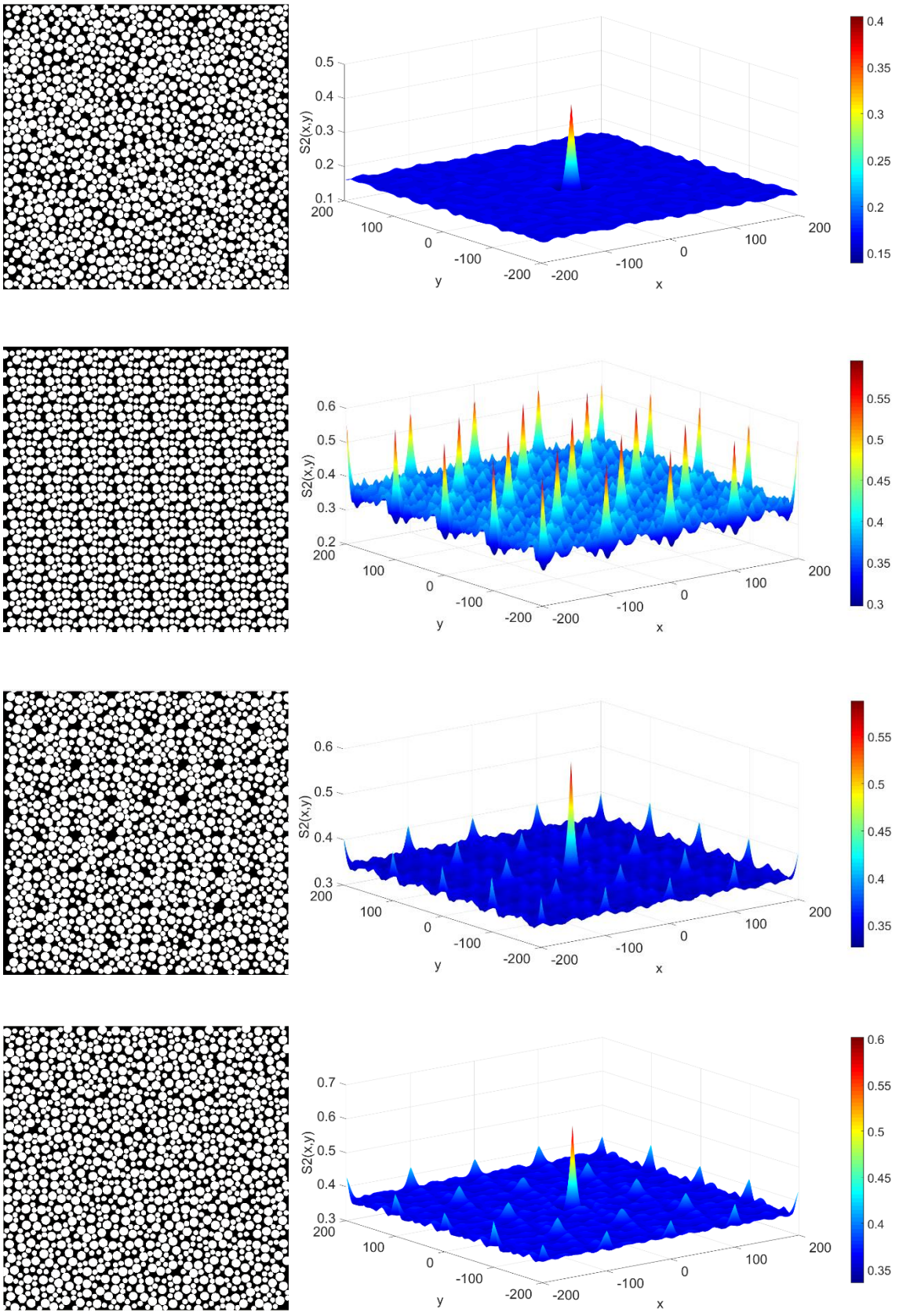

Fig. 3-20 Analysis of 2D polydisperse samples of volume fraction approximately 0.6 Systems from top to bottom: artificial sample, PUC, Wang tiling – VW, Wang tiling – AW. Right – one randomly chosen realization, Left – S2 function (average of all realizations).

3.2.5.3 Monodisperse 3D sets

The Wang tiling extension allows creation of 3D structures. The samples represent monodisperse impenetrable hard spheres in a continuous phase. Generated structures are composed of the PUCs and the Wang cubes with both the VW and the AW boundary conditions. The comparison of approaches is in terms of unwanted artefacts of artificial periodicity. The final position of inclusions is randomized, or in other words depends on initial random velocity vectors. The tested tiling sequence has a shape of cube and consist of 125 individual 3D tiles. Each cube has a size of 40 pixels and contain 12 particles with radius of 5 pixels. Such a description is valid for tiles with periodic and the Wang tiles with the AW boundary conditions. Tiles with the VW follow similar rules as for 2D applications. Duplicated particles in border areas are reduced in final tiling. But in the beginning of the generation algorithm particles are distributed as follows: one sphere to every border part and the others to the central part. Contrary to the 2D samples, the ratio of particle number in border regions to the sum of particles in central parts is lower than the ratio of these tile part volumes. This scheme has been chosen deliberately in order to demonstrate benefits of tiling with the VW and to reduce periodicity.

The results of the two-point probability descriptor for 3D applications are hardly visually interpretable. Therefore a histogram reflecting the number of particles in the spherical shell at a distance r from the certain particle centre is chosen to describe basic statistics, Fig 3-21. Concurrently, the last tested spherical shell is in distance equal to the tile dimension, which is sufficient from the tiling periodicity point of view.

The observed periodicity phenomenon can be retrieved from the data in the last column as well as from the graph trends. Moreover, the situation, when any column is much higher than its nearest neighbours, indicate observed phenomenon as well. Mentioned events can be seen from the statistic of the PUC structure. The last column corresponds to the cube size and include sphere copies in main orthogonal directions. Higher values in zone 13, 17, 24, or 29 contain distances of particles in two closest cubes, but they are significantly affected with copies of particles inside one periodic cell.

The frequency of particles with relative distance equal to the cube size is significantly lower for Wang tiling with VW in comparison with the PUC concept. The difference level is based on the number of particles in border volume space. In general, marginal role plays also a structure of tiling. Despite the stochastic tiling process, the final sequence may include neighbours of the same cubes. In our case such a sequence occurs in less than six percent of the neighbours. The histogram for Wang tiling with the AW is in agreement with the goal to reduce periodicity artefacts. In here the frequency in the last column is the lowest from the generated structures. Moreover the growth rate is fluent indicating uniform distribution without extremes.

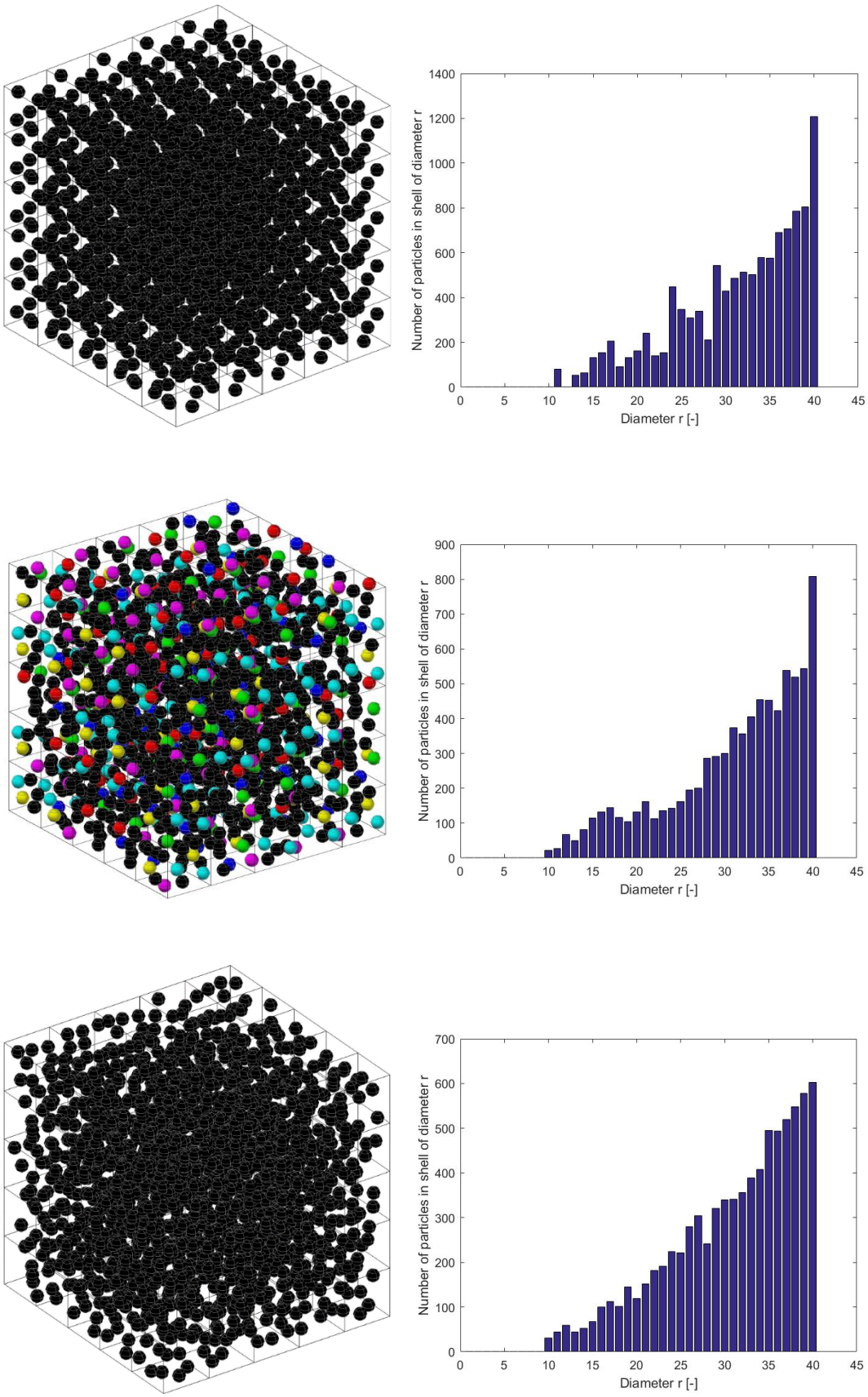

Fig. 3-21 Analysis of 3D monodisperse samples of volume fraction approximately 0.08 Right: Realizations with system of PUC, Wang cubes with VW, Wang Cubes with AW, Left: appropriate histograms of particle distances

3.3 Tile size

Consider six structures with monodisperse discs of identical particle fraction composed with stochastic Wang tiling. Each tile set W8/2-2 of generated structures is created via proposed modified molecular dynamic algorithm with Adaptive Walls approach as described in previous chapters. The algorithm stops when particles reach the final radii of 7.5 pixels. Every single sample contains 900 particles, whereas size and number of tiles in tiling differs. The first sample form grid of 900 tiles with just one particle inside. Each tile in other samples contain 4, 9, 25, 36, and 100 particles respectively.

It is obvious from the Fig. 3-22 with 3 of representatives, that the first simulation (1 particle/tile) represents S arrangement, whereas the second (9 particles/tile) and the third tiling (100 particles/tile) forms rather R arrangement [45]. The term R arrangement means random particle placement and S represents regular or uniform particle positioning over whole area. One can also easily observe differences in the degree of heterogeneity, where in the first sample there are visible interferences and the structure is closer to the ordered system in comparison with the last tiling with both particle clusters and rattlers. The main goal of this part is to provide simulations and build up recommendations for particle-tile size relation with emphasis on specific range of volume fraction similar to optimized structure within next chapter, overall arrangement and different states of heterogeneity for structures.

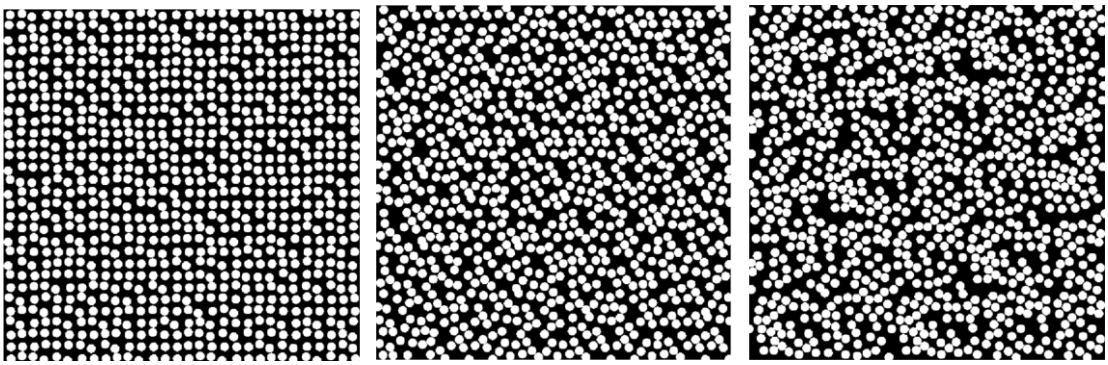

Fig. 3-22 Samples of tiling for tile size investigation
1 inclusion/tile (30×30 tiles), 4 inclusions/tile (15×15 tiles), 36 inclusions/tile (5×5 tiles);
Wang tiling set W8/2-2.

In general every tile within the Wang tiling concept used to be of unit size. But for modelling practice, the base block has to have a size of certain value or at least to be in the certain ratio with other structural dimensions. The determination of the tile size can be divided into two consecutive steps. In the first one there is need to define minimal geometry demands, in order to be able to reach various states of packings. Within the second step the size of tiles as well as tiling is compared to the characteristic structural sizes of a modelled sample and/or modified with emphasis on overall required material properties. We focus, in this stage of investigation, mostly on the first condition.

The very first issue for a definition of the tile size is identification of possible packing states. When a required material is fully packed or domain should have clusters of particles, it is necessary to cogitate the close dense packing. Since the dynamic algorithm involves Adaptive Walls, it is theoretically possible to achieve the maximal hexagonal dense packing of equal-sized inclusions with the volume fraction of 0.9069. But for real random heterogeneous microstructures more common are limits of jammed states (mechanical stable states) or random jammed state respectively [18]. The most disordered jammed state used to be called maximally random. Nevertheless in our simulation we aim at tiling with lower particle fraction in order to simulate specific range of structural domains with higher degree of freedom and R arrangement.

Two assumptions, the same number of particles in every tile and probability of accepting a tile from the appropriate pair of possible tiles, assure overall required volume fraction. The term volume fraction, or in this case a packing fraction, is defined as ratio of the sum of particle areas to overall space. The dimension of space is relative to tile size, therefore the number of particles within a tile defines (with respect to the required packing fraction) the size of each tile. In the following examples, where are different number of particles in tiles, we will compare how this setting affects tiled model in terms of simplified basic statistical description.

For all analysed cases the packing fraction is 0.442. The size of a final tiling is 600×600 pixels/microns. There are 6 examples where the tile size increases gradually. In the first case we have only one inclusion in every tile. Since the size of tile is 20 pixels, the final tiling consists of 30×30 tiles. The table Tab 3-2 summarizes investigated cases with appropriate settings. Figures Fig 3-23 – 3-28 show one tiling set with appropriate tiled structure for given settings and pore size distribution histogram [46] from five different realizations. In this case one realization represents domain with the same tiling sequence but different random particle positions in comparison with other structures within particular tile size. The separation of pores uses watershed segmentation algorithm [47]. Since these are test files, microns in pore size distribution equals to pixels.

Tab. 3-2: Settings for comparison of tile sizes

Set No.	Tile lattice	Total number of tiles	Particles per tile	Total number of particles
1	30x30	900	1	900
2	15x15	225	4	900
3	10x10	100	9	900
4	6x6	36	25	900
5	5x5	25	36	900
6	3x3	9	100	900

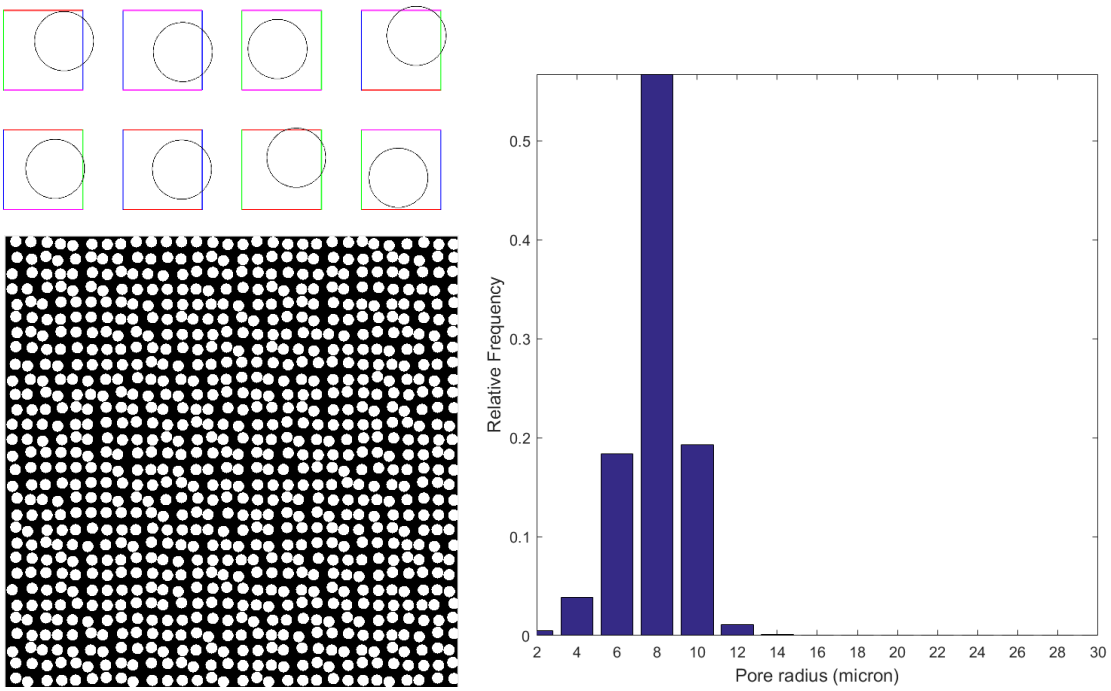

Fig. 3-23 Particle distribution – 1st example 1 inclusion/tile: one sample of Wang tile set with tiling (30×30 tiles), average pore size distribution over 5 realizations

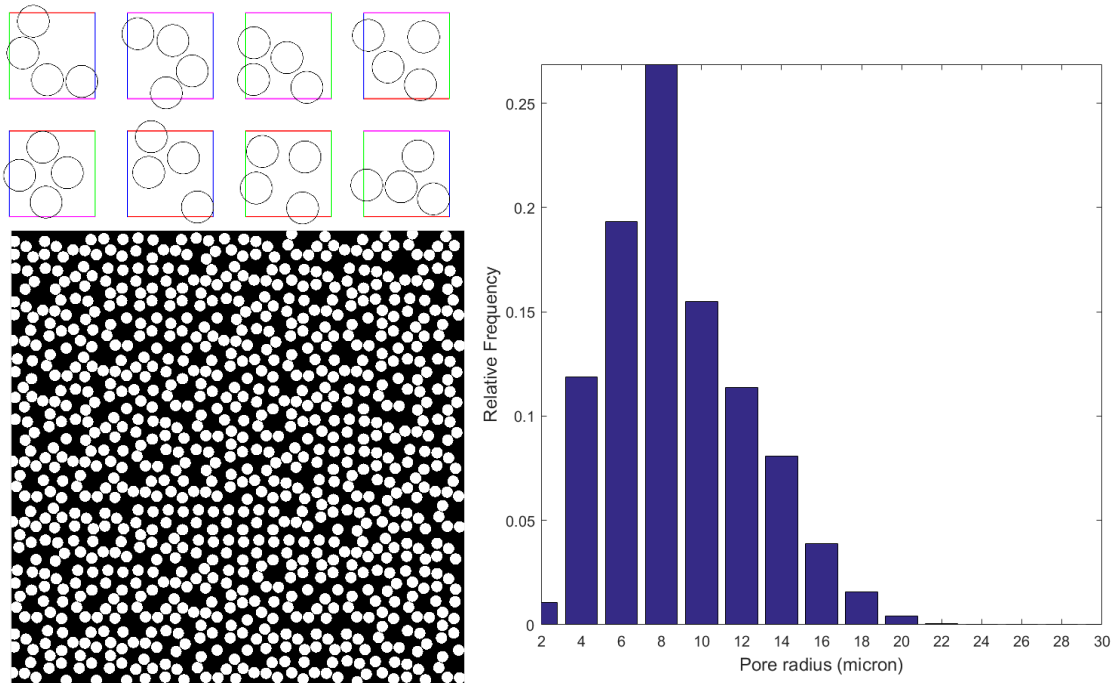

Fig. 3-24 Particle distribution – 2nd example 4 inclusions/tile one sample of Wang tile set with tiling (15×15 tiles), average pore size distribution over 5 realizations

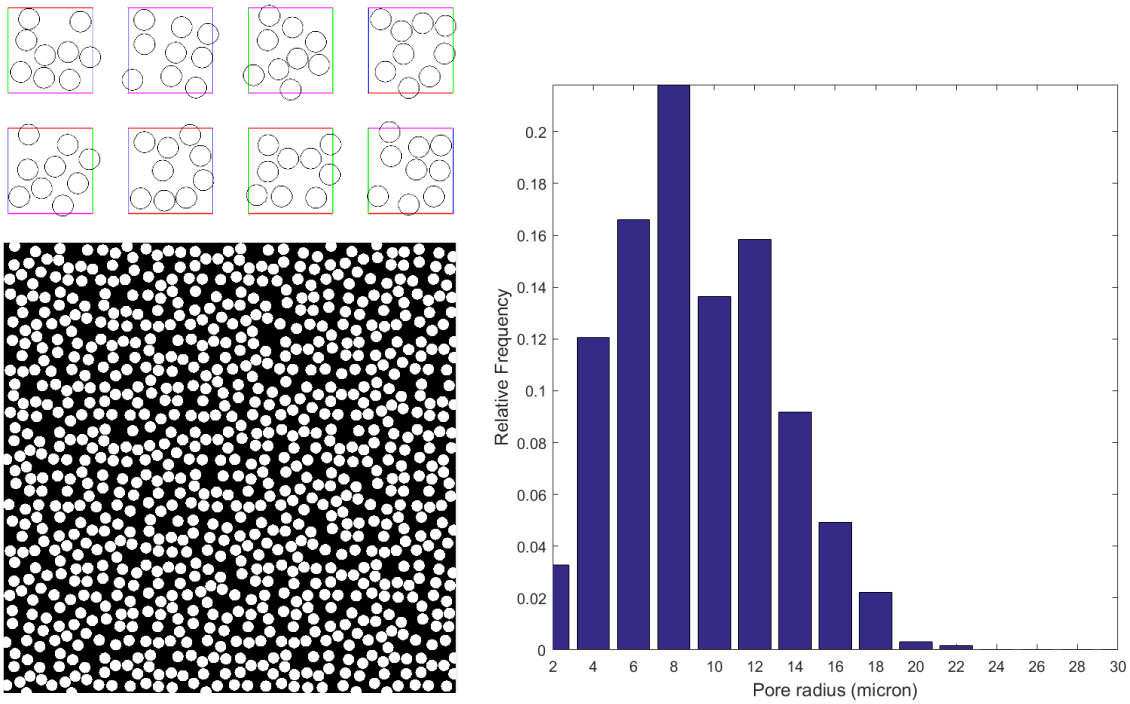

Fig. 3-25 Particle distribution – 3rd example 9 inclusions/tile one sample of Wang tile set with tiling (10×10 tiles), average pore size distribution over 5 realizations

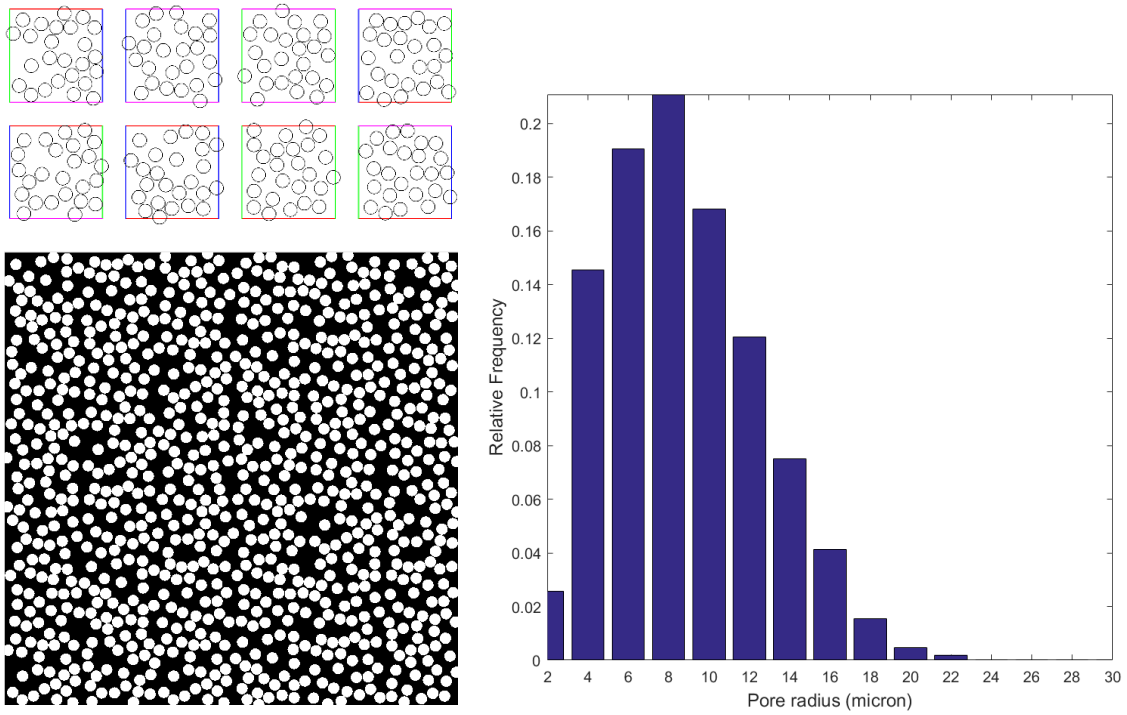

Fig. 3-26 Particle distribution – 4th example 25 inclusions/tile one sample of Wang tile set with tiling (6×6 tiles), average pore size distribution over 5 realizations

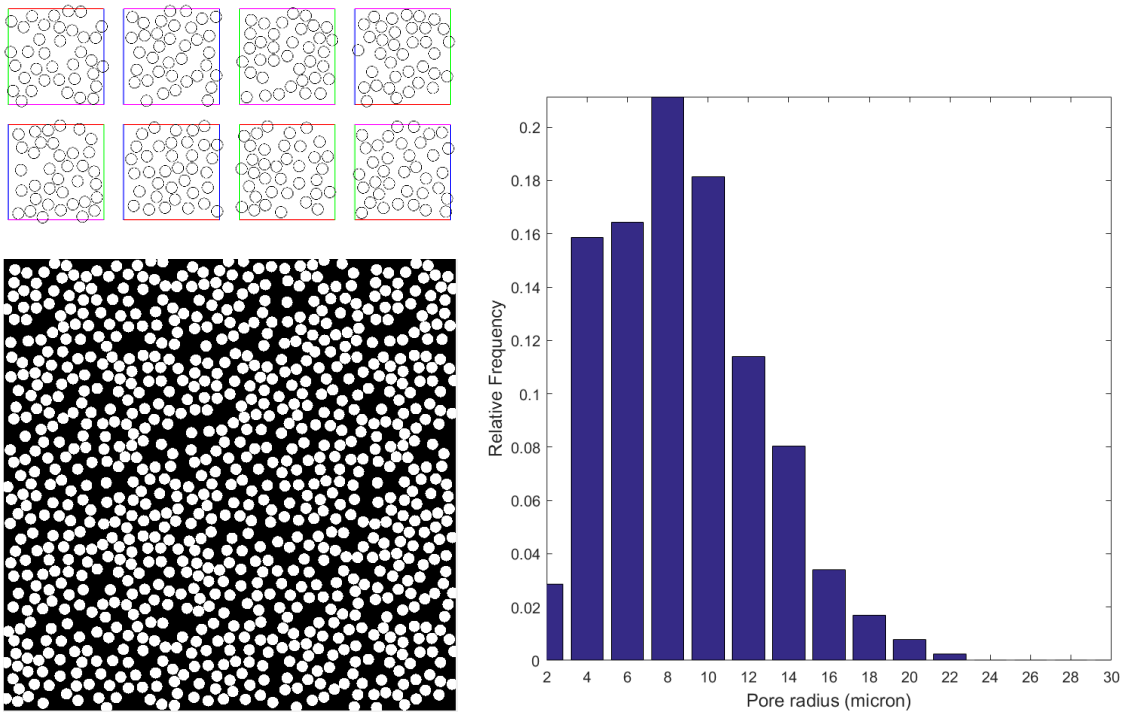

Fig. 3-27 Particle distribution – 5th example 36 inclusions/tile one sample of Wang tile set with tiling (5×5 tiles), average pore size distribution over 5 realizations

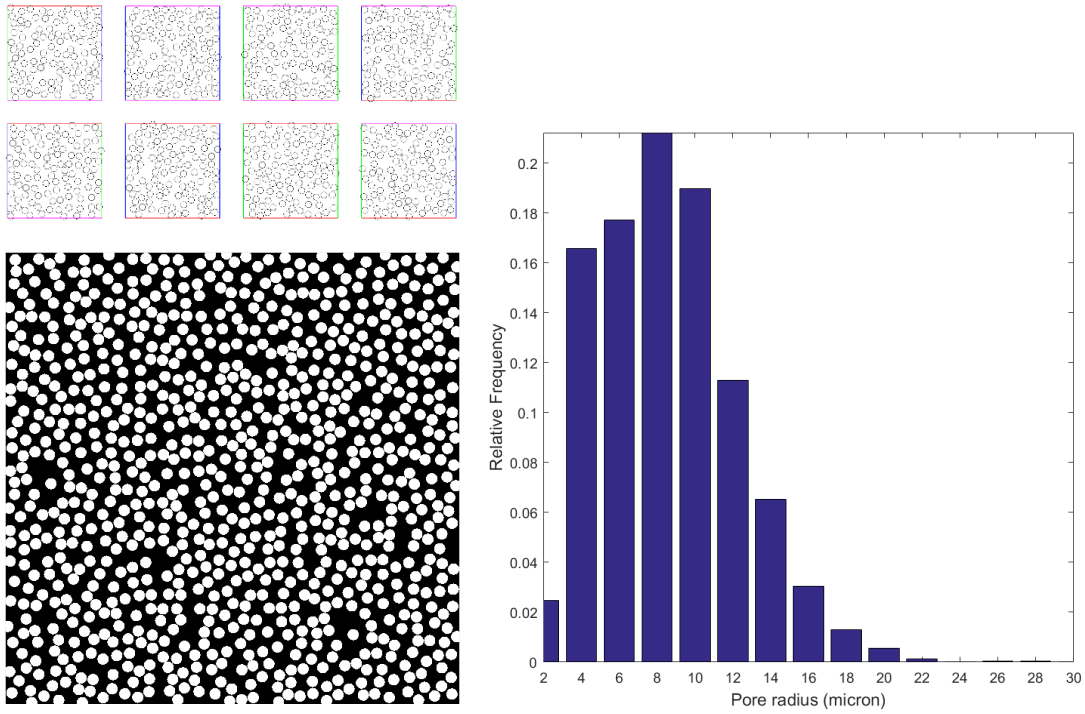

Fig. 3-28 Particle distribution – 6th example 100 inclusions/tile one sample of Wang tile set with tiling (3×3 tiles), average pore size distribution over 5 realizations

In the first case, the tiling exhibits similarity to the material with lattice. The particles in every tile have limited freedom given by the tile size-particle radius ratio which is 0.375. Thus the pore size histogram is quite narrow without existence of large pores. Such setting is valid only for a reconstruction of domain with high-ordered particle system or with a periodic arrangement.

The second simulation with 4 particles in a tile enables to create structures with wider pore distribution. This was achieved mainly due to larger space for particle motion. Nevertheless there is still a dominated pore size indicating lower level of disordering. Moreover in visualisation of one structure occur many local particle clusters caused by small particle number in a tile and the nature of the stochastic tiling.

The histograms from the third and the fourth tested settings display quite similar results in term of range of pore size and maximal relative frequency. Differences in height of bars is given by the size of tile (ability of achieving various states) and relatively low number of tests. Despite the fact of randomized particle positions, the samples of the set with 9 particles in a tile exhibits similarity and therefore pores with size of 12 pixels appear more often than pores with size of 10 pixels. This phenomenon has its origin in relatively small number of tested samples.

The results of last two tested settings (36 and 100 particles per tile) bring no significant benefits in comparison with the previous ones (9 and 25 particles per tile), except the ability to reach larger pores but with very low frequency. The shapes of outer curve connecting relative frequencies and capturing the trends of plots are nearly the same.

In general the larger tiles are, keeping the same volume fraction, the greater heterogeneity in terms of pore size we can get. This assumption fits random domains especialy with higher volume fraction. In our case the volume fraction is 0.442. We can observe from results that satisfying degree of heterogeneity for given volume fraction is achieved with particle radii to tile size ratio in range from 0.125 (9 inclusions per tile) to 0.075 (25 inclustions per tile). Benefits in form of larger pores for higher number of particles disappears when taking into account increasing of computer demands.

The resolution is the same for all tested cases, therefore computer demands on calculation of the two-point probability remains the same as well. The main difference for demands on computer power for sets with different tile sizes lies on recalculation of velocity vectors and collision times. The occurrance of these phenomena is affected by initial velocity vectors (direction and magnitude), initial positions of particles, and number of particles in tiles. In order to eliminate influence of the first two settings, we arranged particles reguralrly and assigned them with the same initial velocity vector magnitude. But the number of collisions grew exponentialy. Despite the best of author efforts, algorithm is not fully optimized and the recalculation of the time dependent phenomena takes the greatest time.

There are several ways how to deal with this problem. One is to implement principles of parallelization and compute each tile separately with transfer of knowledge about particle tending to leave the tile. Another solution is based on selection particles only from the nearest neighbourhood while checking collision. With these improvement the worst time dependency may migrate to other parts of the algorithm.

The tested sets consist of tiles with the same number of particles. If a reconstructed sample has particle high degree of heterogeneity, it may require Wang tiling with different number of particles in tiles. The Fig. 3-29 shows a visualisation of such a domain with large pores. But with different tile particle packing other issues arise. The most critical one is design of tiling algorithm in terms of prescribed overall volume fraction. When the set includes very varying tiles and tiling is made of small number of tiles, the tiling algorithm cannot assure required volume fraction because of the uniform acceptance probability. This problem can be solved with observation of tiling process, where acceptance probability varies over tile set. After a certain part of the Wang tiling is complete, the temporary packing fraction can be recalculated and tiles will be assigned with an updated acceptance probability. Another solution but with similar main idea is to scan reference medium with a tile of given size. Then provide a tile volume fraction histogram, where number of bins equals the number of tiles in the Wang tile set. After this sorting a tiling sequence is made based on histogram values and overall volume fraction. Such an algorithm has been used for reconstruction of real material domains in following chapter.

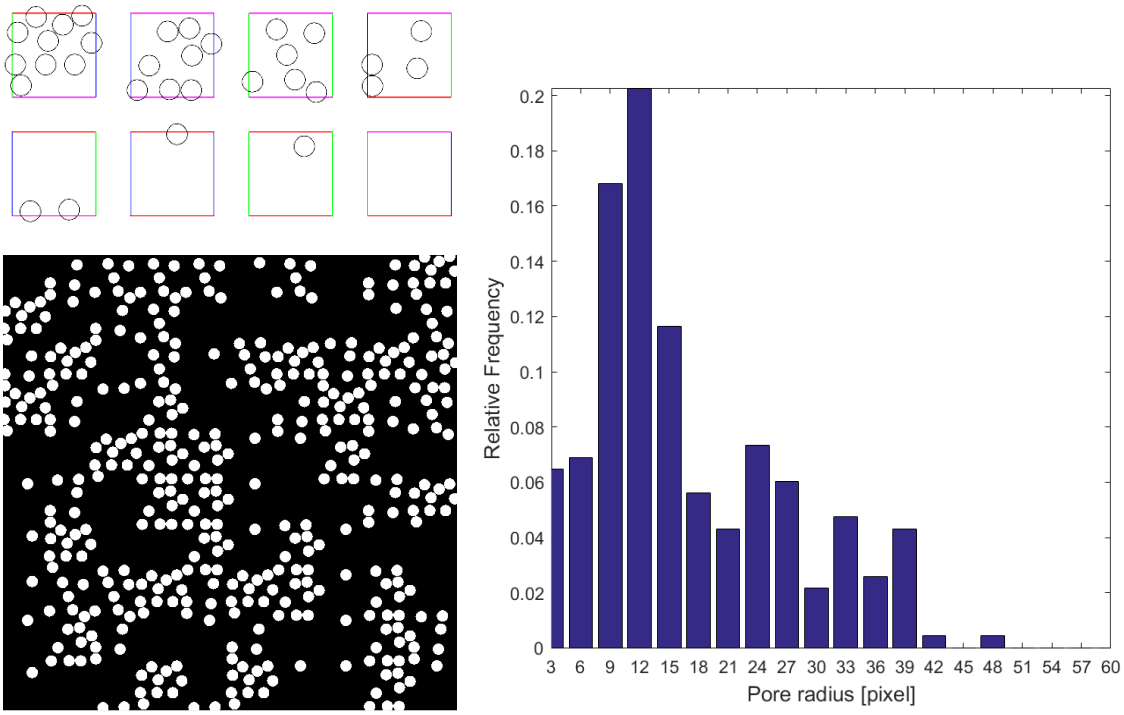

Fig. 3-29 Particle distribution – different number of particles in Wang tiles
one sample of Wang tile set with tiling (10×10 tiles), appropriate Pore size distribution

4 Optimization

The final microstructures, which were created in the preceding chapters using Wang tiling with adaptive edges and molecular dynamics, depended on random initial velocity vectors and initial positions. The stopping criterion was to achieve maximum particle sizes, which represented one of input parameters of the entire algorithm. When comparing the two-point probability descriptor of the reference and generated structures, only the primary tops of the graphs were in agreement. These represented the probability of two-points lying on each other are located in the observed phase. The nature of the descriptor indicates, that these values represent a volume fraction that remained unchanged for the investigated sets. The error in comparing descriptors nearby primary extremes is infinitial for monodispersion sets with very low volume fraction. The probability of finding two pixels in the same phase in this area corresponds to the particle size. However, if we want to construct real-time tiling, which would have a minimal error with the reference sample when comparing descriptors, it is necessary to incorporate elements of optimization techniques into the algorithm.

In the case of a general microstructure, the process of searching for a corresponding sample is based on changing the phase of the selected pixels [1], [10]. The complexity of the problem then mainly lies on the binary representation of the media. Here it is necessary to think of a mistake on the statistical descriptor, which arises with the gross binary representation of media [48]. In view of the above, it is necessary to choose from robust optimization methods, which are able to work with the discrete problem and have the possibility to escape from the local extrema. For example [1] uses the simulated anealing method [49] [50] for the reconstruction of random media. If it is possible to simply define particles in a microstructure, then pixel scattering and compatibility check of particles are ineffective. In [10] an optimization problem with Wang tiles includes two criteria, which were combined into the objective function with weighting principles. Here hard particles in a matrix form reconstructed medium. The change of objective function occurs after a shift of the whole particle template not only one pixel.

The optimization process of domain reconstruction via Wang tiling could be divided into four phases. The first is to find the size of the tile which reflects structural lengths or clusters. The second one defines particle numbers in tiles. The third focuses on optimization of tiling sequence, while the last one deals with the position of particles within each tile. In our case, with respect to the types of reconstructed media, the size of the tile is determined in certain relation with the size of the particle. The number of prarticles in tiles follow the histogram after scenning of reference domain. The tiling sequence for reconstructed samples remains unchanged for appropriate material domain. But the final position of particles is based up on the modified Particle Swarm Optimization method.

4.1 Particle swarm optimization

The definition of the optimization problem for the task of the reconstruction of random heterogeneous structures with circular particles can be written as follows: Find the position of the inclusions in the Wang set which minimize the error on the static descriptor between the final tile and the reference sample. In general case the final position of the particle is determined by its initial position and velocity vector, when boundary conditions and the principle of elastic collision are met. It can be seen, by its physical nature, as a flock of an individual searching a space to find the best position. With regard to this visual form, the optimization problem is solved via Particle Swarm Optimization (PSO) with certain modifications.

4.1.1 History

The PSO belongs to a family of evolutionary techniques that are based on the behavior of the individuals living in the nature. Roots of the PSO reach the second half of the 80's, when Reynolds established the basic rules of individual behavior simulating the movement of flocks in flight phases: Avoid collision with your neighbours, try to balance your speed with your nearest colleagues and stay at their neighbourhood [51]. Later in 1995 Kennedy and Eberhart extended and modified the work of Reynlods and use it to optimize continuous non-linear functions [52]. The behavior of their population corresponded more closely with the principles of intelligence of the swarm, as presented by Millonas [53]. Hence, the term Particle Swarm Optimization.

In the PSO each individual represents a potential solution which depends on its own experiences as well as on knowledge of its neighbours. In the beginning population of particles is assigned with random positions and random velocities. The position and velocity vector of each individual are adjusted within every iteration step. In original approach, these parameters of particle motion in iteration k + 1 are defined as follows:

$$v_{id}^{k+1} = w \cdot v_{id}^{k} + c_1 \cdot rand() \cdot (p_{id} - x_{id}) + c_2 \cdot Rand() \cdot (p_{gd} - x_{id}) \tag{4.9}$$

$$x_{id}^{k+1} = x_{id}^{k} + v_{id}^{k+1} \tag{4.10}$$

where x_{id}^{k} and v_{id}^{k} is a position and velocity of a particle I in iteration k and p_{id} stands for the personal best position so far while p_{gd} means global best postion of a swarm. Coeficients c_1 and c_2 represents cognitive and social factor respectively. Rand designates a member from uniform distributed randomized numbers in range from 0 to 1. Finaly w is a weigted factor, which missed in the original form or can be set to 1. Over the years basic PSO definition has been modified in various ways. A list of improvements can be found in [54], [55], [56] or [57]. Here we discuss only modifications which have direct impact to finalized version of PSO utilized in next parts of this work.

4.1.2 Modification

Modifications and improvements of the method have different purposes. Someof them can only be used for specific tasks, for example, to increase the speed of convergence or to find global extreme. Others try to improve the behavior of the method independently on the type of optimization task. A general modification was proposed by Shi and Eberhard, which introduced inertia weight factor omega as a tool for swarm velocity control and method stability. This parameter is responsible for exploration whereas cognitive and social factors are responsible for attraction and convergence [58].

It is necessary to note that in our case the bearer of the objective function is not each particle, but it depends on position of all particles in the Wang tiles set at any given time. This, in general, leads to a so-called social model where cognitive part is eliminated [49]. In order to be able to search large space in the beginning of the algorithm, the social factor c_2 is defined with linear growth rate and maximal value of 1.5. This is set with regard to recommendations from contribution where Clerk and Kennedy studied the stability and convergence of the PSO [60]. Because of the absence of classical cognitive factor, the weight factor in this work is different from their proposal and set to 1. Thus the inclusions move only in direction defined by their initial velocity vectors. In order to be able to escape from local extremes, each particle in every iteration is assigned with random velocity vector in the range 0-5 multiplied by coefficient for the initial velocity relative to the dimension of the tile. This parameter prevents too fast movement of the inclusions at the beginning of the process, where these can move maximaly by five hundredths of the tile size. The velocity vectors of the whole system are then reduced linearly with a decreasing coefficient which is 1 in the beginning of the algorithm and ends with 0.5. The velocity vectors and position of particles for the next time step are according to following formulas.

$$v_{id}^{k+1} = (v_{id}^{k} + c_1 \cdot \mathrm{Rand} + \frac{c_2}{t_{max}} \cdot t^k \cdot \mathrm{Rand} \cdot \left(p_{gd} - x_{id}^{k} \right)) \cdot (1 - \frac{0.5}{t_{max}} \cdot t^k) \tag{4.11}$$

$$x_{id}^{k+1} = x_{id}^{k} + v_{id}^{k} \cdot dt \tag{4.12}$$

Not only the PSO parameter settings but also the number of particles affect results. It is recommended to use maximally 100 individuals [57] In our work we follow this recommendation as well. The tile dimension for following optimization tasks equals four diameters of the largest particle in a domain. Overal volume fraction of benchmarks and real microstructures is below 60%, this means the average number of particles in a tile is below 12.2. The total number of individals for the modified PSO method with assumptions like this do not exceed 98 and the requirement is fulfilled.

4.2 Verification

Before generation of real sample reconstruction, the algorithm should be tested for a series of basic artificial microstructures. This will give us an overview of the algorithm and help us to set specific parameters to get. In accordance to the results from subchapter 3.2, which compared marginal conditions with respect to the size and the secondary extremes of the statistical descriptor, all of generated samples uses Wang tiling approach with Adaptive Walls.

4.2.1 Reference structure via Periodic Unit Cells

The first test reference medium represents the tiling of periodic unit cells in a regular lattice of 64 cells. The cell has a size of 100 pixels and contains only one particle with a radius of 12.5 pixels. The volume fraction is therefore 0.049. The sequence of tiles for the generated sample is consistent with the samples from Fig. 3-13 up to Fig. 3-20. Due to the nature of the unit cell approach, the number of inclusions in each Wang tile is the same. These inputs reduce the task of finding optimal particle positions on the basis of the two-point probability function to process of reaching constant distance between particles. This assumption is fulfilled whenever the inclusion in each of the tiles are in the same position. However, for the purpose of the algorithm verification for complex systems, the objective function is defined as a sum of the quadratic differential of two-point probabilities.

The algorithm for tile generation calculates with the particles gradually growing to their final desired size. But in order to eliminate the error on the descriptor by different particle size during the algorithm, the compared medium has the current particle positions but with the final dimensions. This may lead to the theoretical overlap if a pair of particles centres are closer than the sum of their final radii. Anyhow this problem is solved automatically in the end of a trial due to the nature of molecular dynamics. Alternatively, it is possible to build up a function for overlapping penalty.

For the first test case, when we have a very small volume fraction and only one part in a tile, the overlapping can only occure when a particle cross with its surface a tile edge. Therefore no penalty is applied here. The dimension of compared descriptor areas is reduced to 400x400 pixels. The reduction would be higher in the case of the reference medium with periodic repetition. Nevertheless, more complex structures requires comparison of larger areas. That is why we have decided to keep this size the same even for the first example. The basic setting of both the algorithm and the optimization method is summarized in Tab. 4-3. Summary of results is in Tab. 4-4. In the Fig. 4-30 is shown the reference and reconstructed tiling with corresponding graphical form of the descriptor.

Tab. 4-3: Settings for reference structure via Periodic Unit Cells 1

Settings of algorithm		Settings of optimization method	
Initial velocity factor:	0.05	Constant weight factor:	1.00
Random velocity factor:	0.25	Constant social factor:	1.50
Number of time steps:	1000	Random social range	0.0 – 1.0

Tab. 4-4: Results for reference structure via Periodic Unit Cells 1

Number of realizations	5
Minimal value of objective function	1.6 e-4
Average value of objective function	5.2 e-4

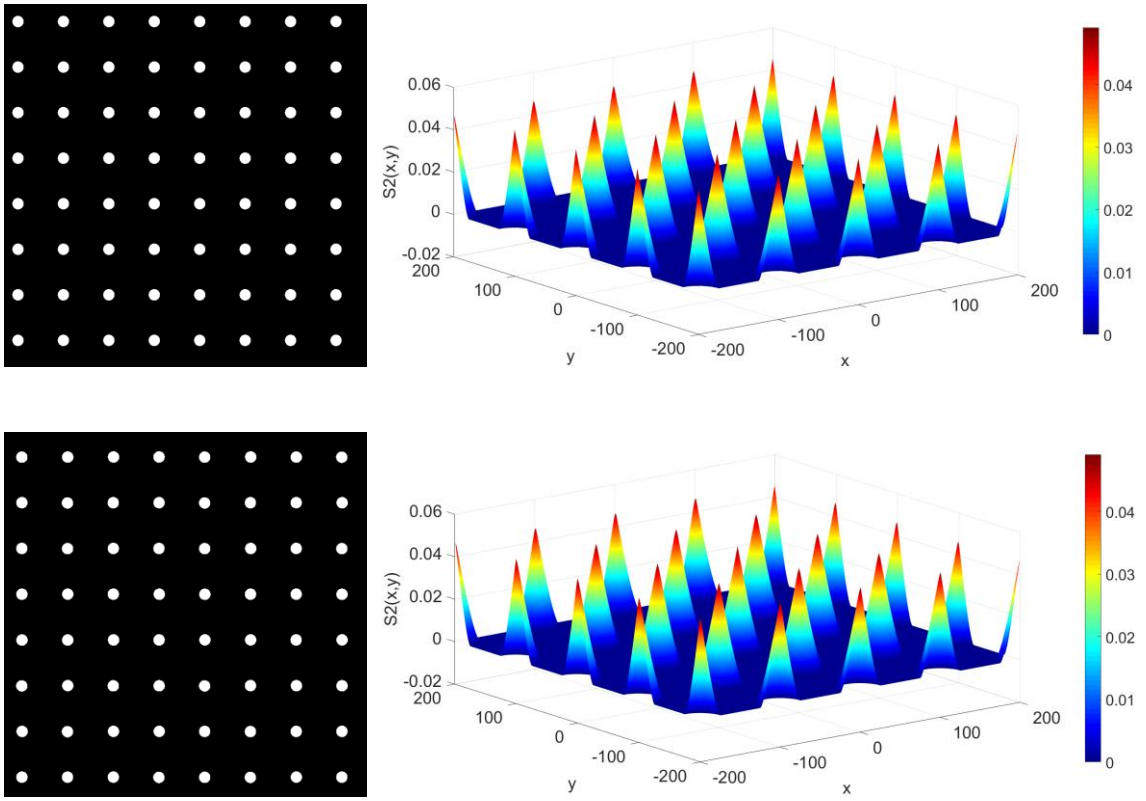

Fig. 4-30 Verification of optimization – Reference structure via Periodic Unit Cells 1
Top: Reference tiling and appropriate statistical descriptor
Bottom: The best arrangement and appropriate statistical descriptor

Visual comparison of both binary representation of the microstructure and statistical descriptor confirm success of optimization technique for this type of domain. The distance between particles has been minimized which forms the regular lattice of particles. The exact position of particles in reconstructed microstructure differs from the reference one by a certain value. But this has no negative effect since we set statistical homogeneity for statistical description. That means independence of the system of any shifting.

The second artificial samples is composed with repetition of one cell as well. Now it contains two inclusions. The sequence of tiling for reconstruction is similar to the first tested domain. Again, each tile is assigned with the same number of particles. The position of particles in reference domain forbids simple reduction of the problem to minimization of mutual particle distance. The comparison is made on a reduced of 400x400 pixels. The algorithm settings is the same as for previous test, see Tab. 4-3. The results are shown on Tab. 4-5. The results are shown on Fig. 4-31, where both reference and optimized structure binary representation is completed with a grapf of appropriate descriptor function.

Tab. 4-5: Results for reference structure via Periodic Unit Cells 2

Number of realizations	5
Minimal value of objective function	3.5
Average value of objective function	4.2

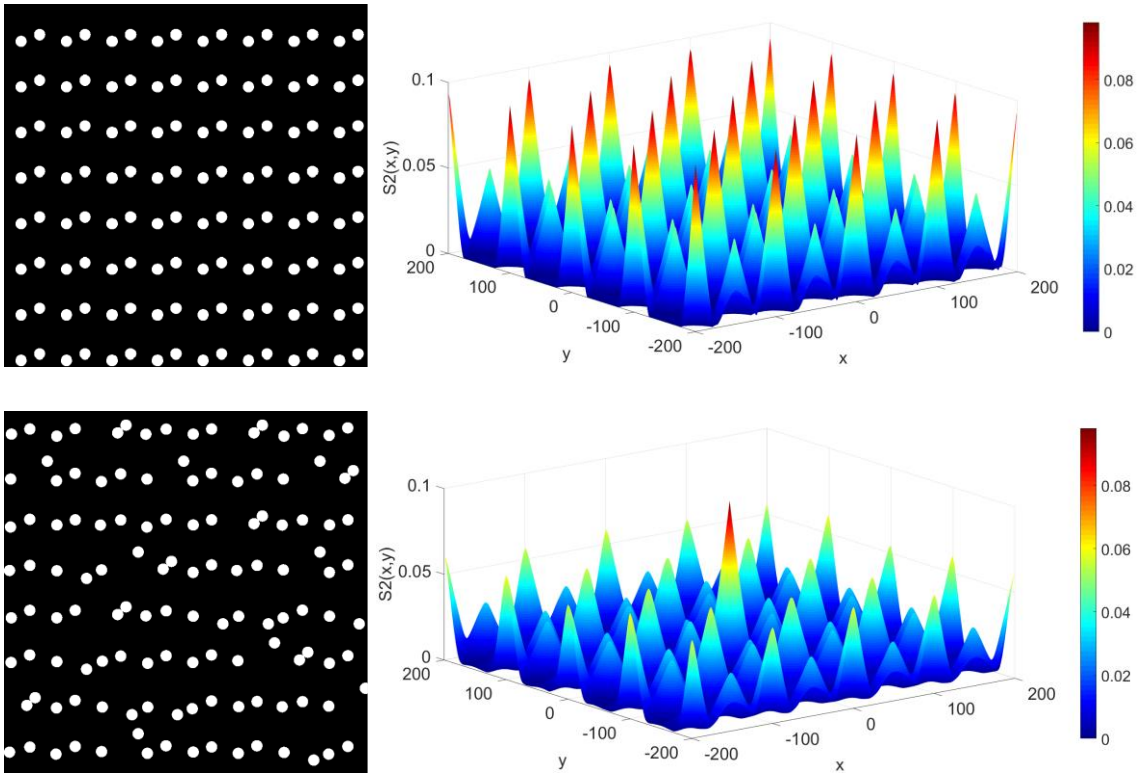

Fig. 4-31 Verification of optimization – Reference structure via Periodic Unit Cells 2
Top: Reference tiling and appropriate statistical descriptor
Bottom: The best arrangement and appropriate statistical descriptor

The result of the second case are not so satisfactory. Obviously we get a microstructure with local minimal difference between compared statistical descriptors. The most of tiles contain particles with the same mutual distance as in reference sample. But some of them are closer. This points to a possible reserve in parameters settings since the algorithm cannot force badly placed particle to move to better position in the end of the process.

4.2.2 Reference structure via Wang tiling

The third specimen is composed of Wang tiles. The sequence of tiles is the same as for domains that served for comparison of various boundary conditions. Concretely the last sample from the Fig. 3-15, where Wang tiles meet the boundary conditions of Adaptive Walls, has been chosen. The reconstructed tiling consists of the same number, sequence and tile dimensions. Each cell of the set includes 8 particles of radius 12.5 pixel. Finial tiling contain total number of 512 particles placed in a matrix phase. An optimization task can be reduced for this type of reference to problem of finding identical copies of original set. However, optimization algorithm should be blind and work in general sense. The precondition would only lead to trivial solution, which requires even less robust methods. The algorithm setings are still the same, see Tab. 4-3, except total number of time steps which is 5000. The results are summarized in the Tab. 4-6. A graphical form of reference and one optimized sample with two-point probability function are shown on Fig. 4-32.

Tab. 4-6: Results for reference structure via Wang tiling

Number of realizations	5
Minimal value of objective function	1,9
Average value of objective function	2,4

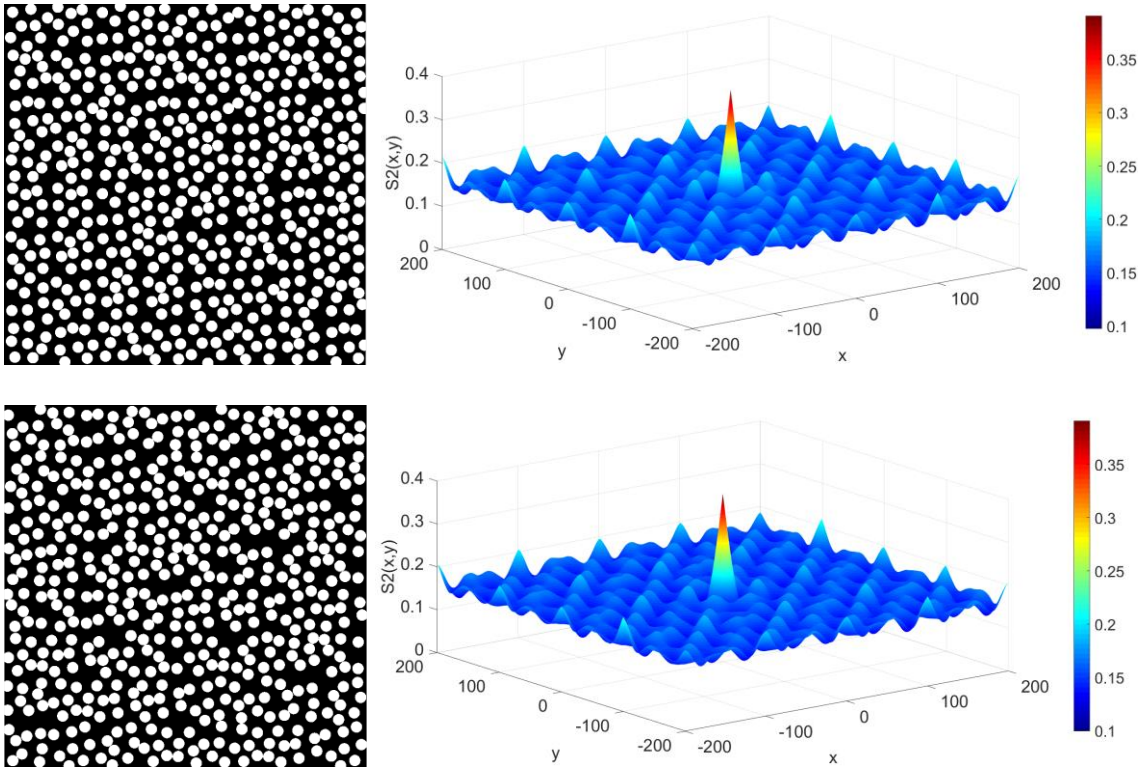

Fig. 4-32 Verification of optimization – Reference structure via Wang tiling
Top: Reference tiling and appropriate statistical descriptor
Bottom: The best arrangement and appropriate statistical descriptor

There is no obvious visual match of the optimized domain with the reference one as in previous two examples. Therefore the best result is compared with other artificial samples with particular inclustion positions. The first artificial structure is composed of tile set, where particle positions are the same for every tile. Thus the final domain is equvivalent with the system of the Periodic Unit Cell. Moreover particles are arranged to regular form corresponding with the tile shape.

The Wang tile set for the second case include randomly arranged particles. Such a domain can be achived by means of sequential adsorbtion or with utilization of the proposed algorithm for tile set generation but without modificiation of velocities during the process.

The third and the fourth comparative samples are based on the original reference media. The first modification rests on shift of randomly chosen particle in each tile by approximately particle radius. With the second modification on half of shifted inclusion from the previous case turn back to the original positions. Since a number of each tile copies in the final tiling is the same, the set modificiatios are proportionally identical to the number of adjusted positions of all particles. The error on descriptor comparison is given by 12.5% shifted particles (from all particles in the tiling) for the first case and by 6.25% for the second case. The Wang tile set of the observed cases are shown on Fig. 4-33. The next figure, Fig. 4-34, displays binary form and descriptor of a realization for each case under investigation.

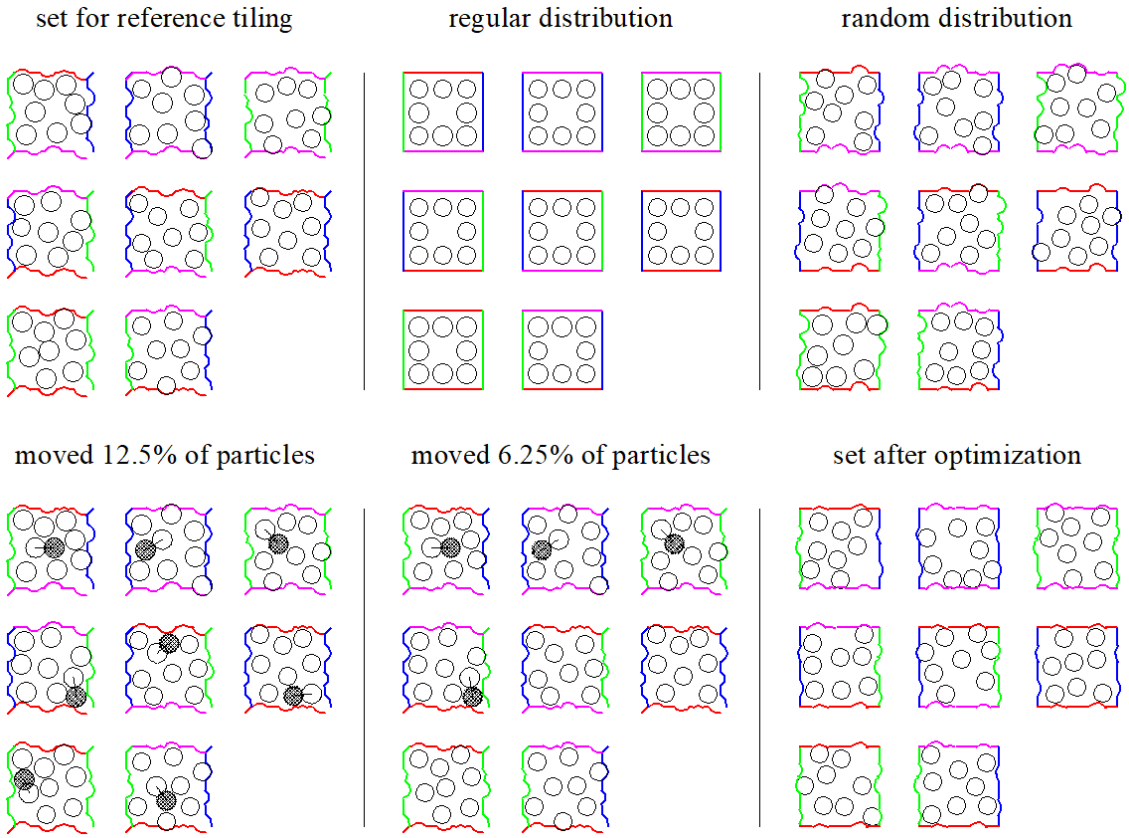

Fig. 4-33 Wang tile sets for verification of optimization technique

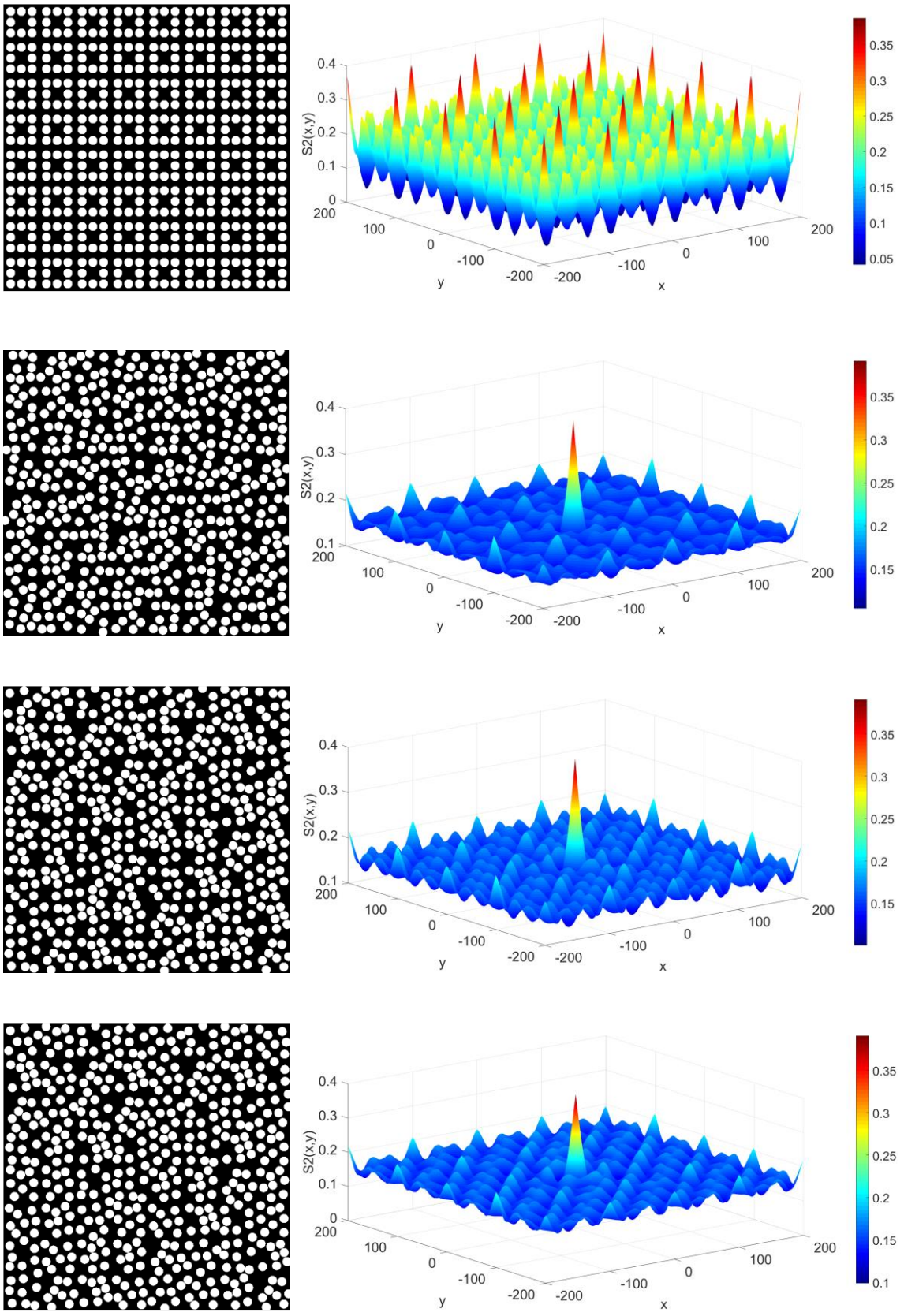

Fig. 4-34 Tilings for verification of optimization technique
regular distribution of particles, random dibstribution of particles,
12.5 % particles moved, 6.25% particles moved (both in comparison with reference tiling)

Comprisons of the error of the individual tests together with the optimized solution are in Tab. 4-7. It is obvious that the optimized solution by its error on the statistical desktoptor corresponds to the realization of the sample, in which less than 6% of the particles have been shifted compared to particle arrangement of the reference tile set. With proposed algorithm we get a state which can be designated as a local optimum. The reaching of the global one is not in scope of this work.

In Fig. 4-35 is the convergence of the optimization method or the objective function respectively for a single realization. The secondary image maps the overlap of particles with final dimension during the algorithm. Here, the overlap represents the sum of the differences between the theoretical minimal and the current distance distance of centres of investigated particle pair. The trends of the graphs correspond to each other. In order to prefer those solution, which offers minimal or zero overlap, a total overlap is increased tenfold and this value is added to the objective function as a penalty.

Tab. 4-7: Results for reference structure via Wang tiling - comparison

Regular particle distribution	296.6
Random particle distribution	20.1
12.5 % particles moved	5.5
6.25 % particles moved	2.3
Number of optimized realizations	5
Minimal value of objective function	1.9
Average value of objective function	2.4

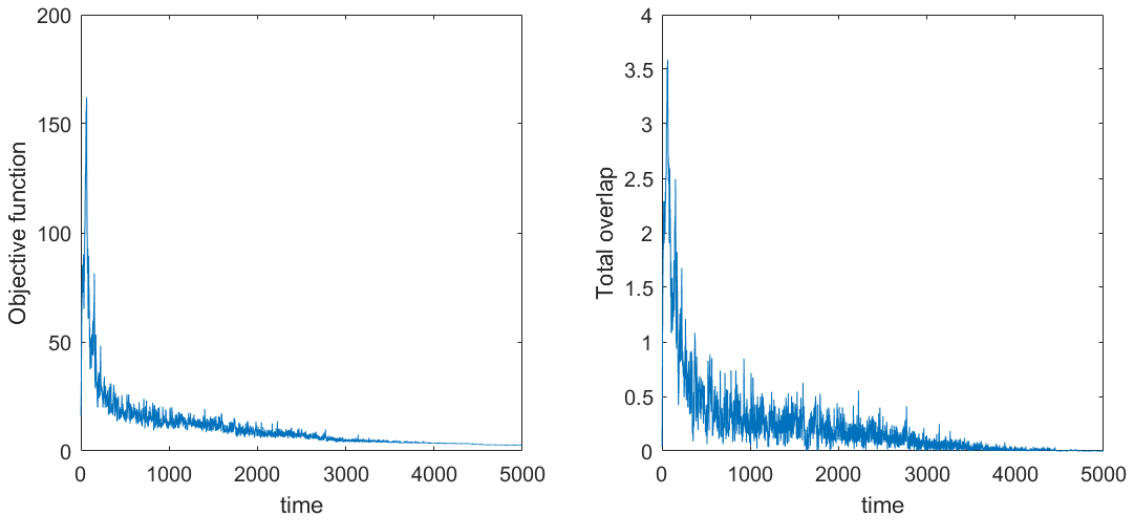

Fig. 4-35 Convergence of optimization and overlapping

4.3 Microstructure reconstruction

This part of the thesis deals with models of real material structures using knowledge of the previous chapters. Here we have two samples that represent systems where the base material is reinforced with long unidirectional fibers. Specifically, the first material is a ceramic matrix composite reinforced with silicon carbide fibers [61]. The second sample is the aluminium basic material reinforced with carbon fibres [62]. By their very nature, both samples represent 2D microstructure with circular hard monodisperse particles in a matrix. Our main goal is to create a Wang tiling sample, which corresponds the original one when compared statistical descriptions.

4.3.1 Ceramic composite – settings

The first microstructure in Fig. 4-36 contains 207 inclusions. We count to this value only particles with centres inside the sample. Inclusions with center out of the micrograph are excluded from any other investigation. Thus the volume fraction is approximately 0.31. The arrangement of inclusion is not uniform, but fibres form both clusters and areas with rattlers. This is confirmed by the pore size histogram in Fig. 4-36. The size of the sample and number of inclusions within allows to mimic microstructure with just one tile or a cell. But we do not leave the idea of utilization of small Wang tile set W8/2-2 with low number of individuals inside. If we compare the pore size histogram to samples where tile size has been investigated, subchapter 3.3, the number of particles has to be different for at least some of tiles from the set.

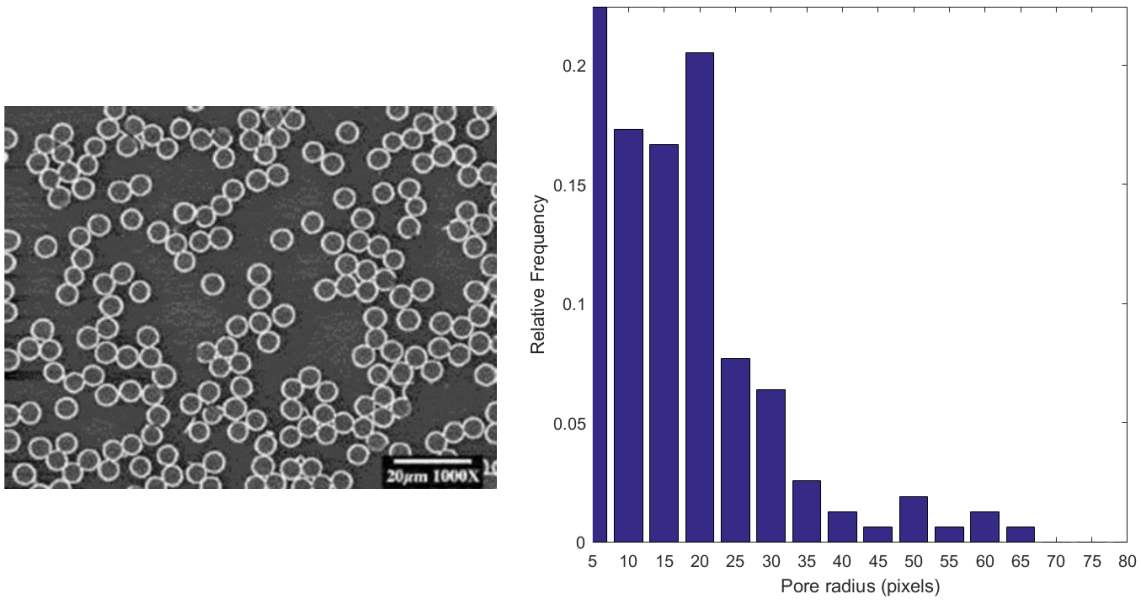

Fig. 4-36 The first reference [61] and apropriate pore size distribution

To determine the number of particles in every individual tiles we use the concept where the reference sample is scanned by a frame of the tile size. This can be done with several ways. The first option is to place a frame randomly, for example with Monte Carlo principles, in the area of reference sample and count for every iteration the number of particles inside. Simplifying version requires division of the medium into a lattice, where size of cells equal size of tiles. Recording the number of particles and creation of a frequency histogram are the same for both principles. Here we use the second option. Since the dimension of the reference sample does not correspond exactly to any multiple of tile size, its peripheral areas have been cut off. The graphic form of the whole process is shown in FIG 4-37, including the number of inclusions inside the cells. Here, again, particle is assigned to certain cell only if its center lies inside. The number of particles varies in range from 2 to 11, but 10 particles include no tile. Now we have 9 types of cells based on a number of inclusions, Wang tiling W8/2-2 offers only 8 tiles. In addition, the first and the last number shows up only once in the whole lattice, while the cells with 7 particles can be found eight times. Therefore, it is necessary to determine the individual tile volume franctions with emphasis on both the range and the frequency of particle numbers.

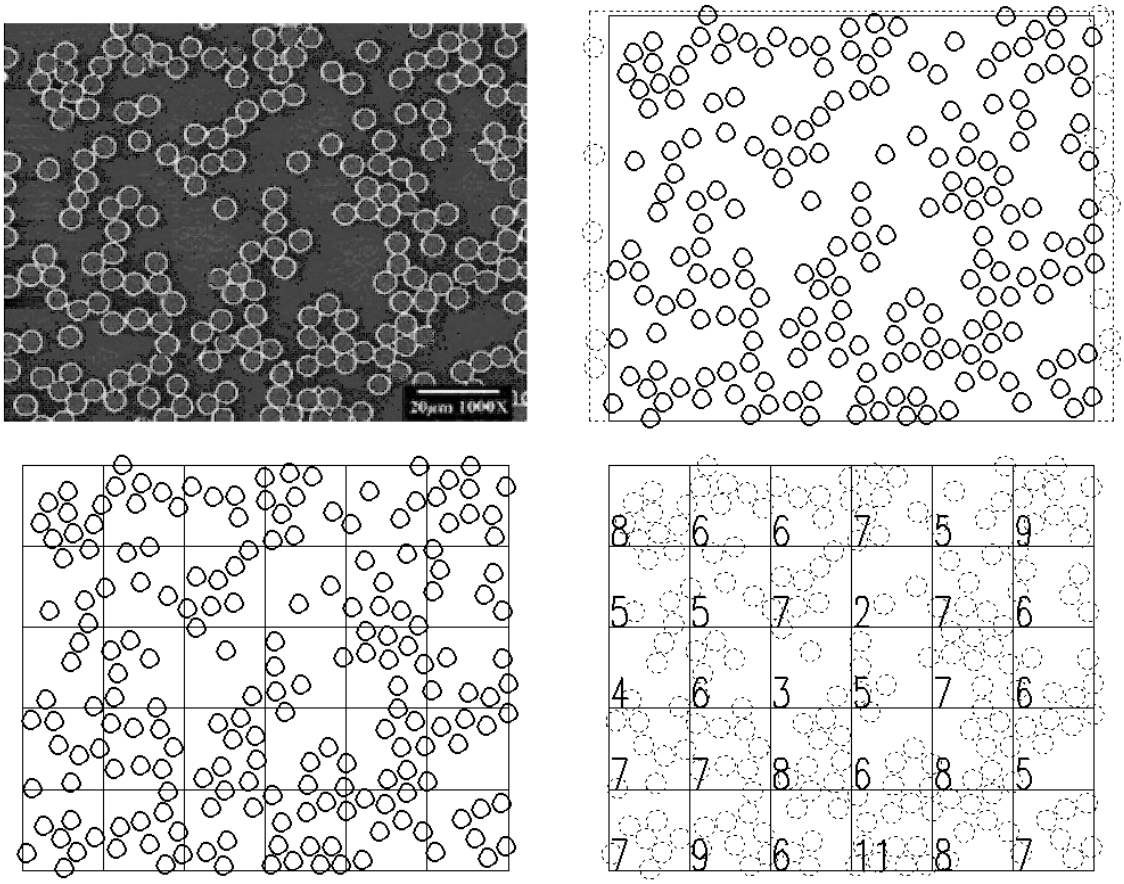

Fig. 4-37 The first reference – partition for estimation of particle number in tiles from upper left row by row to lower rlght: reference sample, cut off for tiling, tiling lattice, number of particles in a cell

Determining the number of particles in the set of tiles is according to the following algorithm. Sequences of cells from the reduced and divided reference sample are assembled ascending based on the number of inclusions contained therein. This string of cells is divided into number of parts corresponding with the number of tiles in Wang tile set, where each portion include the same number of cells (not necessarily integers). Then we calculate the weighted average for each part. These values after rounding define the number of particles in each tile. An exception is the last tile where the number of inclusions prefers the highest number in lattice. Final tiling for the reconstruction of the first real sample include 30 tiles. This number is not completely divisible by the number of tiles in Wang tiling set. Therefore it is not possible to reach the same probability of occurrence of all tile types. The basic set of Wang tiles is shown in Fig. 4-38 together with tiling sequence that will enter the optimization process. The particle arrangement is here only illustrative but exhibits real number of particles assigned to appropriate tile. The radius of inclusion is 12.5 pixels and size of each tile edge is 100 pixels in order to keep the system clear and simple with possible comparison to tilings in previous chapters.

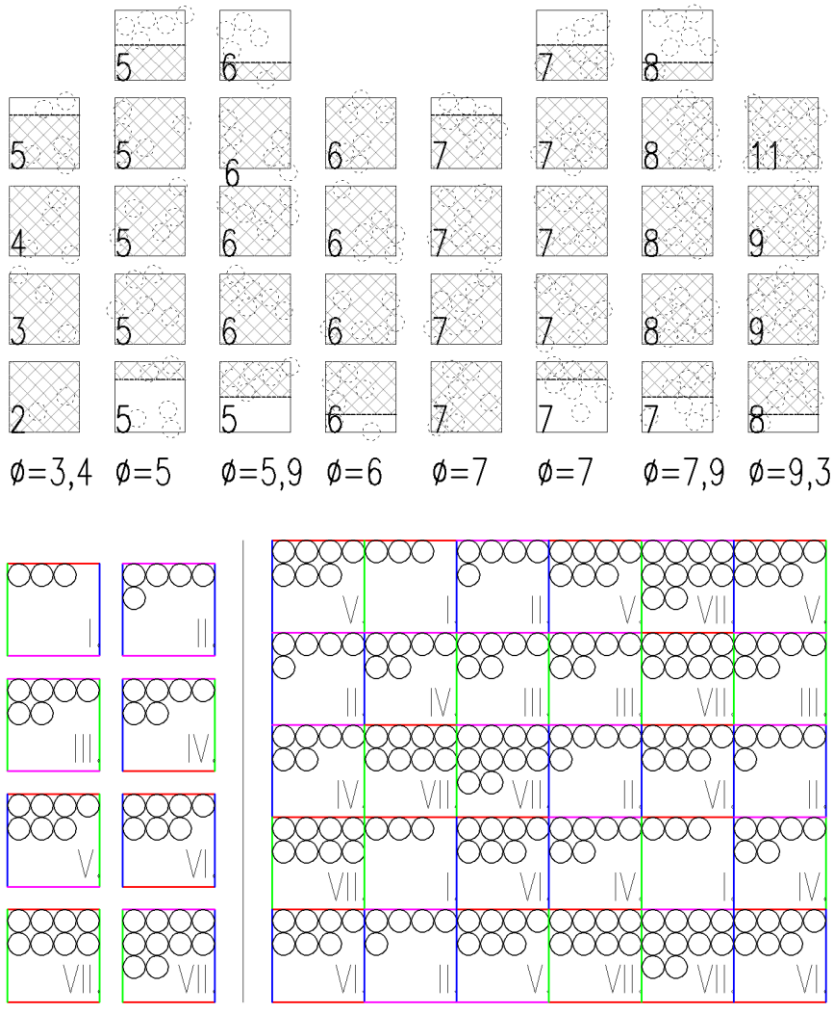

Fig. 4-38 The first reference – definition of Wang tile set W8/2-2, tiling sequence

4.3.2 Ceramic composite – results

The reference samples for verification of the optimization process consist of Periodic Unit Cell or utilize Wang tile set W8/2-2, see subchapter 4.2 Verification. The results of the two-point probability descriptor for the reference and optimized sample have taken into account secondary extremes. If we compare tiling of the same type and sequence, the error on the descriptor in these areas is minimal compared to situation, where the reference sample represents a real microstructure. Therefore optimization procedure on real samples is divided into three subtasks. First two cases enables to check the results visualy by comparison of descriptor on parts of 2D sections. The first monitors variance on the descriptor only in the area defined by the particle diameter from one side and the size of the tile on the other side and only in one direction. Therefore, the issue is reduced to optimization of 2D curve of given region. Because of these conditions, the algorithm focuses primarily on the inner region of each tile and its closest neighbors. At the same time, the effect of the difference on primary extremes is eliminated. These parts represent the overlapping and the error on the binary representation or volume fraction respectively.

The results of this task are shown of Fig. 4-39. Graphic form of descriptor for 3 structures are depicted here. One respresents the reference sample, while the others are based on Wang tiling. The red curve corresponds to reference sample, the green one to the best optimized structure and the last (blue one) represents one realization of system with randomized particle positions. The right side graph shows results in perpendicular direction in order to underline optimized results from the left diagram. The initial part of the graph for all systems is the same due to the nature of descriptor and monodispersed particles. In the observed area and direction the reference and reconstructed medium coincide and indicates the success of the algorithm. Conversely, in the second direction without optimization exhibits significant secondary extremes.

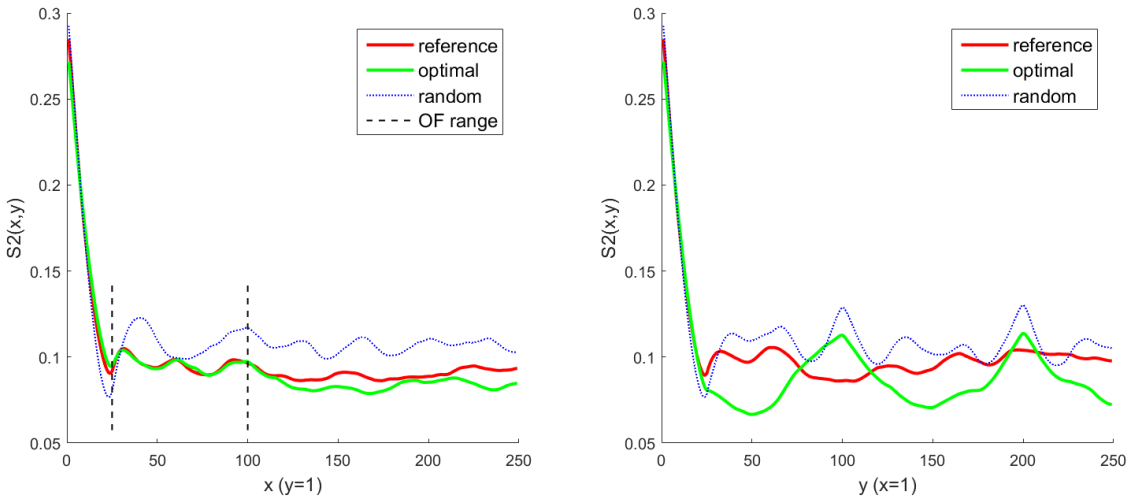

Fig. 4-39 The first reference – optimization only in horizontal direction
left: descriptor in horizontal direction; right: descriptor in vertial direction

The second case focuses on representatives of both horizontal and vertical direction. The objective fuction is based on comparison of two sets both with the same importance. Moreover there is no reduction of observed area. Results take into account both initial area, where particle can overlap during the algorithm, and secondary peaks caused by tiling nature. The diagram on Fig. 4-40 shows curves of three microstructures: the reference one, the best of optimization process, and one with randomized particles.

The reconstructed medium with its statistical description trace the reference one. The main difference is in area that corresponds to the size of the tile. Nevertheless, this effect is considerably reduced in comparison with system of random particle positions. Such a reduction can be reached because of Adaptive Walls concept but also due to the low overall tile numbers.

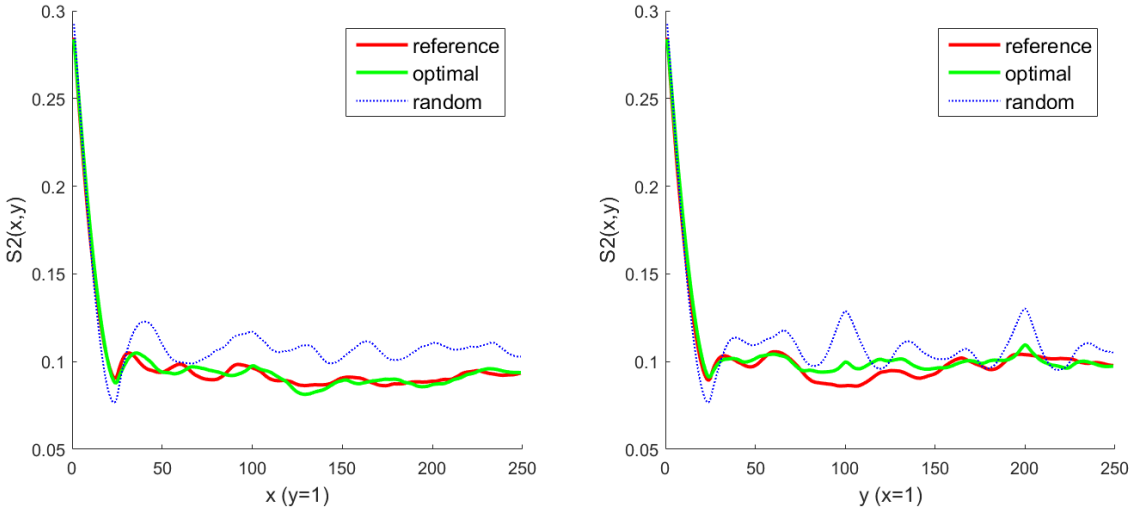

Fig. 4-40 The first reference – optimization in both horizontal and vertical direction
left: descriptor in horizontal direction; right: descriptor in vertial direction

In order to generate optimal images of the real microstructure, the desired areas of exploration are extended to all directions. The following Fig. 4-41 presents binary form and appropriate probability function of reference, best optimized, and randomized domains. The distribution of pore size or matrix islands respectievely appears in the Fig. 4-42. Unfortunately, the visual analysis of these results is not conclusive in terms of confirmation of optimization usefullness. The two-point probability graph is smoothed in the area of secondary extremes, but pore size distribution exhibits random behavior than corresponing to the reference medium. As a comparable parameter serves value of objective function as definied in the beginning of this chapter. These characteristics for 10 runs of optimized process are summarized in Tab. 4-8.

Tab. 4-8: Results of optimization for the first real sample

Number of realizations	10
Minimal value of objective function	7,7
Average value of objective function	10,1
Objective function for random arrangement	20.1

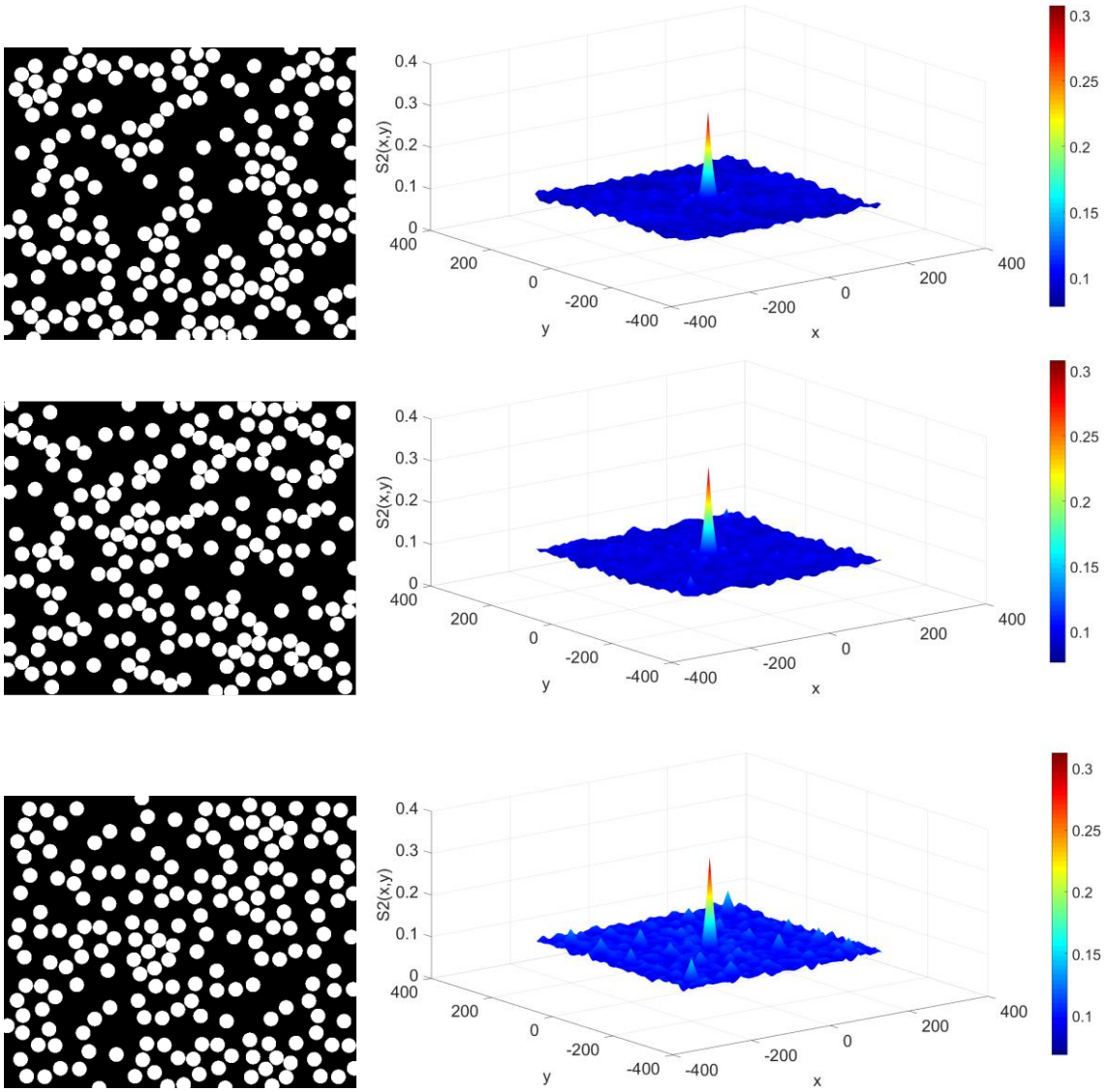

Fig. 4-41 The first reference – results: S2 descriptor comparison
from top: reference sample – cutout, Wang tiling after optimization, Wang tiling random

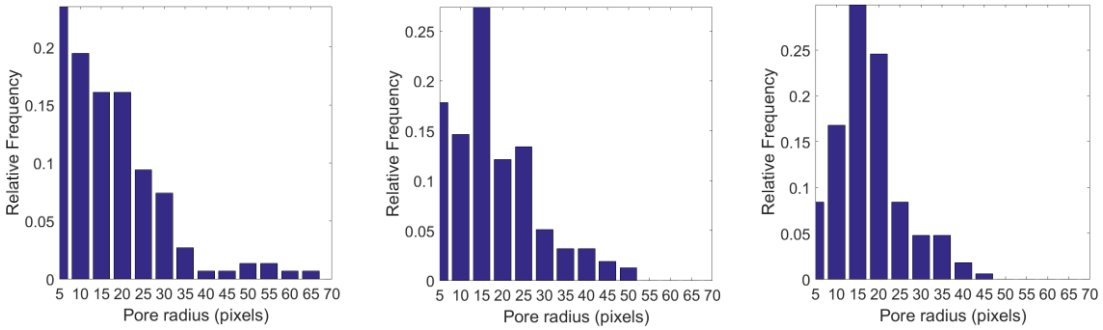

Fig. 4-42 The first reference – results: pore size distribution comparison
from left: reference sample – cutout, Wang tiling after optimization, Wang tiling random

4.3.3 Metal composite – settings

The second real micrograph symbolizes composite where carbon fibres reinforce aluminium matrix. The fragment is smaller than for the first case, but the particle volume fraction is higher. Although the range of pore size and its frequency is not as diverse as in the first sample, it is still necessary to define a base tile set with a different number of particles within. All of this with assumption of normalized 25 pixel diameter and the 100 pixel edge of the tile. The principle of determining the number of particles in each tile is analogous to the previous case. This time there is a lattice of 3x4 cells, thus the tiling consists of 12 tiles. Further investigation is done on reduced sample with total number of particles equal to 125. Separation of inclusions to cells build basis for estimation of volume fractions for Wang tile set.

The graphical form of above described process is on Fig. 4-43, while pore size histogram is shown on Fig. 4-44. And finaly Fig. 4-45 illustrates the creation of tile set in terms of particle numbers and displays tiling sequence for microstructures under optimization procedure. The number of discs in appropriate tile is defined by weighted average after division of order cell string. An exception is the fifth member of the set that reflects both the weighted average and representative numbers in cells of original domain.

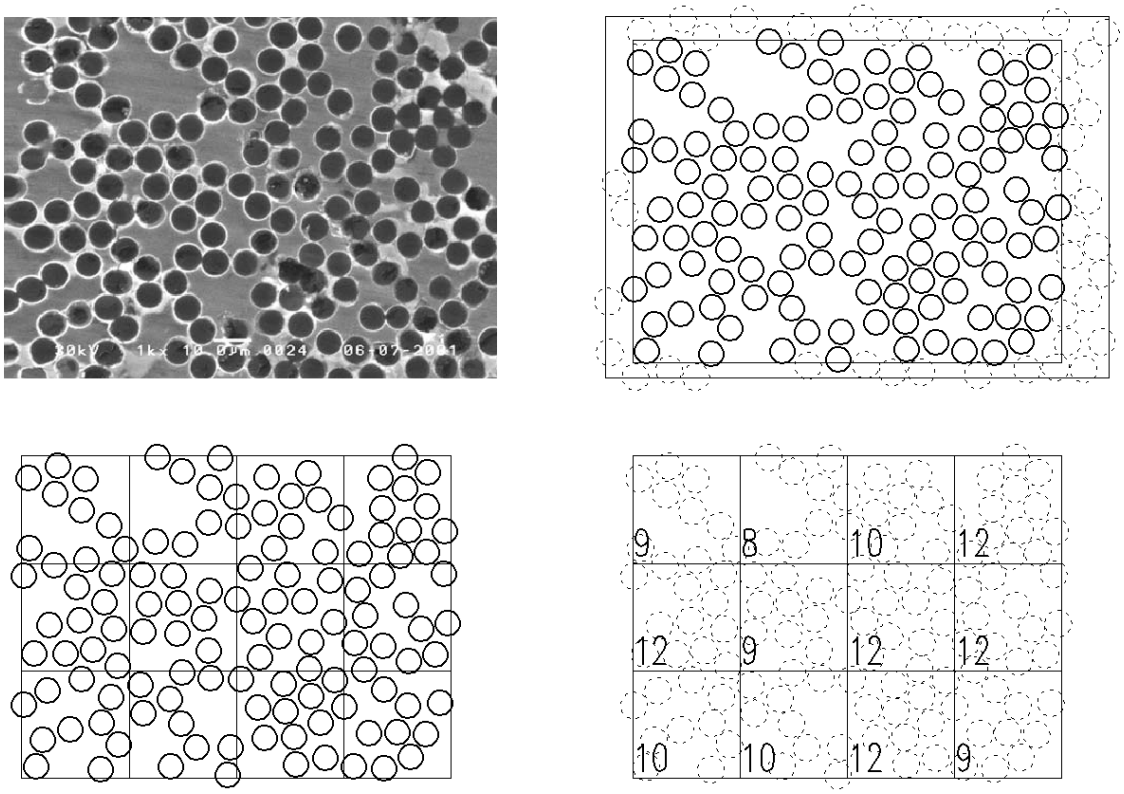

Fig. 4-43 The second reference – partition for estimation of particle number in tiles from upper left row by row to lower rlght: reference sample [62] cut off for tiling, tiling lattice, number of particles in a cell

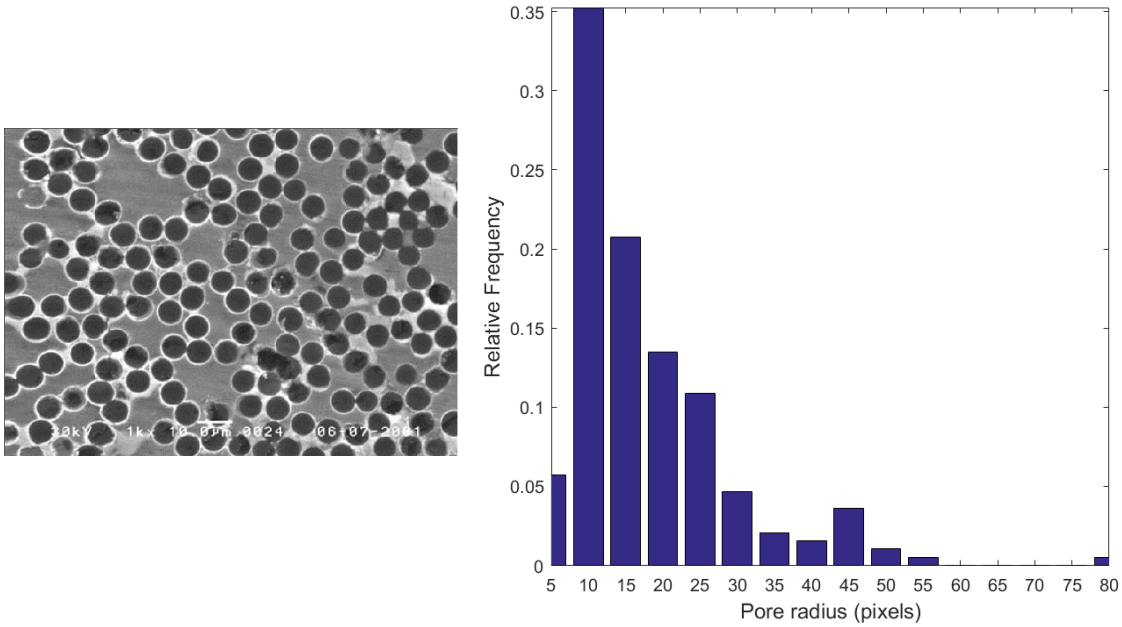

Fig. 4-44 The second reference – pore size distribution
Reference sample [62] and pore size distribution

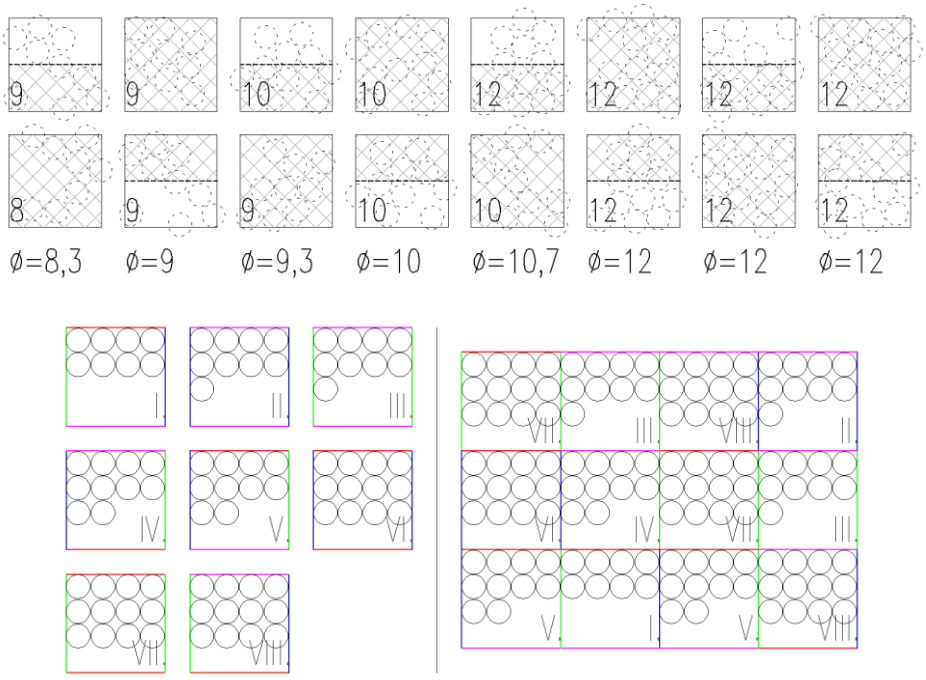

Fig. 4-45 The second reference – definition of Wang tile set W8/2-2, tiling sequence

The particle arrangement in tiles is illustrative. The initial positions of particles remain randomized. Because of the small size of the reference and the chosen tiling sequence, one half of tiles is used in tiling just once. Therefore benefits of Adaptive Walls on final optimized domain are reduced in comparison with tests of boundary conditions, see subchapter 3.2.

4.3.4 Metal composite – results

We use for the second real domain the same optimization schemes as for the previous one. The first objective function observes descriptors in horizontal direction in range of 25-100 pixels. This setting does not take into account the differences in volume fractions due to the theoretical overlaps of particles with final sizes in the course of the algorithm. On the contrary, the range is chosen to cover the size of the tile and related secondary extremes, if they occur. The results of the first optimization process are shown in Fig. 4-45. This figure exhibits, in addition to curves for the reference and optimized sample, result for randomized microstructure. Here, the term randomized represents microstructure composed via Wang tiling of the same tiling sequence as the optimized one but with random positions of non-overlaped particles. This arrangement is achieved by proposed principles for Wang tiling with molecular dynamics but without modification of velocity vectors. In order to highlight the results, the second group of curves on Fig. 4-45 displays statistical description of described domain in direction which is not a part of the optimization process.

The recorded results are the best known in the course of the algoritm, but they are not the final ones. Since the first part of the diagram has not been considered or penalized, the curves are slightly diverted in this area. However, in the investigated area, the reference and generated medium, respectively their statistical description, coincides. The curves differ both in the end part of the first plot and completely in the opposite direction.

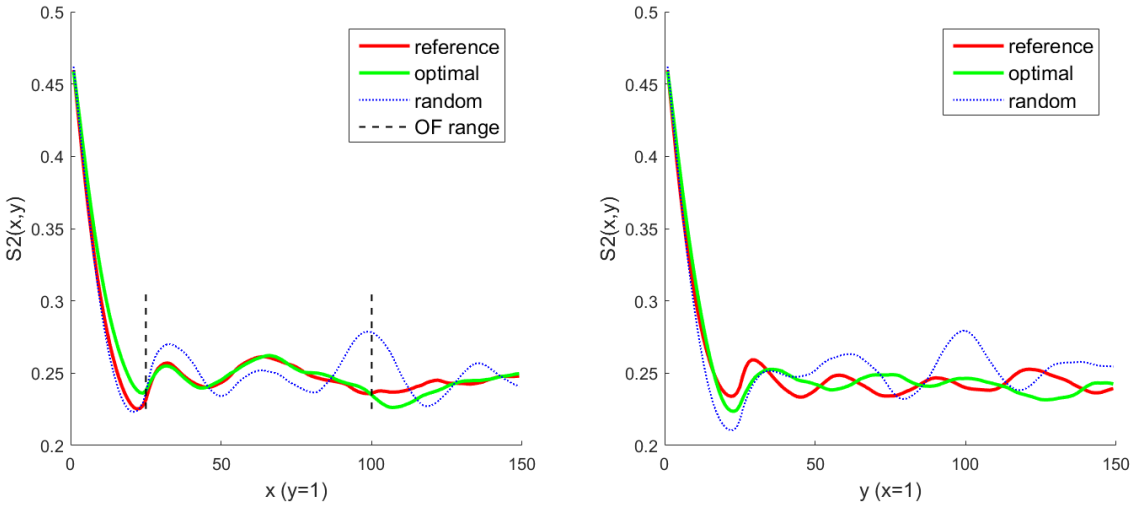

Fig. 4-46 The second reference – optimization only in horizontal direction
left: descriptor in horizontal direction; right: descriptor in vertial direction

An expansion of the area for objective function definition is a part of the second case. The optimization process include information from comparison of both horizontal and vertical direction. The range of compared area is 0-150 pixels. Such a settings takes into account both reduction of secondary extremes and theoretical overlapping during the optimization.

The best match for the observed area is achieved with an arrangement that do not contain overlapping particles. Comparing the curves for random and optimal microstructure, we can detect minimization of the secondary extremes. However, in these areas, which corresponds to the dimension of the tile, still remains the most striking difference between the compared trajectories. This phenomenon is based on the nature of the tiling and its influence in general cases can only be minimized, not eliminated.

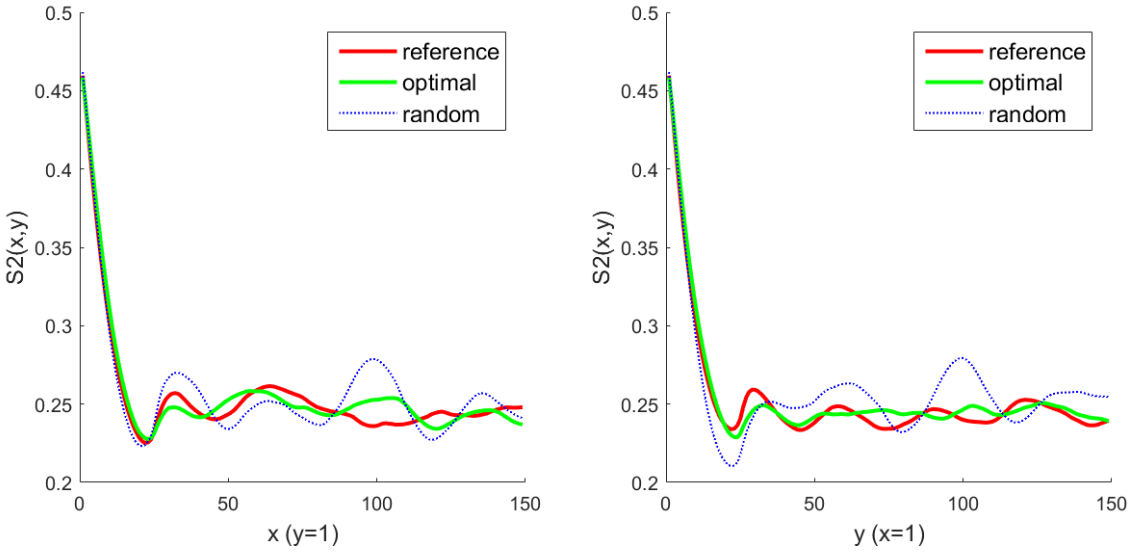

Fig. 4-47 The second reference – optimization in both horizontal and vertical direction left: descriptor in horizontal direction; right: descriptor in vertial direction

The objective function for the last case take into account description square area in range from -150 to 150. The binary representation is displayed in the Fig. 4-46 together with appropriate two-point probability function. Again we have here reference, best optimized and randomized structure. The arrangements of generated systems are the final ones. The next Fig. 4-47 shows the pore size distributions of binarized domains. Here the last randomized microstructure exhibits narrow range of pore sizes. This result corresponds to the binary scheme, where particles are arranged more or less in homogenized form with similar distances between each other. But this is just matter of randomization and has no corresponding value. On the other hand reduction of secondary extremes when compared optimized and randomized structure underline benefits of proposed approach. The comparison of the final values of the objective function serves as one of the best guide of optimization method success, Tab. 4-9. Despite the significant reduction of observed values, there is still a space for improvement, which is discussed in following part of this work.

Tab. 4-9: Results of optimization for the second real sample

Number of realizations	10
Minimal value of objective function	7,2
Average value of objective function	9,8
Objective function for random arrangement	27.7

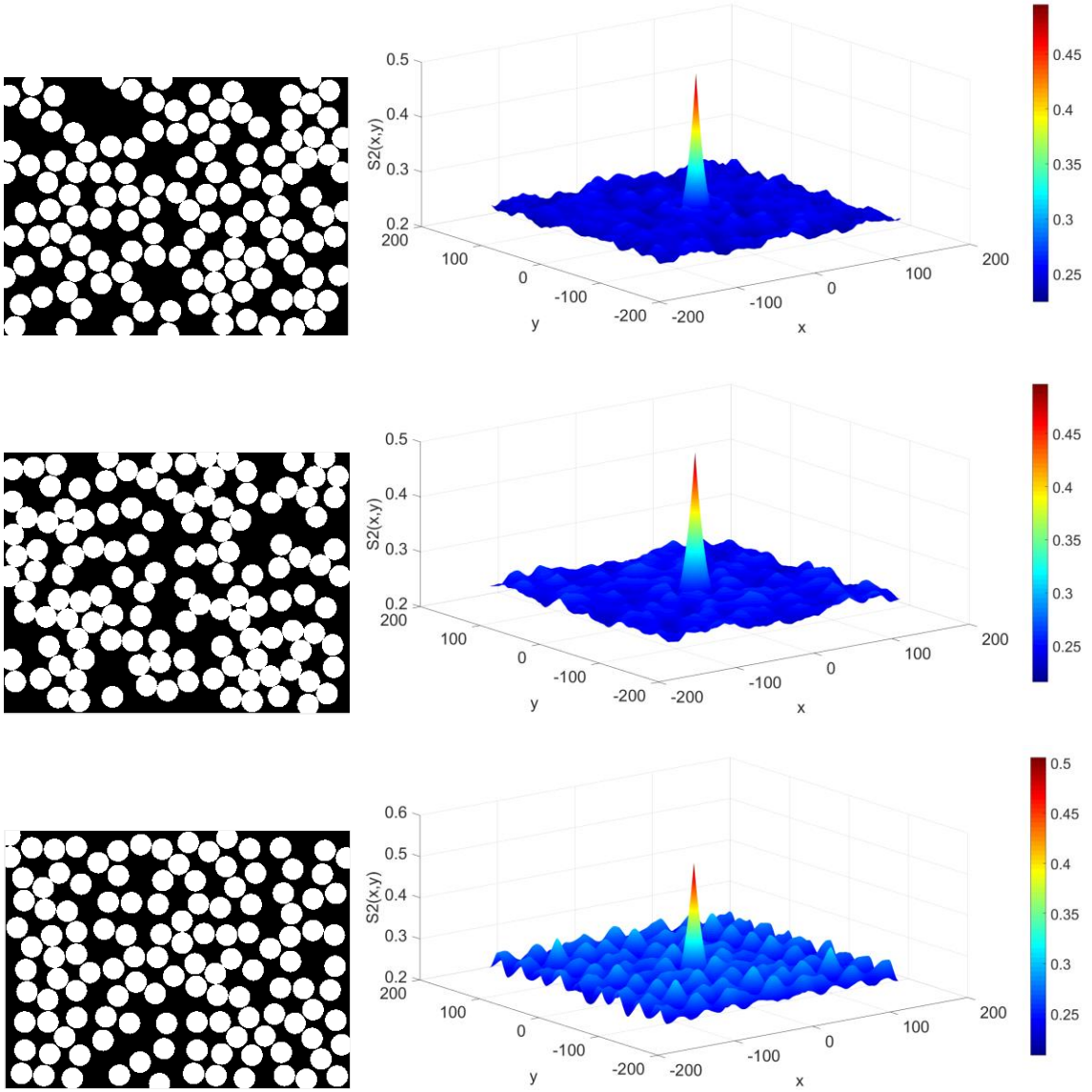

Fig. 4-48 The second reference – results: S2 descriptor comparison
from top: reference sample – cutout, Wang tiling after optimization, Wang tiling random

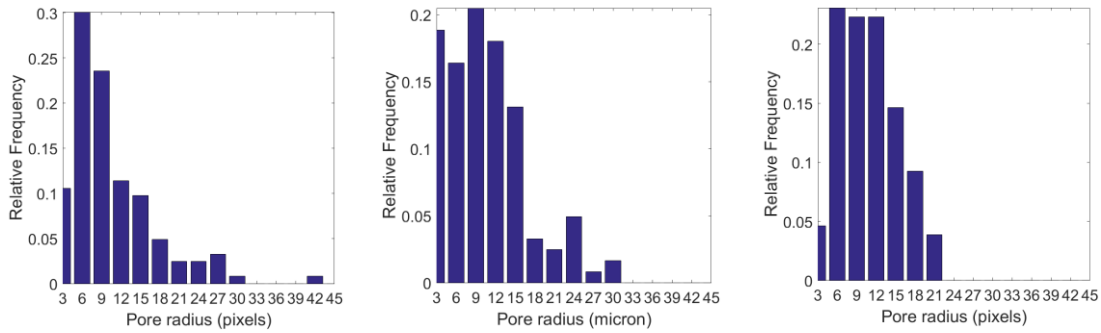

Fig. 4-49 The second reference – results: pore size distribution comparison
from left: reference sample – cutout, Wang tiling after optimization, Wang tiling random

4.4 Discussion

Despite the best author efforts, the optimization as well as tiling process suffer from some shortcoming. In this subchapter we discuss possible reasons why this phenomena occurred and outline possible ways how to eliminate or at least minimized them.

4.4.1 Microstructure description issues

The reference rectangular samples have normalized size of approximately 500x600 or 300x400 pixels. Within these reduced areas of original micrographs we have 193 or 125 particles respectively. Contrary both the pioneer work with Wang tiling approach in material engineering [9] and following contributions [10], [11] deal with multiple times larger samples. The reduction has been made in order to prepare a lattice of tiles of certain dimension. The definition of two-point probability function with hypothesis of ergodicity contains "infinite" sample volume area [1] REF 2-41 This reqirement can be replaced with periodical extension. But in our case we keep the reduced sample dimensions. This simplification leads inter alia to absence of graph convergence to combined probability for large distances of tested pair of pixels. In order to stay consistent, optimized samples are based on the same assumptions as the reference ones. The optimization algorithm focuses only on relative values of compared statistics and therefore simplification of reference sample has no direct impact on evaluation of success of proposed approaches.

On the other hand improvement could be in the form of a reduction of the pixel mesh fineness. In general cases meshes with lower number of pixels cause distorsion and neglection of information on statistical description [48]. But for particle systems with hard inpenetrable circles the resolution affects mainly possibilities in inclusion motion. In our case the diameter of particles has 25 pixels, Novak et al. in [9] work with template where circle has a diameter of 10 pixels. Similar assumptions reduce the degree of freedom of the searching space in optimization process and may help to reach better conformity of the reconstructed microstructure with the reference one. In our case there is space for improvement just in the field of optimization containing information from all direction in comparison with tasks, where objective function observe results in one or two cetain directions.

4.4.2 Improvement in optimization

In the preface of the fourth chapter, general optimization process has been divied into four optimization tasks: optimization of tile size, number of particles in tiles, tiling sequence, and position of particles in tiles. This thesis deals mostly with the last member and here we briefly comment also other issues from the package.

The tile size has a constat value based on investigation of particle arrangements, particle geometry and recommendations for the Particle Swarm Optimization techniques. Specifically, it equals to four diameters of the largest particle size, which allows to be with the specified volume fraction in the area of the R arrangement. The overall number of particles is bellow maximal number of individuals for space searching of the traditional PSO. It is important to note that the number of inclusions in the tile set varied based on the material scan. But if we want to create a set with the same number of particles, it is necessary to choose the size of the tile with respect to the required volume fraction. In general, the size of the tile is another variable in deffinion of the tile set and corresponding realizations of reference sample. In contribution [10] authors observed the particle size dependence on the results of the optimization task with objective function consisting of the two-point probability statistical descriptor and a mechanical compatibility. In general, the increase of tile size also shifts the secondary extremes of the two-point probability function. Nevertheless, new proposed Adaptive Walls concept of boundary conditions allows to reduce these influences and tile size as well. The secondary advantage of this proposal lies on savings of computer demands.

The number of particles in the tile and their optimal arrangement is closely related to the tile size. Either with regards to dense packing or general volume fractions. If the medium exhibits higher heterogeneity, the problem of particle numbers in tile can be solved in two ways. The first is based on mirrostructure lengths and the total volume fraction, where each tile of the set contains the same number of inclusions. This approach leads to relatively large tiles and to higher computational demands. The second option allows to have a set with tiles of different volume fractions. In this case, it is necessary to track the tiling algorithm in order to meet the conditions of both the total and partial volume fractions. The number of particles in each individual tile can be based on the scan of reference sample. Here we offer also two options. The first one requires sufficient number of randomly thrown epty tiles in the microstructure while with the second one the reference fragment is divided into lattice of cells with the dimension of Wang tile. Both principles later work with histogram of number of particles inside these cells. This approach together with weighted averge allows to create tile set for highly heterogeneous microstructures.

The principles of the stochastic tiing enables to create various realizations of different tile sequences with usage of a single tiles set, where particles has certain positions. The tilings in this work have relatively small number of tiles and optimization procedure works on specific sequence of tiles. Moreover we used tile set with different individual tile volume fractions. This modification together with Adaotive Walls approach easily minimized periodicity artefacts. But for general cases stochastic tiling produces areas with multiple copies of the same tile.

This phenomenon can be solved with modification of tiling algorithms. On one hand there is a possibility to enlarge tiling set, either with full sets or with additional colours (codes) on tile edges. The other group of solutions deals with tiling process. When we track a sequence of tiles and observe tile neighbourhood, the probability of acceptance of certain tile can be modified [63]. Another option is to involve optimization techniques to tilings [64]. The last but not least solution replaces stochastic tiling with aperiodic tiling [15], [16].

The technique for optimization of paticle positions proposed in this work can be improved in several ways. The first is setting of the PSO parameters. In our implementation parameters follow general recommendation. But the part of general algorithm, which reflects the best position of the individual is replaced in our formulation with a random vector in order to escape from local optima. If we focus on convergence of the best so far solution over 4000 time steps of one optimization trial for the task of reduced comparable area Fig. 4-50, obviously the penalty for overlap particles is too small. The absolute minimum has been achieved after approximately 70% of total time steps. But if we equip the penalty with a large value, optimization algorithm became blind. The degree of blindness would depend on tile volume fractions. Materials with high volume fractions and small number of particles in tile exhibits first arrangement without overlapping usualy too late and algorithm converges to this local optimum. Similar behaviour occurs when we set initial arrangement without overlapping particles. Such a system can be generated via proposed algorithms but without velocities optimization. But this solution is preffered to others and proposed optimization technique find the best positions in neighbourhood of initial values. An interesting and promising option is implementation of hybrid techniques or even optimization algorithms based on population of individuals [54].

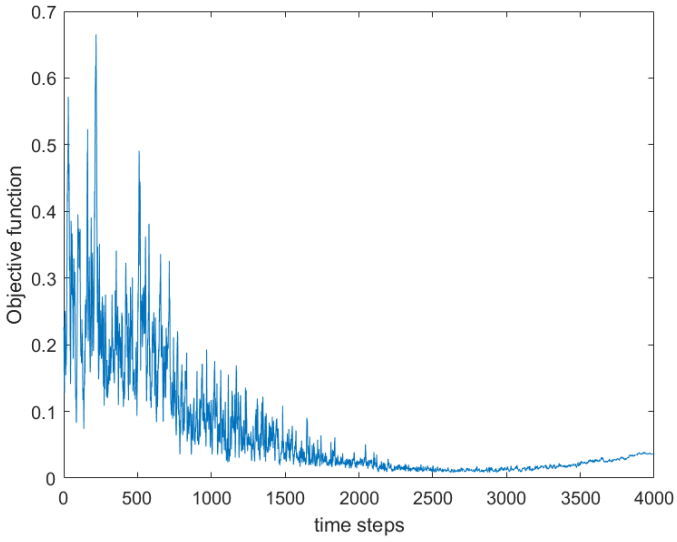

Fig. 4-50 Convergence of optimization technique for the first real sample reduced comparable area

4.4.3 Application of the algorithms

This work deals with optimization of just one function based on comparison of statistical descriptors. But for some issues in material engineering such comparison is inadequate [10]. However, the whole proposed algorithm works in a general sense if we are able to define an objective function. The remaining questions are convergence speed or reaching either local or global extremes of an objective function. These results depend on settings of an optimization method and initial and boundary conditions as well. In order to obtain valid results, we have to define parameters for wide range of optimization tasks or to perform test and gain exact values for settings applicable only to specific function.

The Adaptive Walls approach has been used in this work only for Wang tiling set W8/2-2 for 2D application and W16/2-2-2 for single illustration for 3D case. But the definition allows to use this type of boundary conditions to sets with more edge information or even aperiodic tilings. Nevertheless, we have to keep on mind, especially in connection with molecular dynamics, that faultless behaviour requires check of every possible combination of neighbour tiles where particles tend to leave. Thus any extension of edge information leads to increased computational demands. This disadvantage might be reduced with utilization of parallelization techniques. Then each tile can be solved separately until any particle cross the tile edge. But after recalculation of velocity vector tiles can live their own lives.

In this work we focuse on materials which include circular or spherical particles. But the greatest benefit of this work – Adaptive Walls – is able to be incorporated to modelling of materials with various particle shapes. If we implement border areas where phases of pixels can be switched, the method became universal and capable to deal with models even without particles or with particles of general form. A simplified visualization of Wang tiling set W8/2-2 is shown in Fig. 4-51 with Adaptive Walls concept and particles of various shapes.

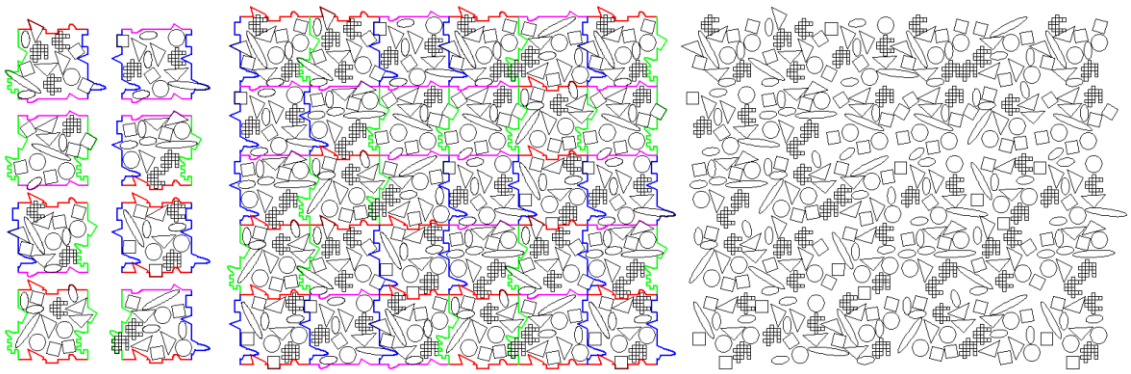

Fig. 4-51 Wang tiling with Adaptive Walls – particles of various shape

5 Conclusions

This work deals with modeling of random heterogeneous microstructures. Particular emphasis is placed on particle material domains, where circular or spherical inclusions are arranged in the matrix. Traditionally, such structures are modeled by a system of the same cells with periodic boundary conditions. However, in material engineering there are tasks where it is necessary to keep sample heterogeneity and minimize periodic artifacts. The solution, how to preserve randomness and heterogeneity is an application of the Wang tiling. This method is able to generate infinite aperiodic tiling via a small finite set of tiles. In the field of material engineering, we are satisfied with the stochastic tiling, which was also implemented in this work.

With respect to the type of microstructure, the basic set of tiles is generated by molecular dynamics. Although the tiling itself reduces the periodicity compared to the Periodic Unit Cell concept, the edge information (particle beyond the tile edge) is repeated with every single occurrence of the same colour on the edge. With a new type of boundary conditions - Adaptive Wall - it is no longer necessary to assign the particles to the edges. This significantly reduces extremes on two point probability function even for tile set with low number of particles. The veracity of these theses was tested on a number of artificial 2D microstructures both mono and polydisperse and on a single sample of 3D spherical microstructure.

In the next part of the thesis we focused on generation of optimal microstructures via comparing the statistical descriptors with the reference medium. It was represented by both 2D artificial samples and chosen real composite microstructures. We introduced the principles of the modified Particle Swarm Optimization (PSO) method into molecular dynamics. The modification consisted of the absence of the cognitive part replace by random vectors, but also of the other control parameters settings. The generated microstructures coincided with the reference, if this is an artificial samples composed of tiles. For real microstructure, the algorithm was highly reliable in optimizing statistical descriptor segments. There is a space for improvement especialy for tasks with comparison of large areas, but proposed algorithm determined local minimum even for this kind of problem.

The most of proposed procedures and algorithms are valid for a wider range of types of material structures. Thus in further investigation it would be appropriate to extend modelled particle microstructures by including different inclusion shapes or to implement algorithms to non-particle material domains. This would, however, make the tasks more computationally demanding. Such a problem would be successfully solved by implementation of parallelization techniques. Last but not least we need to focus on the optimization method in order to reach global extremes of investigated functions.

References

[1] TORQUATO, S. *Random heterogeneous materials: microstructure and macroscopic properties.* New York: Springer, 2002. ISBN 0-387-95167-9.

[2] VOJTĚCH, D. *Kovové materiály.* Praha: Vydavatelství VŠCHT, 2006. ISBN 80-708-0600-1.

[3] LAGAE, Ares. TILE-BASED METHODS IN COMPUTER GRAPHICS. Leuven, 2007. Ph.D. thesis. KATHOLIEKE UNIVERSITEIT LEUVEN, FACULTEIT INGENIEURSWETENSCHAPPEN, DEPARTEMENT COMPUTERWETENSCHAPPEN AFDELING INFORMATICA. Supervisor: prof. dr. ir. Philip Dutré.

[4] COHEN, Michael F., Jonathan SHADE, Stefan HILLER and Oliver DEUSSEN. Wang Tiles for image and texture generation. In: ACM SIGGRAPH 2003 Papers on – SIGGRAPH '03 [online]. New York, New York, USA: ACM Press, 2003, pp. 287–294 [cit. 2019-01-10]. DOI: 10.1145/1201775.882265. ISBN 1581137095.

[5] WINFREE, Erik, Furong LIU, Lisa A. WENZLER and Nadrian C. SEEMAN. Design and self-assembly of two-dimensional DNA crystals. *Nature: International journal of science*. 1998, **394**, pp. 539-544.

[6] MAO, Chengde, Thomas H. LABEAN, John H. REIF and Nadrian C. SEEMAN. Logical computation using algorithmic self-assembly of DNA triple-crossover molecules. *Nature: International journal of science.* 2000, **407**, pp. 493-496.

[7] WANG, Hao. Proving theorems by pattern recognition I. *Communications of the ACM* [online]. **3**(4), pp. 220-234 [cit. 2019-01-10]. DOI: 10.1145/367177.367224. ISSN 00010782.

[8] WANG, Hao. Proving Theorems by Pattern Recognition – II. *Bell System Technical Journal* [online]. 1961, **40**(1), 1-41 [cit. 2019-01-10]. DOI: 10.1002/j.1538-7305.1961.tb03975.x. ISSN 00058580

[9] NOVÁK, Jan, Anna KUČEROVÁ and Jan ZEMAN. Compressing random microstructures via stochastic Wang tilings. *Physical Review E* [online]. 2012, **86**(4) [cit. 2019-01-10]. DOI: 10.1103/PhysRevE.86.040104. ISSN 1539-3755.

[10] NOVÁK, Jan, Anna KUČEROVÁ and Jan ZEMAN. Microstructural enrichment functions based on stochastic Wang tilings. *Modelling and Simulation in Materials Science and Engineering* [online]. 2013, **21**(2) [cit. 2019-01-10]. DOI: 10.1088/0965-0393/21/2/025014. ISSN 0965-0393.

[11] DOŠKÁŘ, Martin, Jan NOVÁK and Jan ZEMAN. Aperiodic compression and reconstruction of real-world material systems based on Wang tiles. *Physical Review E* [online]. 2014, **90**(6) [cit. 2019-01-10]. DOI: 10.1103/PhysRevE.90.062118. ISSN 1539-3755.

[12] TURING, A. M. On Computable Numbers, with an Application to the Entscheidungsproblem. *Proceedings of the London Mathematical Society* [online]. 1937, **s2-42**(1), pp. 230-265 [cit. 2019-01-10]. DOI: 10.1112/plms/s2-42.1.230. ISSN 00246115.

[13] CHURCH, Alonzo. An Unsolvable Problem of Elementary Number Theory. *American Journal of Mathematics* [online]. 1936, **58**(2) [cit. 2019-01-10]. DOI: 10.2307/2371045. ISSN 00029327.

[14] BERGER, Robert. The undecidability of the domino problem. *Memoirs of the American Mathematical Society* [online]. 1966, (66), 0-0 [cit. 2019-02-06]. DOI: 10.1090/memo/0066. ISSN 0065-9266.

[15] CULIK, Karel. An aperiodic set of 13 Wang tiles. *Discrete Mathematics*. ELSEVIER, 1996, **160**, pp. 245-251. Available from: https://core.ac.uk/download/pdf/82646448.pdf.

[16] JEANDEL, Emmanuel and Michael RAO. An aperiodic set of 11 Wang tiles. 2015. <hal-01166053v2> Available from: https://arxiv.org/pdf/1506.06492v1.pdf.

[17] BARGMANN, Swantje, Benjamin KLUSEMANN, Jürgen MARKMANN, Jan Eike SCHNABEL, Konrad SCHNEIDER, Celal SOYARSLAN and Jana WILMERS. Generation of 3D representative volume elements for heterogeneous materials: A review. *Progress in Materials Science*[online]. 2018, **96**, pp. 322-384 [cit. 2019-01-10]. DOI: 10.1016/j.pmatsci.2018.02.003. ISSN 00796425.

[18] DONEV, Aleksandar. Jammed Packings of Hard Particles. Princeton, 2006. Disertation. Princeton University. Advisors Dr. Sal Torquato and Dr. Frank Stillinger.

[19] ADAMCZYK, Zbigniew. Particles at Interfaces: Interactions, deposition, structure. Second edition. London: Academic Press, 2017. ISBN 978-0-08-101248-2.

[20] VISSCHER, WILLIAM M. and M. BOLSTERLI. Random Packing of Equal and Unequal Spheres in Two and Three Dimensions. *Nature* [online]. 1972, **239**(5374), pp. 504-507 [cit. 2019-01-10]. DOI: 10.1038/239504a0. ISSN 0028-0836.

[21] WILLIAMS, S. R. a A. P. PHILIPSE. Random packings of spheres and spherocylinders simulated by mechanical contraction. *Physical Review E* [online]. 2003, **67**(5) [cit. 2019-01-10]. DOI: 10.1103/PhysRevE.67.051301. ISSN 1063-651X.

[22] JODREY, W. S. and E. M. TORY. Computer simulation of close random packing of equal spheres. *Physical Review A* [online]. 1985, **32**(4), pp. 2347-2351 [cit. 2019-02-10]. DOI: 10.1103/PhysRevA.32.2347. ISSN 0556-2791.

[23] BEZRUKOV, Alexander, Monika BARGIEL and Dietrich STOYAN. Statistical Analysis of Simulated Random Packings of Spheres. *Paticle & Particle Systems Characterization*. 2002, **19**, 111-118. DOI: 10.1002/1521-4117(200205)19:2<111::AID-PPSC111>3.0.CO;2-M.

[24] ALDER, B. J. a T. E. WAINWRIGHT. Studies in Molecular Dynamics. II. Behavior of a Small Number of Elastic Spheres. *The Journal of Chemical Physics* [online]. 1960, **33**(5), pp. 1439-1451 [cit. 2019-02-10]. DOI: 10.1063/1.1731425. ISSN 0021-9606.

[25] CUNDALL, P. A. a O. D. L. STRACK. A discrete numerical model for granular assemblies. In: *The Essence of Geotechnical Engineering: 60 years of Géotechnique*. 2008, pp. 305-329. Available from: http://websrv.cs.umt.edu/classes/cs477/images/0/0e/Cundall_Strack.pdf

[26] Smilauer V. et al. Yade Documentation 2nd ed., 2015. doi:10.5281/zenodo.32409. http://yade-dem.org

[27] STRÁNSKÝ, Jan. Mesoscale Discrete Element Model for Concrete and Its Combination with FEM. Prague, 2018. Doctoral Thesis. Czeach Technical University in Prague. Advisor Prof. Ing. Milan Jirásek, DrSc.

[28] LUBACHEVSKY, Boris D. and Frank H. STILLINGER. Geometric properties of random disk packings. *Journal of Statistical Physics* [online]. 1990, **60**(5-6), pp. 561-583 [cit. 2019-01-10]. DOI: 10.1007/BF01025983. ISSN 0022-4715.

[29] LUBACHEVSKY, Boris D., Frank H. STILLINGER and Elliot N. PINSON. Disks vs. spheres: Contrasting properties of random packings. *Journal of Statistical Physics* [online]. 1991, **64**(3-4), pp. 501-524 [cit. 2019-01-10]. DOI: 10.1007/BF01048304. ISSN 0022-4715.

[30] ASTE, Tomaso and D. L. WEAIRE. *The pursuit of perfect packing*. 2nd ed. New York: Taylor & Francis, 2008. ISBN 978-1-4200-6817-7.

[31] BERRYMAN, James G. Random close packing of hard spheres and disks. *Physical Review A* [online]. 1983, **27**(2), pp. 1053-1061 [cit. 2019-01-10]. DOI: 10.1103/PhysRevA.27.1053. ISSN 0556-2791.

[32] HALES, T. (2005). A Proof of the Kepler Conjecture. *Annals of Mathematics*, **162**(3), second series, pp. 1065-1185. Available from: http://www.jstor.org/stable/20159940.

[33] WEITZ, D. A. PHYSICS: Packing in the Spheres. *Science* [online]. 2004, **303**(5660), pp. 968-969 [cit. 2019-01-10]. DOI: 10.1126/science.1094581. ISSN 0036-8075.

[34] SCHAER, J. The Densest Packing of 9 Circles in a Square. *Canadian Mathematical Bulletin* [online]. 1965, **8**(03), pp. 273-277 [cit. 2019-01-10]. DOI: 10.4153/CMB-1965-018-9. ISSN 0008-4395.

[35] SCHLÜTER, K. Kreispackung in quadraten. *Elemente der Mathematik.* Math. 1979, **34**, 12-14.

[36] PEIKERT, Ronald. Dichteste Packungen von gleichen Kreisen in einem Quadrat. *Elemente der Mathematik*. 1994, **49**, 16-26. DOI: 10.5169/seals-45416.

[37] WÜRTZ, D., M. MONAGAN and R. PEIKERT. The history of packing circles in a square. *Maple Technical Newsletter*. 1994, pp. 35-42.

[38] STEPHENSON, Kenneth. Circle Packing: *A Mathematical Tale. Notices of the AMS*. 1994, **50**(11), pp. 1376-1388.

[39] STEPHENSON, Kenneth. *Introduction to circle packing: the theory of discrete analytic functions*. New York: Cambridge University Press, 2005. ISBN 0-52182356-0.

[40] HIFI, Mhand and Rym M'HALLAH. A Literature Review on Circle and Sphere Packing Problems: Models and Methodologies. *Advances in Operations Research* [online]. 2009, pp. 1-22 [cit. 2019-01-10]. DOI: 10.1155/2009/150624. ISSN 1687-9147.

[41] ŠEJNOHA, Michal and Jan ZEMAN. Micromechanics in practice. Ashurst, Southhampton, UK: WIT Press, [2013]. ISBN 978-1-84564-682-0.

[42] ŠEJNOHA, Michal and Jan ZEMAN. Micromechanical analysis of random composites. Prague: Czech Technical University, 2002. *CTU reports*. ISBN 80-01-02523-3.

[43] FULLWOOD, David T., Stephen R. NIEZGODA, Brent L. ADAMS and Surya R. KALIDINDI. Microstructure sensitive design for performance optimization. *Progress in Materials Science* [online]. 2010, **55**(6), pp. 477-562 [cit. 2019-01-10]. DOI: 10.1016/j.pmatsci.2009.08.002. ISSN 00796425.

[44] LAGAE, Ares and Philip DUTRÉ. An alternative for Wang tiles. *ACM Transactions on Graphics* [online]. 2006, **25**(4), pp. 1442-1459 [cit. 2019-01-10]. DOI: 10.1145/1183287.1183296. ISSN 07300301.

[45] MÜLLNER, Tibor, Klaus K. UNGER and Ulrich TALLAREK. Characterization of microscopic disorder in reconstructed porous materials and assessment of mass transport-relevant structural descriptors. *New J. Chem* [online]. 2016, **40**(5), pp. 3993-4015 [cit. 2019-01-10]. DOI: 10.1039/C5NJ03346B. ISSN 1144-0546.

[46] RABBANI, Arash, Saeid JAMSHIDI and Saeed SALEHI. An automated simple algorithm for realistic pore network extraction from micro-tomography images. *Journal of Petroleum Science and Engineering*[online]. 2014, **123**, pp. 164-171 [cit. 2019-01-10]. DOI: 10.1016/j.petrol.2014.08.020. ISSN 09204105.

[47] BEUCHER, S. and C. LANTUEJOUL. Use of watersheds in contour detection. In: *Proceedings of the International Workshop on Image Processing: Real-time Edge and Motion detection / estimation*. Rennes, France, 1979.

[48] LEDESMA-ALONSO, René, Romeli BARBOSA and Jaime ORTEGÓN. Effect of the image resolution on the statistical descriptors of heterogeneous media. *Physical Review E* [online]. 2018, **97**(2) [cit. 2019-01-10]. DOI: 10.1103/PhysRevE.97.023304. ISSN 2470-0045.

[49] ČERNÝ, V. Thermodynamical approach to the traveling salesman problem: An efficient simulation algorithm. *Journal of Optimization Theory and Applications* [online]. 1985, **45**(1), pp. 41-51 [cit. 2019-01-10]. DOI: 10.1007/BF00940812. ISSN 0022-3239.

[50] KIRKPATRICK, S., C. D. GELATT and M. P. VECCHI. Optimization by Simulated Annealing. Science [online]. 1983, **220**(4598), pp. 671-680 [cit. 2019-01-10]. DOI: 10.1126/science.220.4598.671. ISSN 0036-8075.

[51] REYNOLDS, Craig W. Flocks, herds and schools: *A distributed behavioral model. ACM SIGGRAPH Computer Graphics* [online]. 1987, **21**(4), pp. 25-34 [cit. 2019-01-10]. DOI: 10.1145/37402.37406. ISSN 00978930.

[52] KENNEDY, J., and R. C. Eberhart. *Particle swarm optimization. In Proceedings of the 1995 IEEE international conference on neural networks* (Perth, Australia), pp. 1942–1948. Piscataway, NJ: IEEE Service Center.

[53] MILLONAS, Mark M. Swarms, Phase Transitions, and Collective Intelligence (Paper 1); and A Nonequilibrium Statistical Field Theory of Swarms and Other Spatially Extended Complex Systems (Paper 2), Working Papers, 1993, 93-06-039, Santa Fe Institute.

[54] SENGUPTA, Saptarshi, Sanchita BASAK and Richard PETERS. Particle Swarm Optimization: A Survey of Historical and Recent Developments with Hybridization Perspectives. Machine Learning and Knowledge Extraction [online]. 2018, **1**(1), pp. 157-191 [cit. 2019-01-10]. DOI: 10.3390/make1010010. ISSN 2504-4990.

[55] BANKS, Alec, Jonathan VINCENT and Chukwudi ANYAKOHA. A review of particle swarm optimization. Part I: background and development. Natural Computing [online]. 2007, **6**(4), pp. 467-484 [cit. 2019-01-10]. DOI: 10.1007/s11047-007-9049-5. ISSN 1567-7818.

[56] BANKS, Alec, Jonathan VINCENT and Chukwudi ANYAKOHA. A review of particle swarm optimization. Part II: hybridisation, combinatorial, multicriteria and constrained optimization, and indicative applications. *Natural Computing* [online]. 2008, **7**(1), pp. 109-124 [cit. 2019-01-10]. DOI: 10.1007/s11047-007-9050-z. ISSN 1567-7818.

[57] GARCÍA-GONZALO, E. and J. L. FERNÁNDEZ-MARTÍNEZ. A Brief Historical Review of Particle Swarm Optimization (PSO). *Journal of Bioinformatics and Intelligent Control* [online]. 2012, **1**(1), pp. 3-16 [cit. 2019-01-10]. DOI: 10.1166/jbic.2012.1002. ISSN 23267496.

[58] SHI, Y. and R. EBERHART. A modified particle swarm optimizer. In: 1998 IEEE International Conference on Evolutionary Computation Proceedings. IEEE World Congress on Computational Intelligence (Cat. No.98TH8360) [online]. IEEE, 1998, pp. 69-73 [cit. 2019-01-10]. DOI: 10.1109/ICEC.1998.699146. ISBN 0-7803-4869-9.

[59] KENNEDY, J. The particle swarm: social adaptation of knowledge. In: Proceedings of 1997 IEEE International Conference on Evolutionary Computation (ICEC '97) [online]. IEEE, 1997, pp. 303-308 [cit. 2019-01-10]. DOI: 10.1109/ICEC.1997.592326. ISBN 0-7803-3949-5.

[60] CLERC, M. and J. KENNEDY. The particle swarm - explosion, stability, and convergence in a multidimensional complex space. IEEE Transactions on Evolutionary Computation [online]. **6**(1), pp. 58-73 [cit. 2019-02-03]. DOI: 10.1109/4235.985692. ISSN 1089778X.

[61] STEWART, Tim, Brian WILIAMS and Jerry BROCKMEYER. Ceramic Industry Magazine [online]. 2014, 1 August 2014 [cit. 2019-01-10]. Available from: https://www.ceramicindustry.com/articles/94101-melt-infiltrated-refractory-ceramic-matrix-composites

[62] NGUYEN, Nguyen Q., Sean D. PETERSON, Nikhil GUPTA and Pradeep K. ROHATGI. Modeling the Effect of Active Fiber Cooling on the Microstructure of Fiber-Reinforced Metal Matrix Composites. *Metallurgical and Materials Transactions A* [online]. 2009, **40**(8), 1911-1922 [cit. 2019-02-10]. DOI: 10.1007/s11661-009-9885-2. ISSN 1073-5623.

[63] ZRŮBEK, Lukáš, Martin DOŠKÁŘ, Anna KUČEROVÁ, Marcela MENESES-GUZMÁN, Francisco RODRÍGUEZ-MÉNDEZ and Bruno CHINÉ. IMAGE SYNTHESIS OF METAL FOAM MICRO-STRUCTURE WITH THE USE OF WANG TILES. *Acta Polytechnica CTU Proceedings* [online]. 2018, **15**, pp. 142-147 [cit. 2019-01-10]. DOI: 10.14311/APP.2018.15.0142. ISSN 2336-5382

[64] TYBUREC, Marek a Jan ZEMAN. OPTIMIZATION-BASED APPROACH TO TILING OF FINITE AREAS WITH ARBITRARY SETS OF WANG TILES. Acta Polytechnica CTU Proceedings [online]. 2017, 13, pp. 135-141 [cit. 2019-02-10]. DOI: 10.14311/APP.2017.13.0135. ISSN 2336-5382.

Cited publications of the author

[I] ŠEDLBAUER, David. Wang Tiles Size in Terms of Circular Particle Dynamics. In: *NMM 2017 - Nano & Macro Mechanics 2017: Acta Polytechnica CTU Proceedings.* Vol. 13. Prague: Czech Technical University in Prague, 2017, pp. 102-108. ISBN 978-80-01-06346-0. ISSN 2336-5382.

[II] ŠEDLBAUER, David. Adaptive Boundaries of Wang Tiles for Heterogenous Material Modelling. In: Modern Methods of Experimental and Computational Investigations in Area of Construction II: Acta Polytechnica CTU Proceedings. Pfaffikon: Trans Tech Publications, 2017, pp. 159-166. ISBN 978-3-0357-1092-2. ISSN 1022-6680.

[III] ŠEDLBAUER, David and Martin DOŠKÁŘ. Optimized Wang Tiles Generation for Heterogenous Materials Modelling. In: *Modern Methods of Experimental and Computational Investigations in Area of Construction: Applied Mechanics and Materials*. Vol. 825. Pfaffikon: Trans Tech Publications, 2016, pp. 183-190. ISBN 978-3-03835-603-5. ISSN 1660-9336.

[IV] ŠEDLBAUER, David. Dynamic Packing Algorithm for 3D Wang Cubes Generation. In: *Proceedings of the 5th Conference Nano & Macro Mechanics.* Prague: Czech Technical University in Prague, 2014, pp. 173-180. ISBN 978-80-01-05569-4.

[V] ŠEDLBAUER, David. Heterogenous Material Modelling via Dynamics Packing of Stochastic Wang Tiles. In: *Proceedings of the 4th Conference Nano & Macro Mechanics*. Prague: Czech Technical University in Prague, 2013, pp. 187-192. ISBN 978-80-01-05332-4.